Surface waves : introduction

In addition to body waves, surface waves can be excited by quakes.
The property of interest is their dispersion, phase and group velocity as a function of period.
Main use: study geographical variability of crust and upper mantle.
Period range where characterization as surface waves is convenient is, roughly, 20 sec to 200 sec.

Above 200 sec, finite spherical shape of ⊕ becomes important, more convenient description is as free oscillations of spherical ⊕, the distinction is similar to that between travelling and standing waves on a violin string.

Recall: for body waves in a homogeneous medium:

$\underline{r}$ = particle label
$\underline{s}(\underline{r}, t)$ = displacement of particle $\underline{r}$ at time t

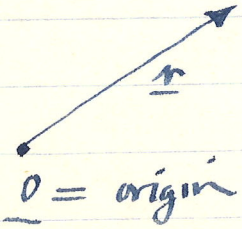

Body waves are possible motions of homog. elastic medium of form:

$$\underline{s}(\underline{r},t) = \underline{A}\cos(\underline{k}\cdot\underline{r} - \omega t)$$

↑ plane wave

amplitude $\underline{A}$ describes polarization of motion as well.

$\underline{k}$ = wavenumber vector

ω = angular frequency

$k = |\underline{k}|$ = wavenumber

$\lambda = 2\pi/k$ = wavelength

$\underline{k}\cdot\underline{r} = k_x x + k_y y + k_z z$

Physically such solutions are waves propagating in direction $\hat{k} = \underline{k}/k$. The phase speed of propagation (velocity of wave "crests" or "troughs") is

$$c = \omega/k$$

We found ∃ two distinct types of waves:

1. P waves:

$$c = \alpha = \sqrt{\frac{K + \frac{4}{3}\mu}{\rho}}$$

particle motion or polarization $\underline{A}$ along direction of propagation

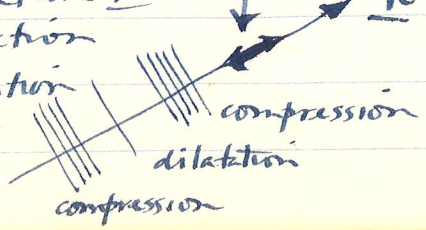

$\underline{k}$ (defines direction of propagation)

$$\underline{A} \parallel \underline{k}$$

2. S waves : $\boxed{c = \beta = \sqrt{\frac{\mu}{\rho}}}$

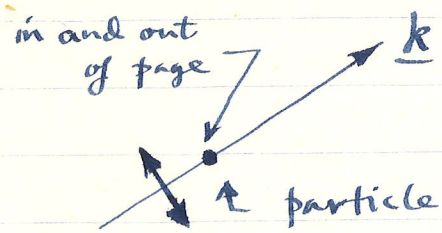

$\boxed{\underline{A} \perp \underline{k} \quad (\underline{k} \cdot \underline{A} = 0)}$

Note : the above is independent of excitation of the waves, concerns only their free propagation, we have looked for all possible freely propagating solns.

We now conduct a similar program for surface waves.

Simplest case possible first :

Homogeneous half-space (vacuum above) :

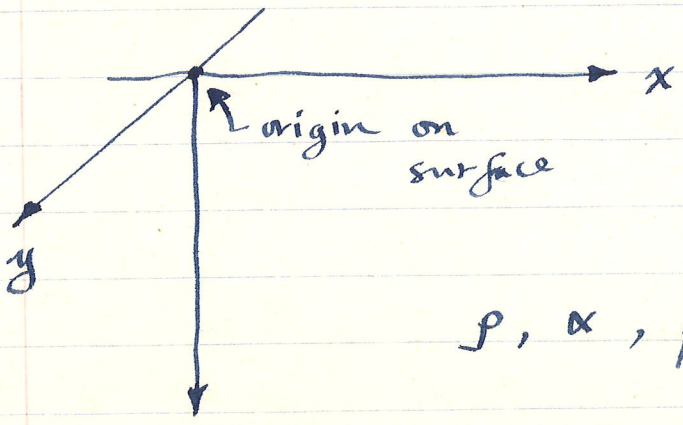

ρ, α, β all constant

Now that ∃ a bdry. the distinction between SH and SV polarization becomes important. As with body waves ∃ two distinct cases: pure SH and P–SV, which are coupled at boundaries.

A freely propagating surface wave is of the form:

$k_x x + k_y y$

$$s(\underline{r},t) = s(\underline{x},z,t) = \underline{A}(z)\cos(\underline{k}\cdot\underline{x} - \omega t)$$

where $\underline{A}(z) \to 0$ as $z \to \infty$ (i.e. confined to surface)

$\underline{k}$: horizontal wavevector

$$\underline{k} = k_x\hat{x} + k_y\hat{y}$$

$\underline{x} = x\hat{x} + y\hat{y}$ so that $\underline{r} = \underline{x} + z\hat{z}$

ω = ang. frequency

$\lambda = 2\pi/k$: horizontal wavelength

$c = \omega/k$: phase speed along surface

The wave is trapped near the surface and propagating horizontally along it.

$A(z)$ will always be either SH or P-SV polarized.

For a homogeneous half-space SH type solutions do not exist.

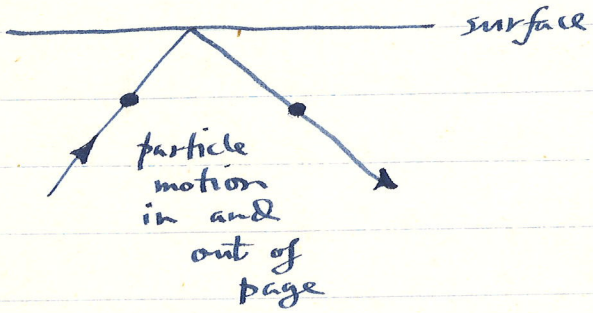

$\exists$ reflected SH body waves but their amplitude does not $\to 0$ as $z \to \infty$ (attenuation doesn't count)

$\exists$ no SH surface-trapped waves in this case

There are however P-SV surface waves called Rayleigh waves (Rayleigh 1885). To find this solution one must solve a boundary value problem (see e.g. Garland Section 4.2). The phase speed $c = \omega/k$ is determined by solving a transcendental equation called the Rayleigh equation.

Also see Gubbins 3.9 & 3.10

It takes the form

$$\left(\frac{1}{\beta^2}-\frac{2}{c^2}\right)^2-\frac{4}{c^2}\left(\frac{1}{c^2}-\frac{1}{\alpha^2}\right)^{1/2}\left(\frac{1}{c^2}-\frac{1}{\beta^2}\right)^{1/2}=0$$

c depends on both α and β but not in this case on ρ (this misleading, more generally it will)

For any reasonable material solution of above eqn. is $c \sim 0.9\beta$. Furthermore c is always $< \beta$.

Poisson solid ($\sigma = 1/4$ or $\alpha = \sqrt{3}\beta$):

$$c = 0.9194\beta$$

P-SV polarization $\Rightarrow$ particle motion is in k, z plane. There is both a vertical and horizontal component

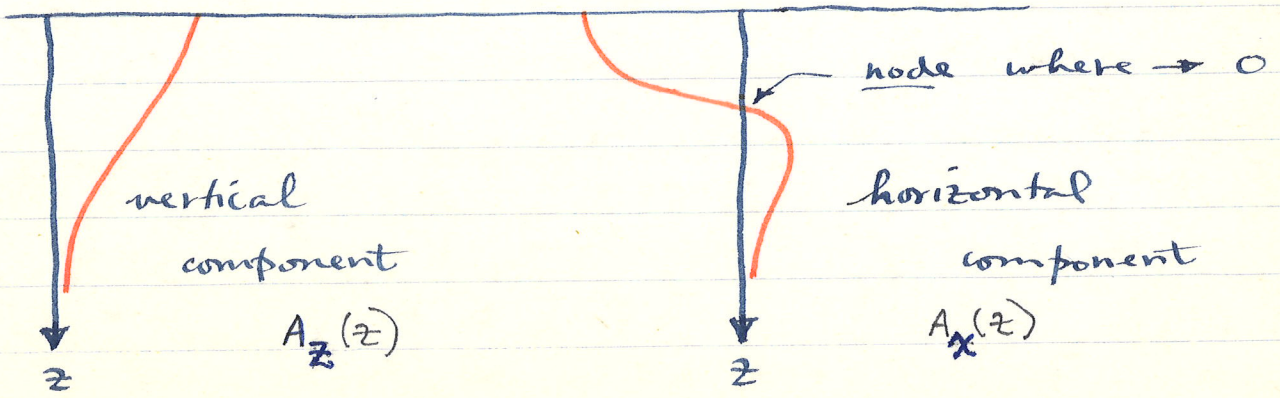

Furthermore the relative phase of vertical and horizontal motion is $\pi/2$ or 90° so particle motion is a closed retrograde ellipse

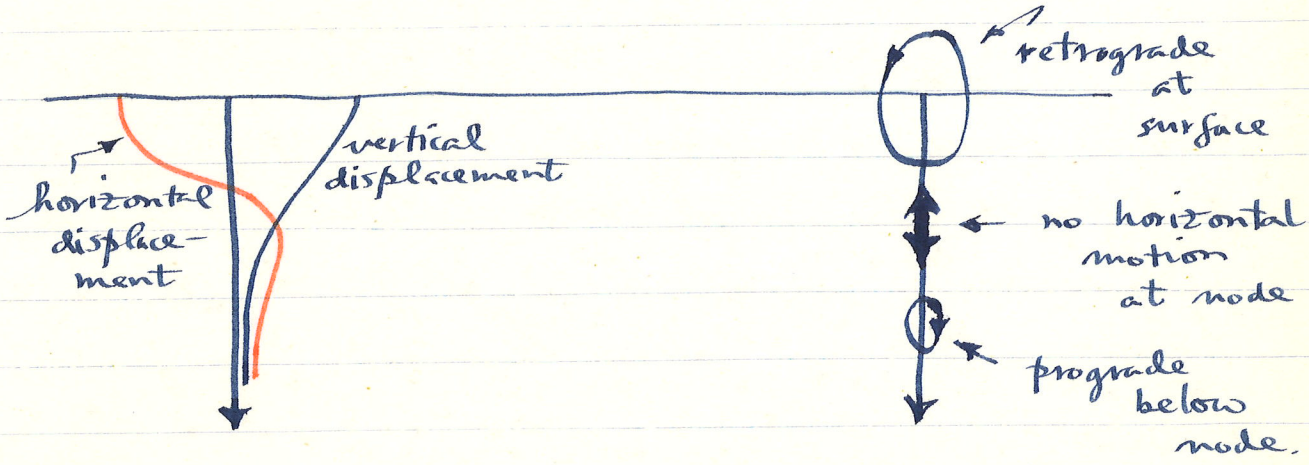

Retrograde elliptical motion at surface is very characteristic of Rayleigh waves, even in layered half-space.

For Poisson solid ($\sigma = 1/4$) vertical axis of ellipse = 1.468 × horizontal axis, in general vertical ~ 1.5 × horizontal.

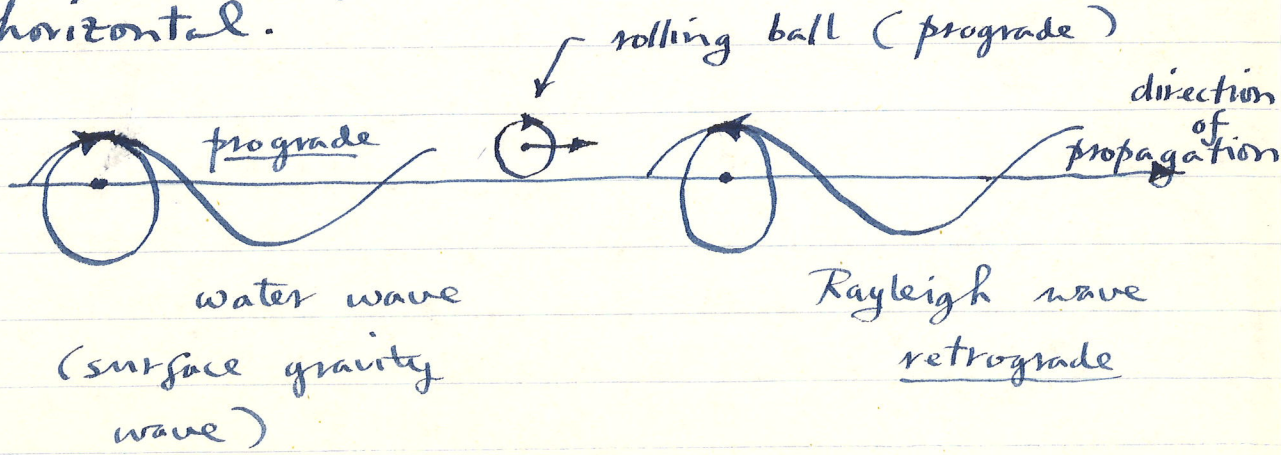

The decay of $\underline{A(z)}$ into the half-space as $z \to \infty$ is <u>exponential</u>

> <u>Poisson solid</u>: both vertical and horizontal $\sim \exp(-0.8475\ kz)$ as $z \to \infty$.

Thus <u>longer wavelength waves</u> penetrate <u>deeper</u>. This characteristic of <u>all</u> surface waves. For <u>Poisson solid</u> the motion is smaller by $1/e$ at a depth $z = \dfrac{\lambda}{2\pi(0.85)} \sim \dfrac{1}{5}\lambda$.

The next most complicated case we can analyze is a single layer over a half-space

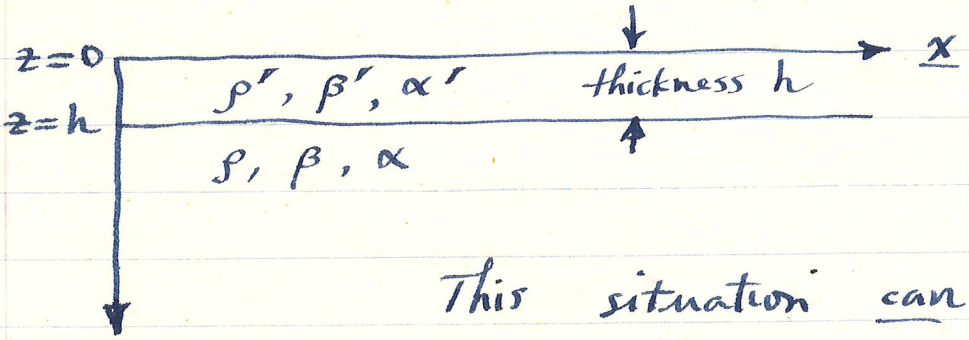

This situation <u>can</u> support SH surface waves, called <u>Love waves</u> (Love 1911). Their properties do <u>not</u> depend on α, α'.

By considering this layered model Love "explained" the existence of <u>observed</u> SH surface waves.

Particle motion in this case is $\perp$ to $\underline{k}, z$ plane, in $\hat{k} \times \hat{z}$ direction, motion is of form

$$\underline{s}(\underline{x}, z, t) = (\hat{k} \times \hat{z})\, u(z) \cos(\underline{k} \cdot \underline{x} - \omega t)$$

($\hat{k} \times \hat{z}$: SH polarization)

Two new features in this case:

1. For a given k, $\exists$ more than one mode of propagation, different modes have different displacement eigenfunctions $u(z)$.
2. the propagation is dispersive, the phase speed depends on the frequency ω and wavenumber k.

Again one must solve a boundary value problem (see Garland Section 4.3). Results conveniently presented in form of dispersion diagram, plot of frequency ω vs. k, frequency of wave with wavenumber k.

First, let us consider form of dispersion diagram for Rayleigh waves in homog. half-space.

$$\omega = ck, \quad c \approx 0.9\beta$$

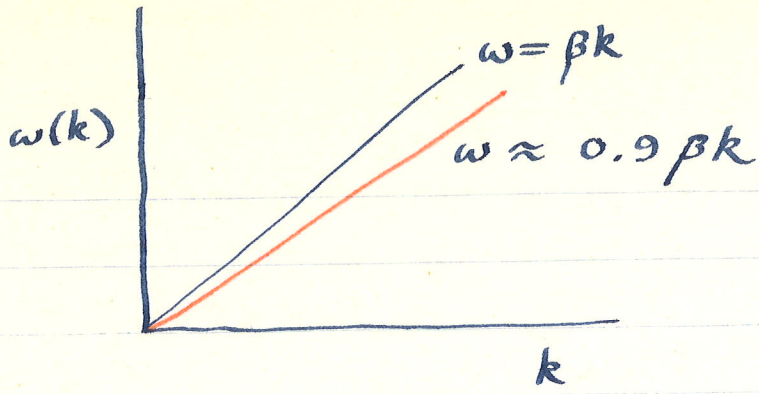

Dispersion diagram is a straight line, slope c = Rayleigh phase speed. This characteristic of non-dispersive waves (body waves in non-attenuating medium also non-dispersive)

Love wave dispersion diagram:

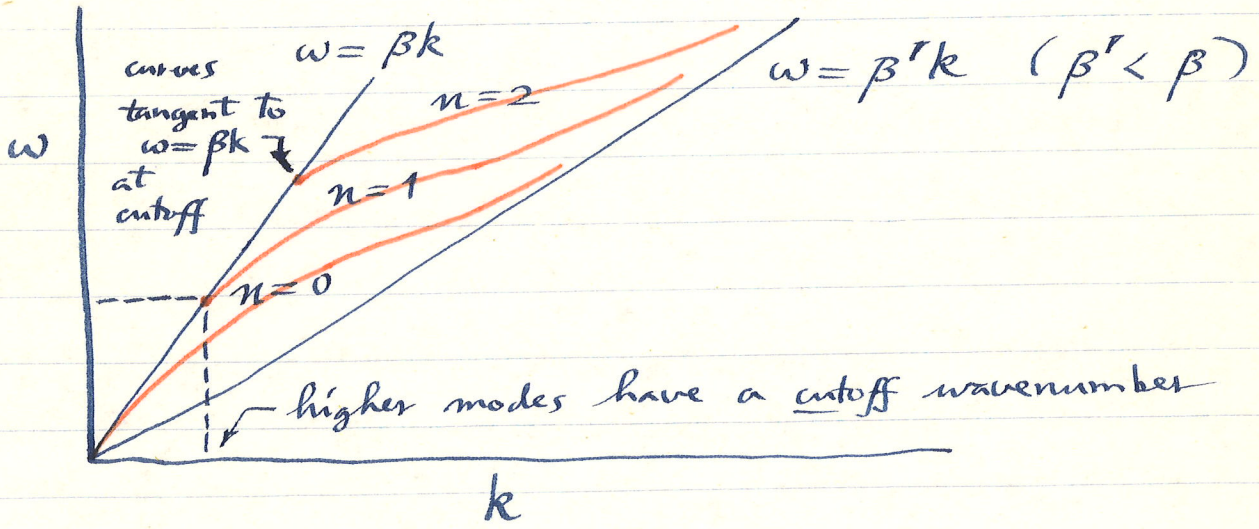

n = 0 : fundamental mode

n = 1, 2, etc. : overtone modes
(first overtone, second overtone, etc.)

Higher modes do not exist for long periods $T = 2\pi/\omega$, long wavelengths $\lambda = 2\pi/k$ (longer than the respective cutoffs).

Phase velocity is now wavelength and frequency-dependent:

$$\boxed{c(k) = \omega(k)/k}$$

Geometrically, it is the slope of the line from origin out to the point

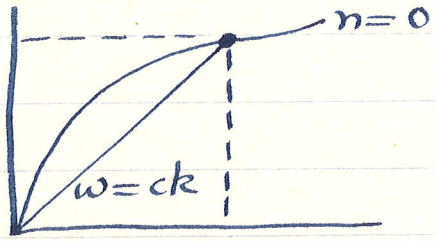

The possible phase speeds $c(k)$ may be shown to satisfy the transcendental equation (Love 1911)

$$\boxed{\tan\left[k\left(\frac{c^2}{\beta'^2}-1\right)^{1/2} h\right] = \frac{\mu\left(1-\frac{c^2}{\beta^2}\right)^{1/2}}{\mu'\left(\frac{c^2}{\beta'^2}-1\right)^{1/2}}}$$

*

Note $\beta' < c < \beta$, easy to see from dispersion diagram

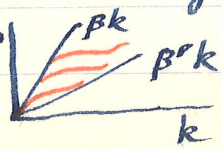

For any given k $\exists$ only a finite number of solutions.

The equation * can also be derived by thinking of Love waves as due to constructive interference of SH body waves reflected successively within the upper layer.

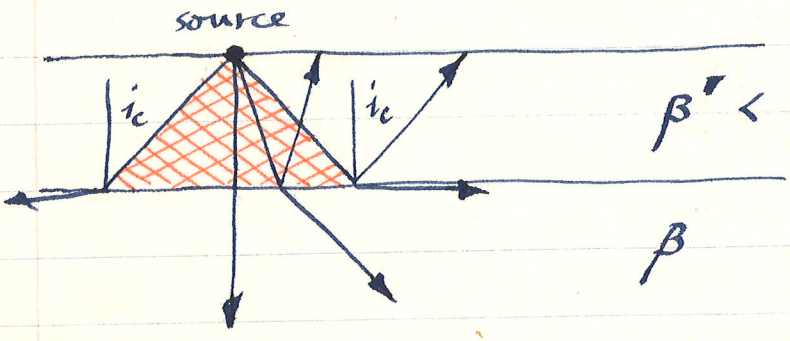

critical angle:

$$\sin i_c = \frac{\beta'}{\beta}$$

for incidence angles $i < i_c$, SH energy can be transmitted to half-space below, but all the SH energy radiated from the source outside shaded cone above propagates as Love waves trapped by total internal reflection in upper layer, only exponential leakage into half-space

Love waves are the result of constructive interference of the reflected SH body waves:

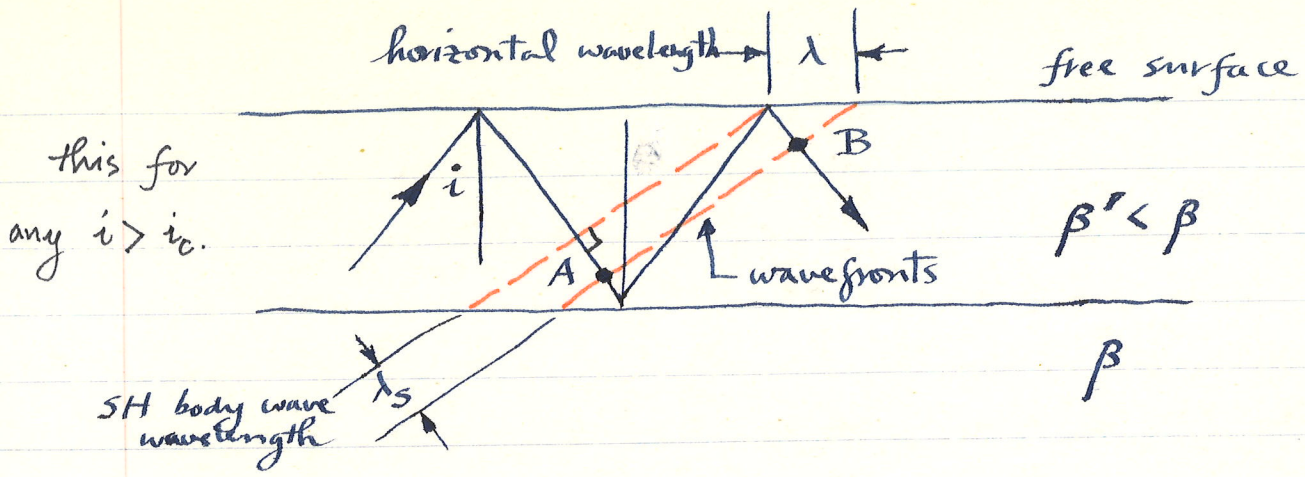

Condition for <u>constructive interference</u> is that:

$$\text{phase at } B = \text{phase at } A + 2n\pi, \quad n = 0, 1, 2 \ldots$$

Let λ_s = wavelength of SH body waves in layer (distance between successive wavefronts). Then

$$\lambda = \frac{\lambda_s}{\sin i}, \quad \text{horizontal wavelength of surface waves.}$$

Also $\sin i = \frac{\beta'}{c}$

$$\sin i = \frac{\lambda_s}{\lambda} = \frac{\beta'}{c}$$

Then: phase at B − phase at A

$$= \frac{2\pi}{\lambda_s}(\text{path length } AB) + \phi_{base} + \phi_{top}$$

ϕ_{base}: phase advance upon reflection at base

ϕ_{top}: phase advance at free surface (zero)

it's the sum of 2 parts: $AB = \frac{h}{\cos i} + \frac{h}{\cos i}(\quad \cos 2i)$

The path length $AB = 2h\cos i$ so

$$\frac{2\pi}{\lambda_s}(AB) = \frac{2kh}{\tan i} = 2kh\sqrt{\frac{c^2}{\beta'^2}-1}$$

Thus:

$$2kh\sqrt{\frac{c^2}{\beta'^2}-1} + \phi_{base} = 2n\pi$$

To find $\phi_{base}(i)$ must consider problem of impingement of SH plane wave on a boundary. Can show that

$$\tan\frac{\phi_{base}}{2} = \frac{\mu\left(1-c^2/\beta^2\right)^{1/2}}{\mu'\left(c^2/\beta'^2-1\right)^{1/2}}$$

↑ note depends on μ, μ' as well as on β, β'.

This leads to

$$kh\left(\frac{c^2}{\beta'^2}-1\right) = \tan^{-1}\frac{\mu\left(1-\frac{c^2}{\beta^2}\right)^{1/2}}{\mu'\left(\frac{c^2}{\beta'^2}-1\right)^{1/2}} + n\pi$$

which is equivalent to *

$n = 0, 1, 2\ldots$ is the overtone number.

Can also plot $c(k) = \omega(k)/k$.

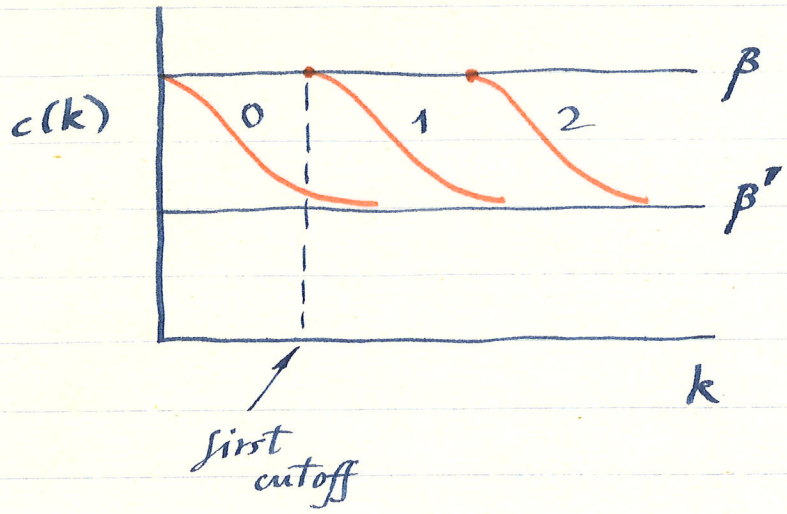

The associated <u>particle motion</u> $u(z)$ looks like:

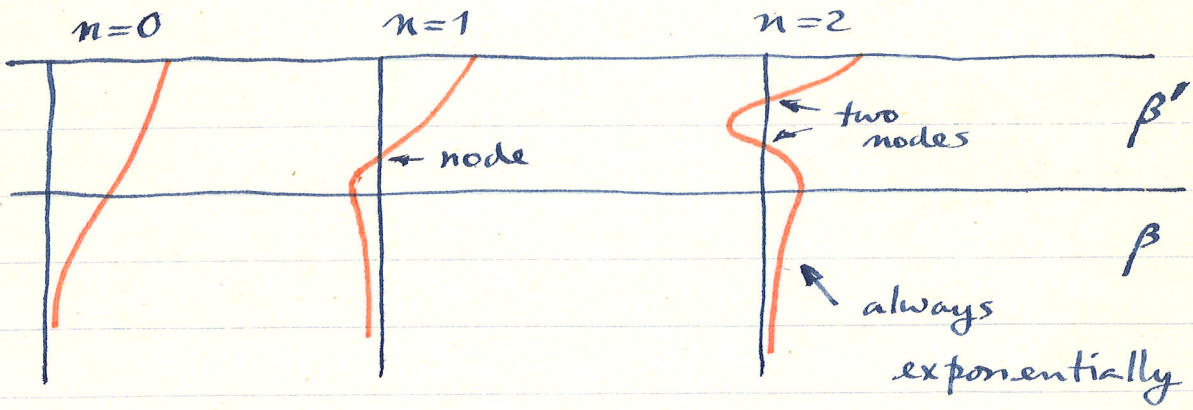

Particle motion in and out of page, n^{th} overtone has n <u>nodal surfaces</u> in top layer

<u>In the half-space</u> $u(z) \sim e^{-(1-\frac{c^2}{\beta^2})^{1/2} kz}$

↳ quote more precise result next page

In the upper layer:

$$u(z) \sim \cos\left(\frac{c^2}{\beta'^2} - 1\right)^{1/2} kz$$

In the half-space below, to be more precise,

$$u(z) \sim \cos\left(\frac{c^2}{\beta'^2} - 1\right)^{1/2} kh \exp\left[-\left(1 - \frac{c^2}{\beta^2}\right)^{1/2} (z-h)\right]$$

Note this continuous at bdry $z=h$ as it must be.

At cutoff of an overtone branch:

1. $c(k) = \beta$

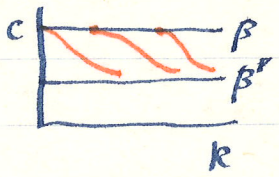

2. $\left(\frac{\beta^2}{\beta'^2} - 1\right)^{1/2} kh = n\pi$

Thus at cutoff of 1st overtone, e.g.

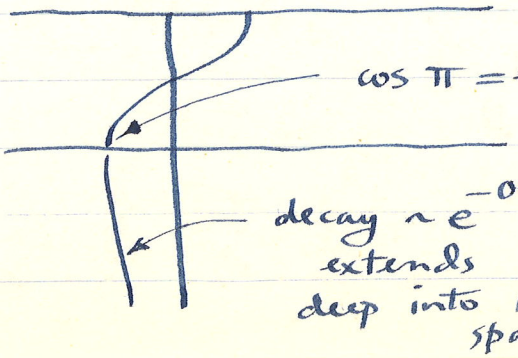

(in general cutoff occurs when $n/2$ cycles of cos can just fit in

As an example: "typical" continental crust – mantle structure

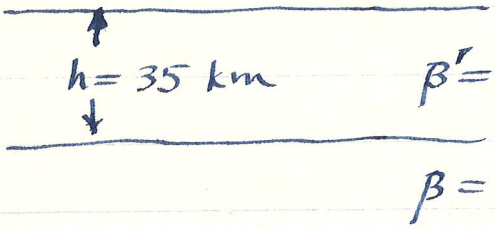

Cutoff of first mode occurs at:

In general for n^{th} mode:

$$\omega_{cutoff} = \frac{n\pi\beta'}{h}\left(1 - \frac{\beta'^2}{\beta^2}\right)^{1/2}$$

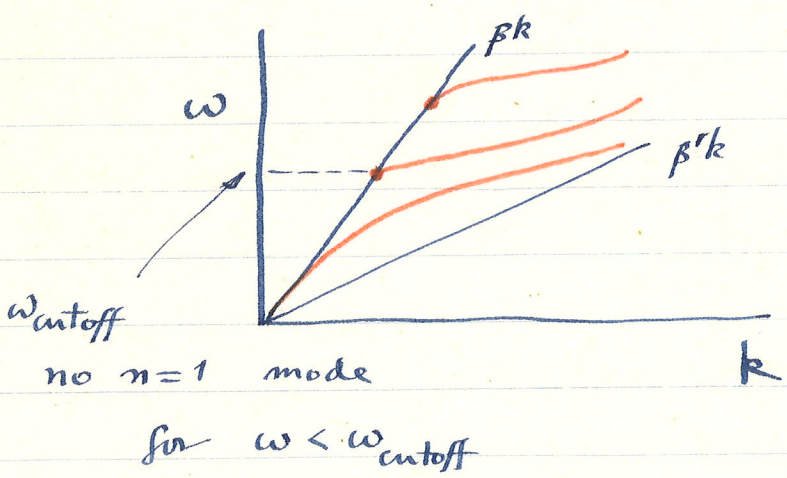

no $n=1$ mode for $\omega < \omega_{cutoff}$

$\omega_{cutoff} = 0.08$ Hz

period $T = 13$ s,

higher mode Love waves have periods shorter than this in above structure.

~~Another characteristic of an mode at cutoff~~

Another characteristic of a mode at cutoff: from constructive interference pt. of view cutoff occurs when SH waves are propagating at the critical angle, since $\sin i = \beta'/c$ $= \beta'/\beta$ at cutoff

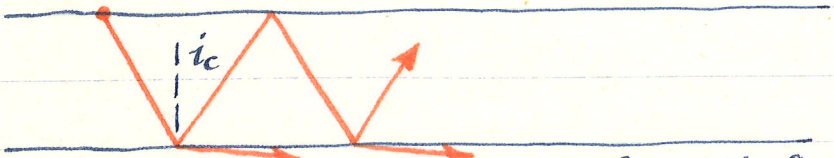

this the reason for decay $\sim e^{-\alpha z}$

↑ this the picture for fundamental mode at $k \to 0$ (its "cutoff") too

The penetration into half-space is maximum at cutoff (or at $k \to 0$ for fundamental mode).

For $kh \gg 1$ the displacement in the half-space is very small.
From SH pt of view looks more and more like horizontally propagating SH

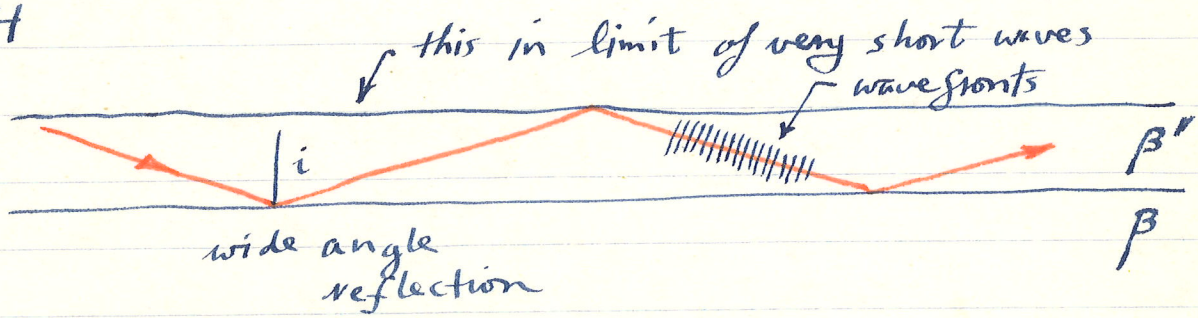

Thus makes sense that $c(k) \to \beta''$ and $k \to k$ of body waves.

Fundamental in other limit ($kh \ll 1$):

looks like

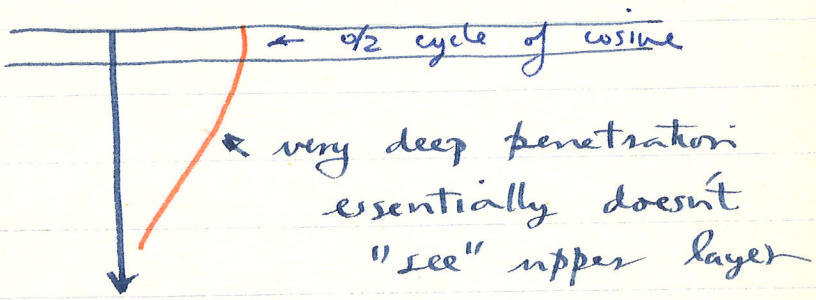

this in limit of very long waves

Thus $c(k) \to \beta$, shear velocity in lower layer

And, recall again, $n = 1$ at cutoff

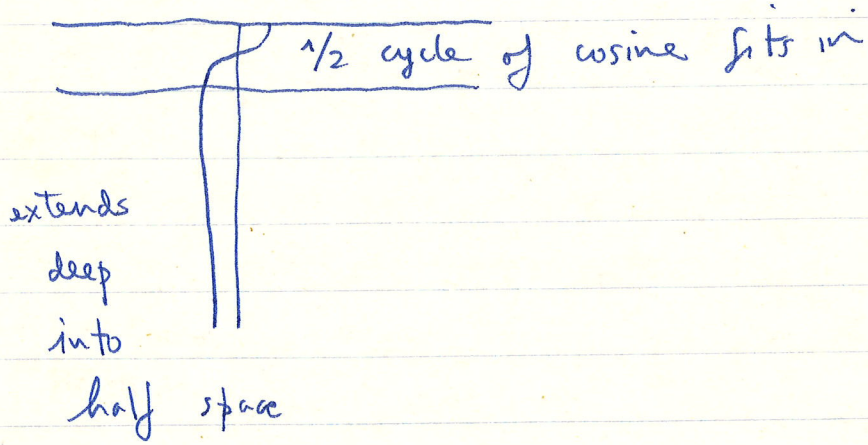

Surface waves in arbitrary layered structures

The constructive interference approach is not easily generalized but the boundary value problem approach can be.

Before advent of computers 2 or 3 layer models were the practical limit. Can now solve b.v. problem numerically for arbitrary structure:

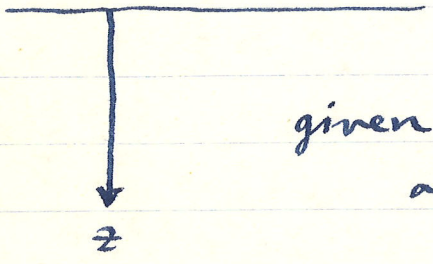

given $\alpha(z)$, $\beta(z)$, $\rho(z)$
all → constant below some depth

Both Love and Rayleigh waves can in general propagate.

Love waves: general properties very similar to 2-layer case.
Suppose that structure looks like:

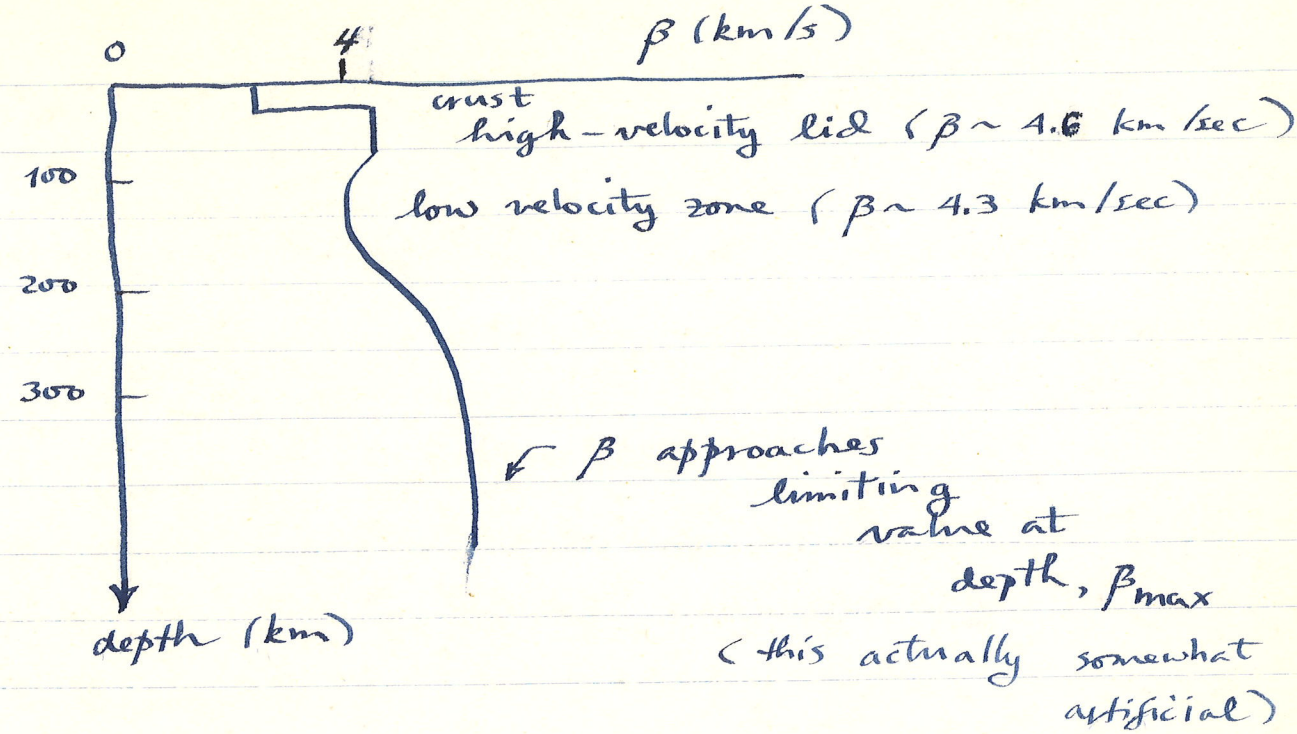

In a general way dispersion diagram then looks like:

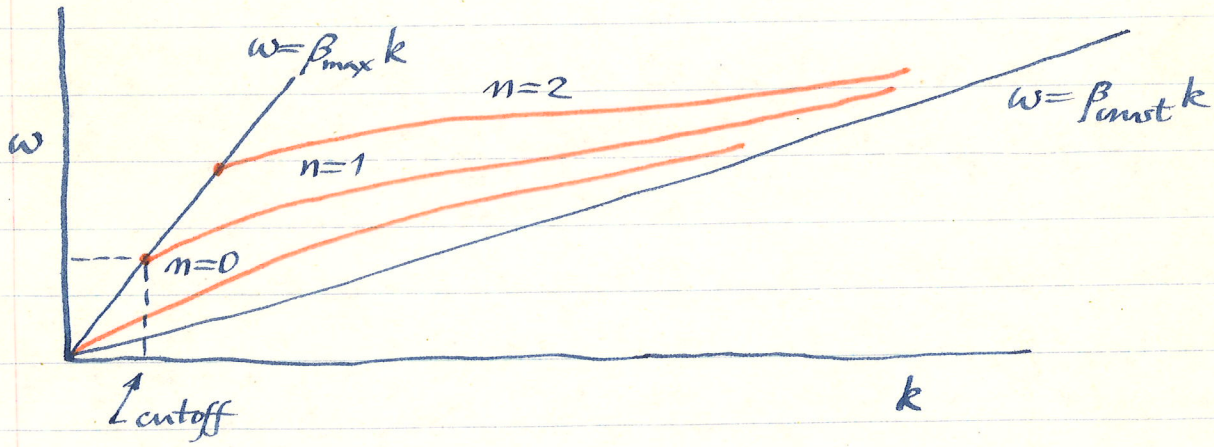

Consider $k \to \infty$, high frequencies, short wavelengths, wave trapped in crustal layer, dispersive properties depend critically on thickness of sedimentary cover, etc.
For the Φ this is periods $\lesssim$ 10 sec, propagating in crust.

Crust is very inhomogeneous laterally, these short-period waves are strongly refracted and scattered, difficult to study.

Consider fundamental mode in limit $k \to 0$, very long wavelength, does not "see" upper structure, looks like a homogeneous half-space, speed β_{max}.

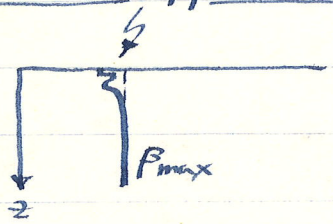

This limit somewhat artificial as β in mantle actually increases with depth down to core-mantle bdry.

Plot of c vs. k looks like (as before):

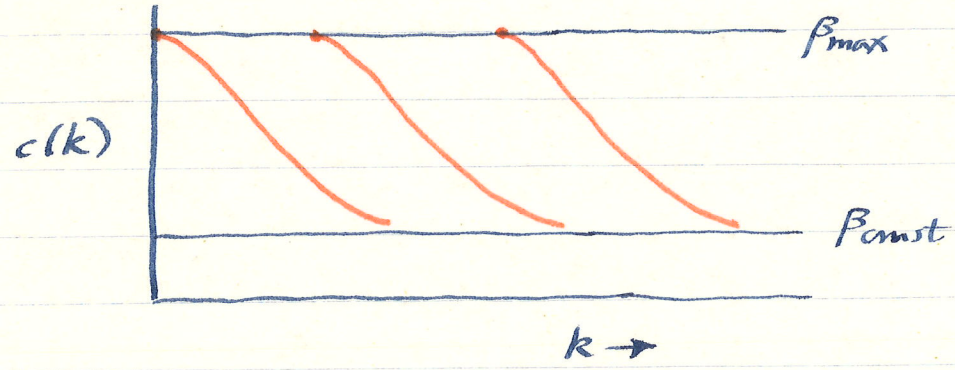

Once again the n^{th} mode has n nodes as a function of depth.

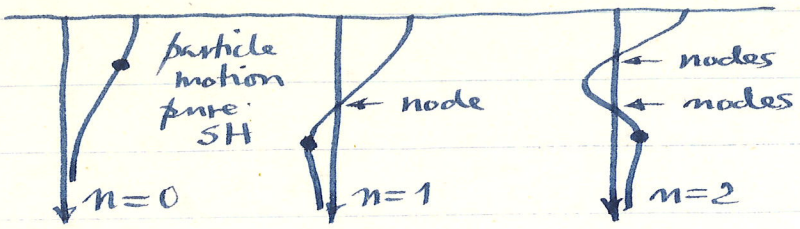

Love eigenfunctions $u(z)$

Details of $\omega(k)$, $c(k)$ and $u(z)$ depend on the structure, in fact on both $\mu(z)$ and $\rho(z)$, or alternatively on $\beta(z)$ and $\rho(z)$. If $\beta(z)$ and $\rho(z)$ chosen as independent variables the dependence on $\beta(z)$ is stronger than on $\rho(z)$.

Rayleigh waves: in a homogeneous medium $\exists$ only a fundamental and it is non-dispersive. More generally Rayleigh waves are dispersive and $\exists$ overtones.

Dispersion diagram has the general form:

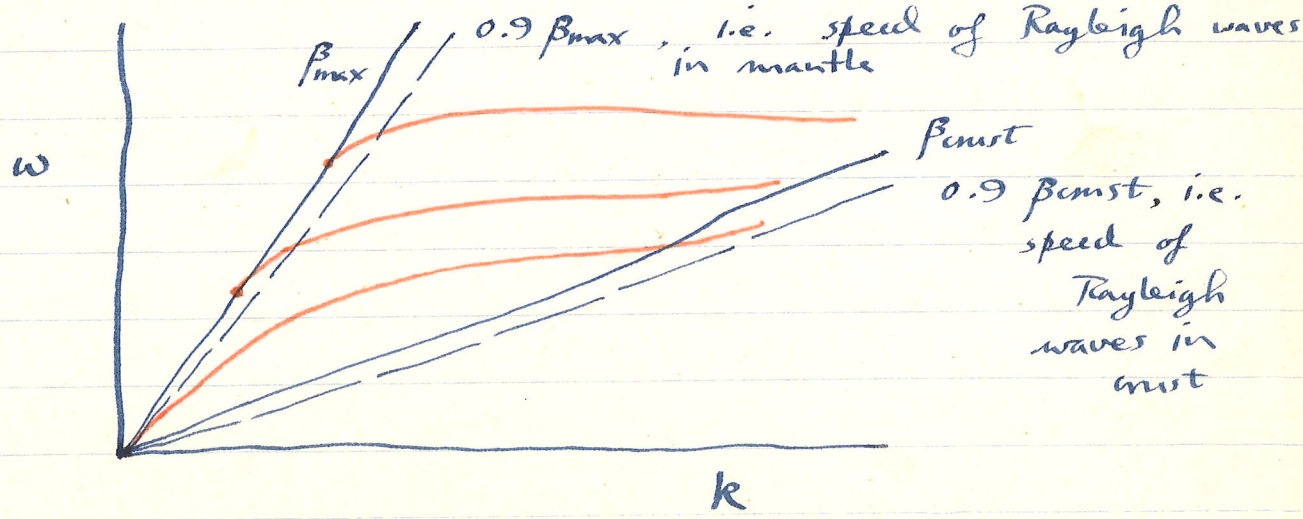

Phase velocity vs. k looks like:

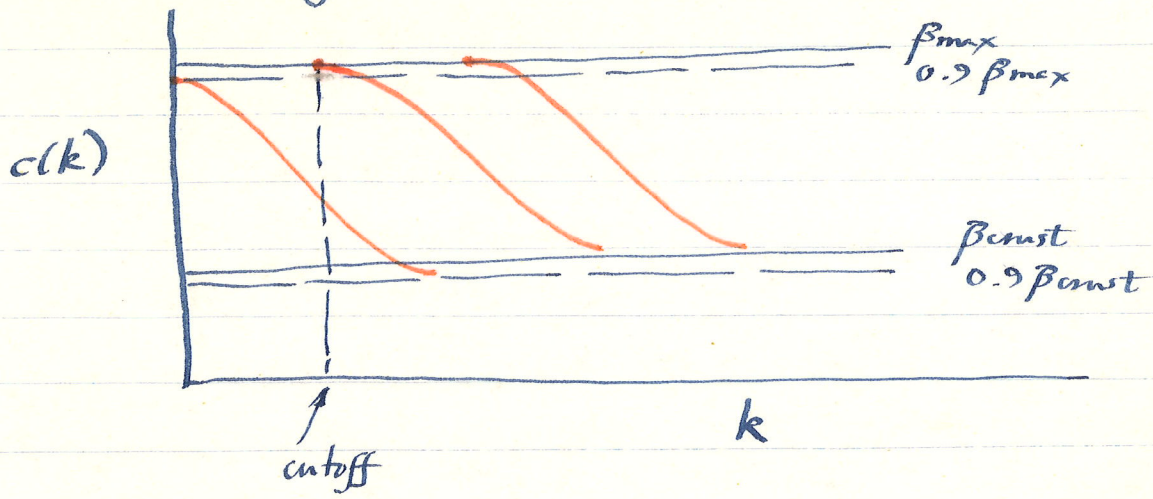

Consider the fundamental Rayleigh mode. For $k \to 0$ does not "see" structure near top, propagates with $c_{Rayleigh}$ of mantle. For $k \to \infty$ propagates in crust with $c_{Rayleigh}$ of crust.

The limiting phase speeds of overtone Rayleigh modes happen to be β_{max} and β_{crust}.

In fact higher mode Rayleigh waves become almost pure SV as n increases. Look like SV counterpart of Love wave, $\omega(k)$ and $c(k)$ quite similar, particle motion looks like

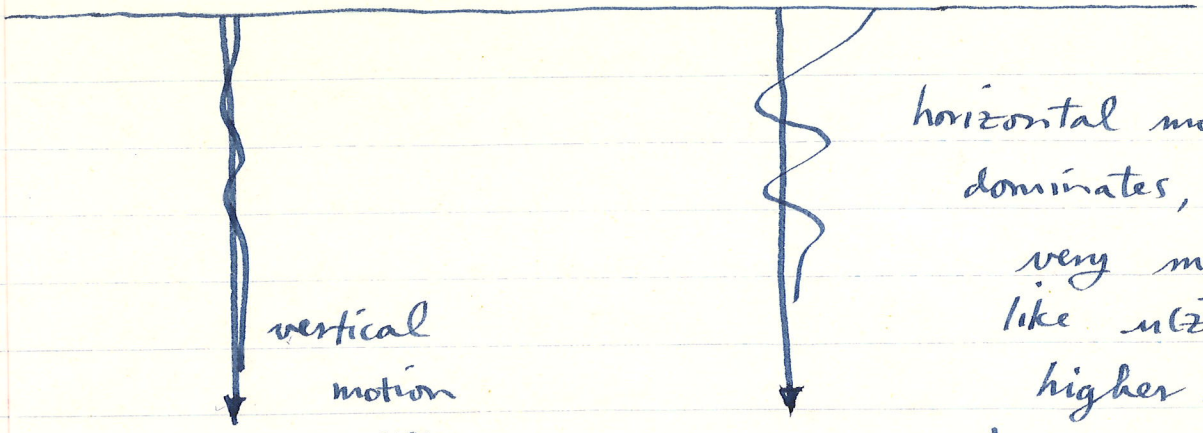

The particle motion of the fundamental Rayleigh is still an ellipse, retrograde at surface

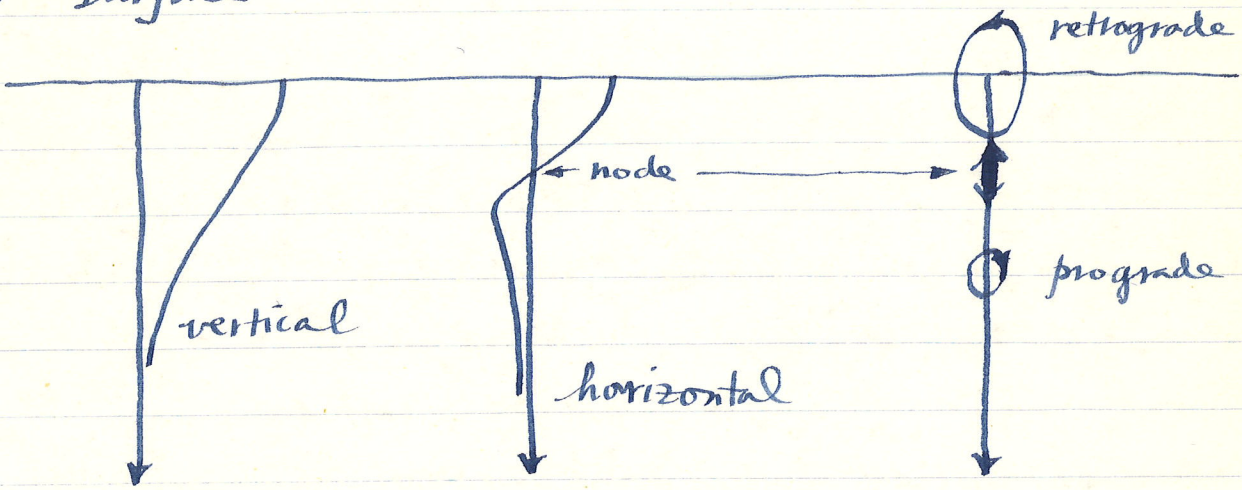

Figures A-E from Aki and Richards textbook show the phase velocity c for Love and Rayleigh fundamental modes, periods 20-100 sec

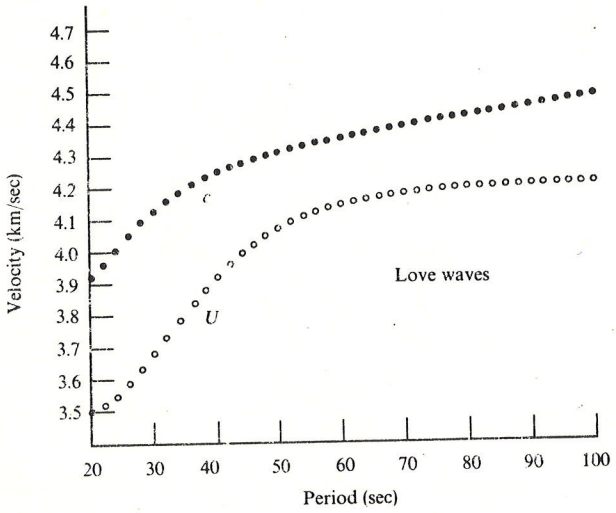

FIGURE **A**

Phase and group velocity of the fundamental-mode Love waves for the Gutenberg Earth model.

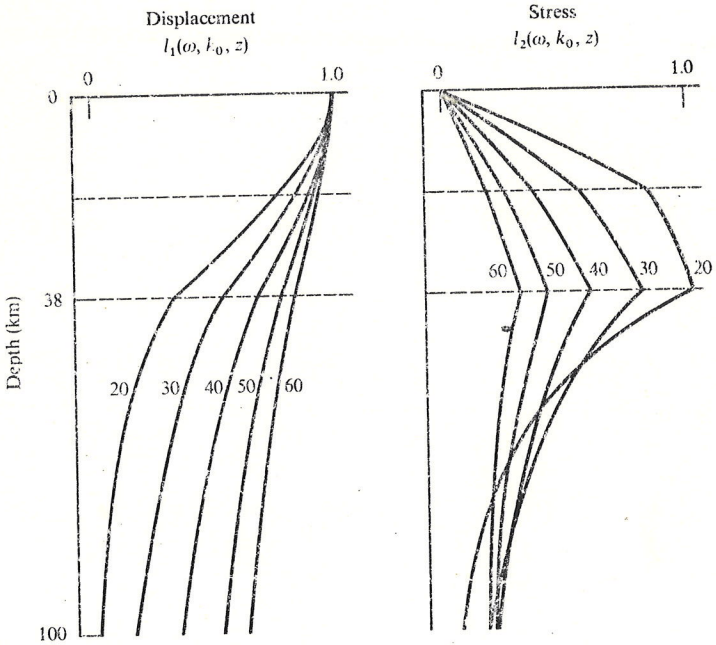

FIGURE **B**

The eigenfunctions for the fundamental-mode Love waves for various periods. The amplitude is normalized to the displacement at $z = 0$.

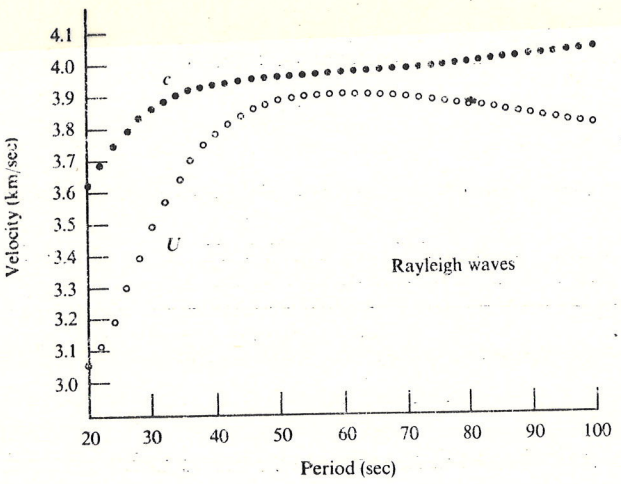

FIGURE C

Phase and group velocity of the fundamental-mode Rayleigh waves for the Gutenberg Earth model.

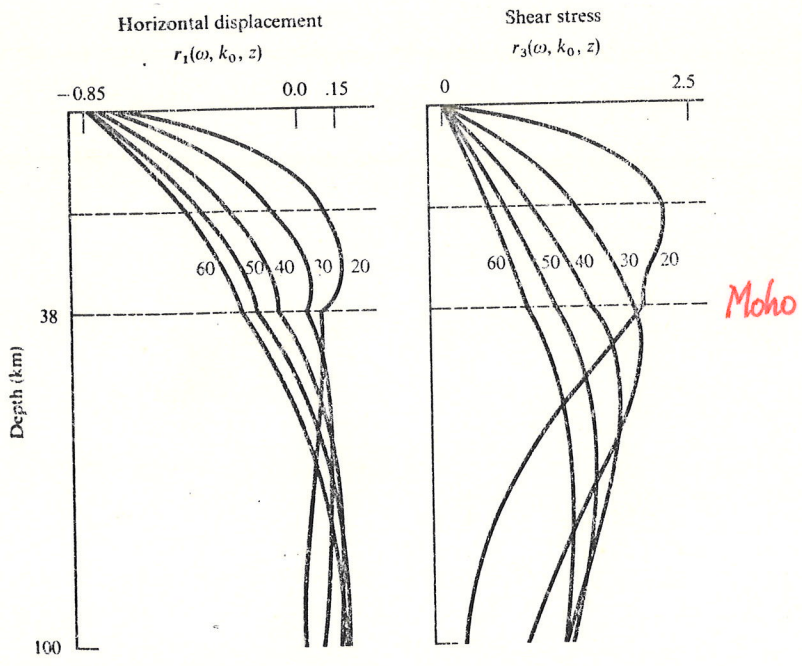

FIGURE D

The horizontal eigenfunctions for the fundamental-mode Rayleigh waves for various periods. The amplitude is normalized to the vertical displacement r_2 at $z = 0$.

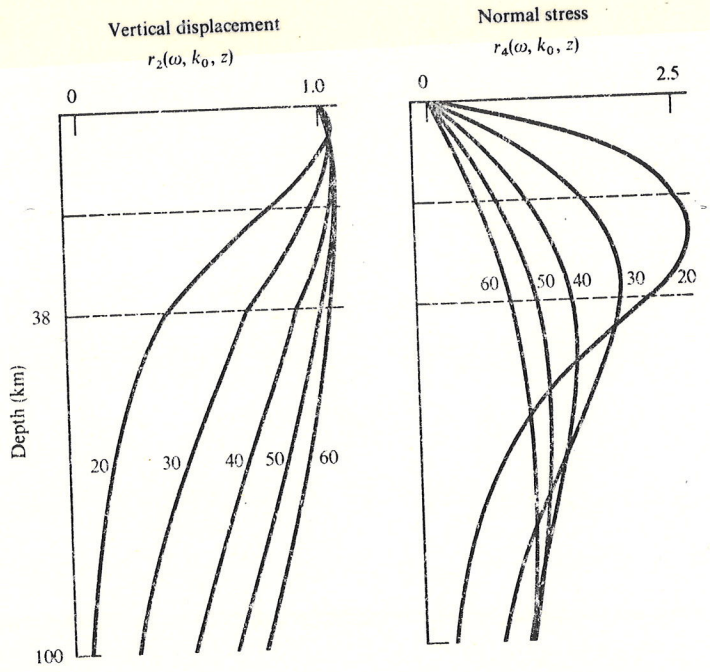

FIGURE E

The vertical eigenfunctions for the fundamental-mode Rayleigh waves for various periods. Again, the amplitude is normalized to the vertical displacement r_2 at $z = 0$.

Gutenberg's layered model of continental structure.

Layer number	*Depth to bottom* (km)	*density* (g/cm^3)	v_p (km/sec)	v_s (km/sec)
1	19	2.74	6.14	3.55
2	38	3.00	6.58	3.80 — Moho
3	50	3.32	8.20	4.65
4	60	3.34	8.17	4.62
5	70	3.35	8.14	4.57
6	80	3.36	8.10	4.51
7	90	3.37	8.07	4.46
8	100	3.38	8.02	4.41
9	125	3.39	7.93	4.37
10	150	3.41	7.85	4.35
11	175	3.43	7.89	4.36
12	200	3.46	7.98	4.38
13	225	3.48	8.10	4.42
14	250	3.50	8.21	4.46
15	300	3.53	8.38	4.54
16	350	3.58	8.62	4.68
17	400	3.62	8.87	4.85
18	450	3.69	9.15	5.04
19	500	3.82	9.45	5.21
20	600	4.01	9.88	5.45
21	700	4.21	10.30	5.76
22	800	4.40	10.71	6.03
23	900	4.56	11.10	6.23
24	1000	4.63	11.35	6.32

The phase velocity is the velocity of monochromatic waves of a given wavenumber k or period T.

The group velocity, also shown, we shall discuss later.

Also shown are the displacement eigenfunctions and stress eigenfunctions (don't worry about these) plotted vs. depth for different period waves: 20, 30, 40, 50, 60 secs.
The calculations are done for a classical ⊕ model due to Gutenberg, a fair depiction of average continental structure, Moho at 38 km, v_p goes from 6.6 km/s to 8.2 km/s and v_s from 3.8 to 4.7 km/sec.

The deeper penetration of longer period waves is clear.

Changes in the structure cause changes in the dispersion curves. Rayleigh's variational principle can be used to quantify this.

This allows one to calculate the partial or Fréchet derivatives of $c(T)$ w.r.t. changes in the model parameters:

$$\frac{\partial c(T)}{\partial \alpha(r)}, \quad \frac{\partial c(T)}{\partial \beta(r)}, \quad \frac{\partial c(T)}{\partial \rho(r)}$$

all for a given mode at a given period T

The plot from Cara shows, e.g., $\partial c/\partial \beta(r)$ for fundamental Love and Rayleigh waves for periods $T = 40, 60, 100, 180$ secs plotted vs. z/λ where λ is the wavelength.

The phase velocities are of order $c \sim 4$ km/sec, so the wavelengths λ are roughly

$$\lambda \sim 4T(\text{sec}) \text{ measured in km}$$

$\lambda \sim 80$ km for $T = 20$ s

$\lambda \sim 400$ km for $T = 100$ s

Love waves are more sensitive to shallower structure. Rayleigh waves of a given period T "see" deeper.

> Very roughly: fundamental Love waves "see" to $z \sim \lambda/4 \sim$ depth in km = period in seconds while fundamental Rayleigh waves "see" to $z \sim \lambda/2 \sim$ depth in km = twice period in seconds.

Partial derivatives very valuable, give very clear idea of sensitivity of measured data to changes in structure of $\oplus$, in this case crust + upper mantle.

Also form basis for modern inversion methods, to be discussed later.

To constrain structure at deeper depths higher mode data is very valuable. Can be seen from Fig. 3.1 from Ph. D. thesis by Guust Nolet.

See also empirical bell-tuning curves from Rossing, The Acoustics of Bells, Am. Sci., 72, 440, 1984.

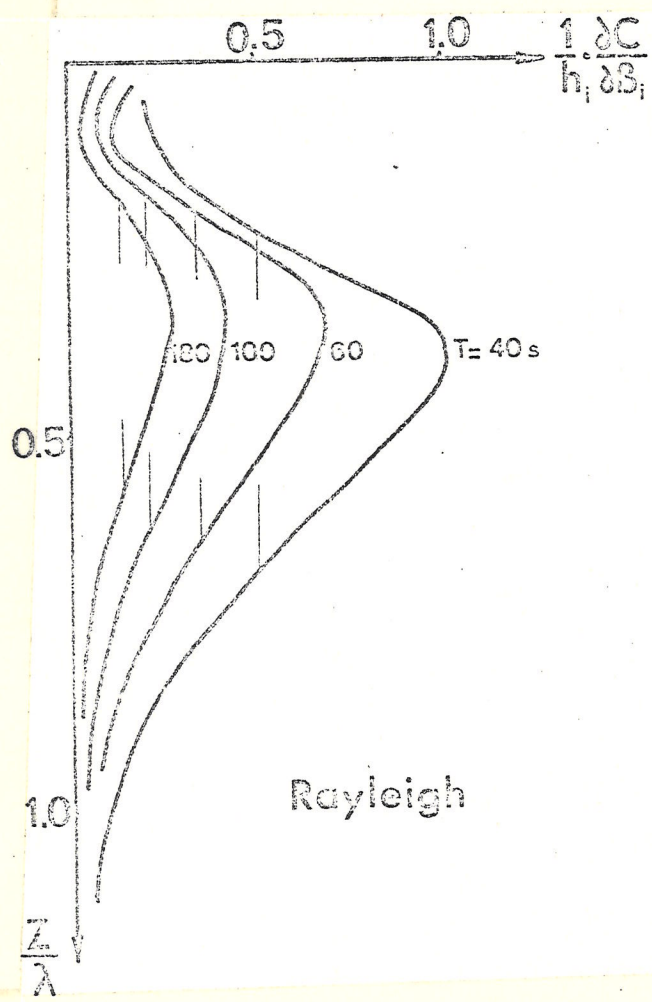
0.5
1.0
$\frac{1}{h_i}\frac{\partial C}{\partial \beta_i}$
180
100
60
T= 40 s
0.5
1.0
$\frac{Z}{\lambda}$
Rayleigh

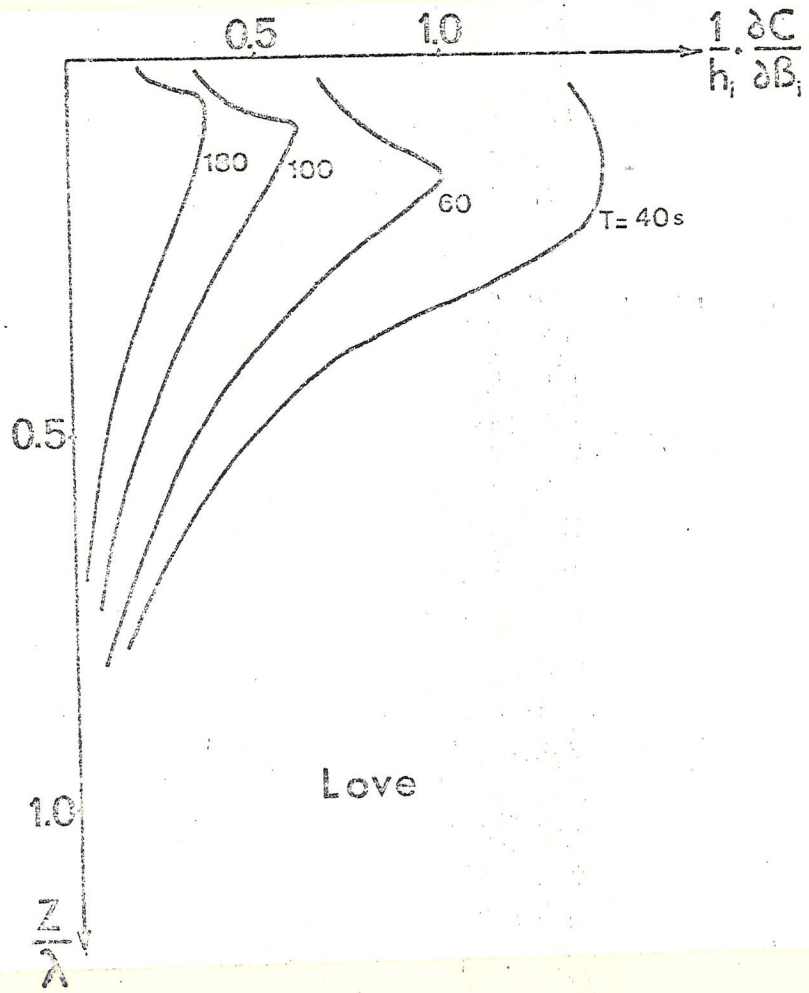
0.5
1.0
$\frac{1}{h_i}\frac{\partial C}{\partial \beta_i}$
180
100
60
T= 40 s
0.5
1.0
$\frac{Z}{\lambda}$
Love

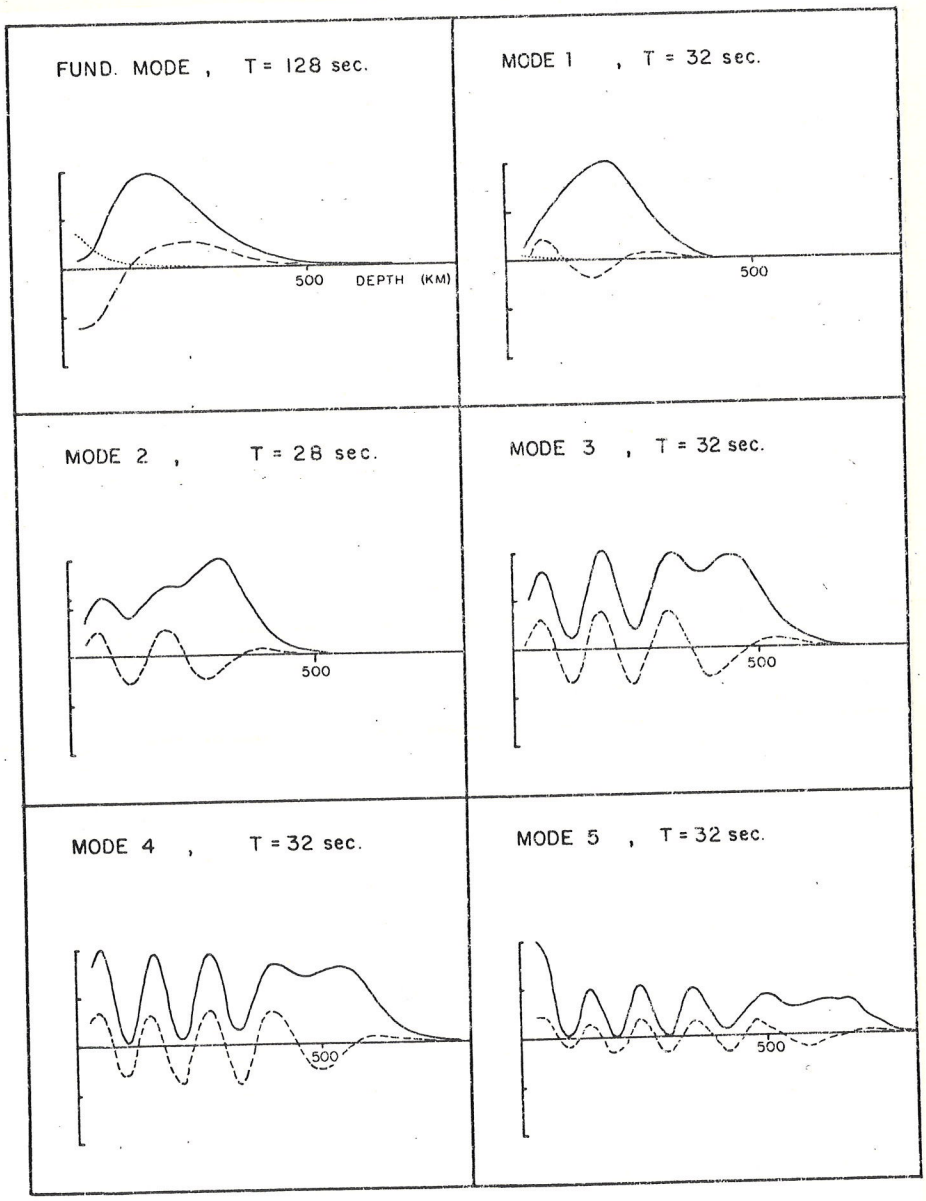

Figure 3.1 Variational parameters for the phase velocity of Rayleigh wave modes with respect to perturbations in the shear wave velocity (solid line), compressional wave velocity (dotted line) and density (broken line) as a function of depth, beneath the crust. The curves for each mode are normalized to an arbitrary scale for units km/sec resp. gr/ccm.

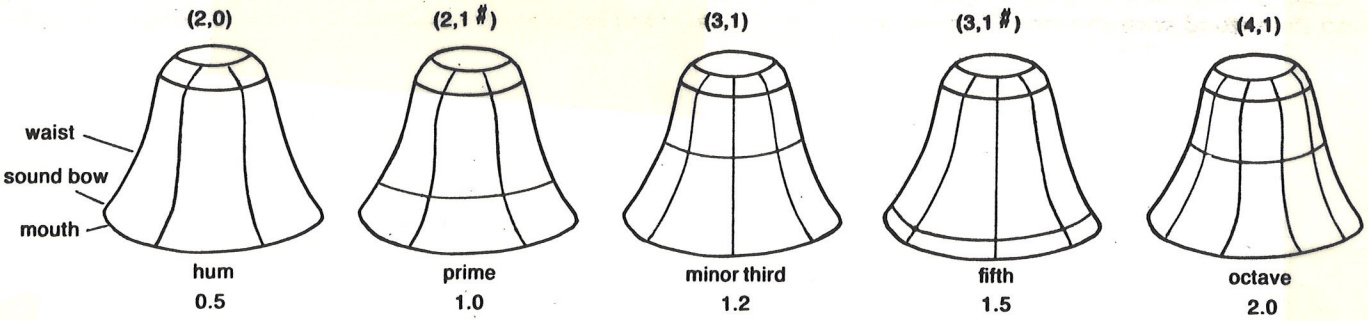

Figure 3. The nodal lines in a vibrating bell are analogous to the diameters and circles of Figure 2, and the same pair of numbers, the first for nodal meridians and the second for nodal circles, designates each mode of vibration. The first five modes of a tuned church bell or carillon bell are shown here; these modes of vibration produce the first five partials shown in Figure 1. The relative frequencies and names of these partials, which vary among bell founders of different countries, are given below each diagram.

Figure 6. After a church bell or carillon bell has been cast, the first five partials must be tuned to a harmonic sequence. The tuner uses a bell lathe, and he consults tuning curves such as those shown in Figure 7 to decide where metal should be removed from the inner surface. (Courtesy of the Dutch National Carillon Museum, Asten.)

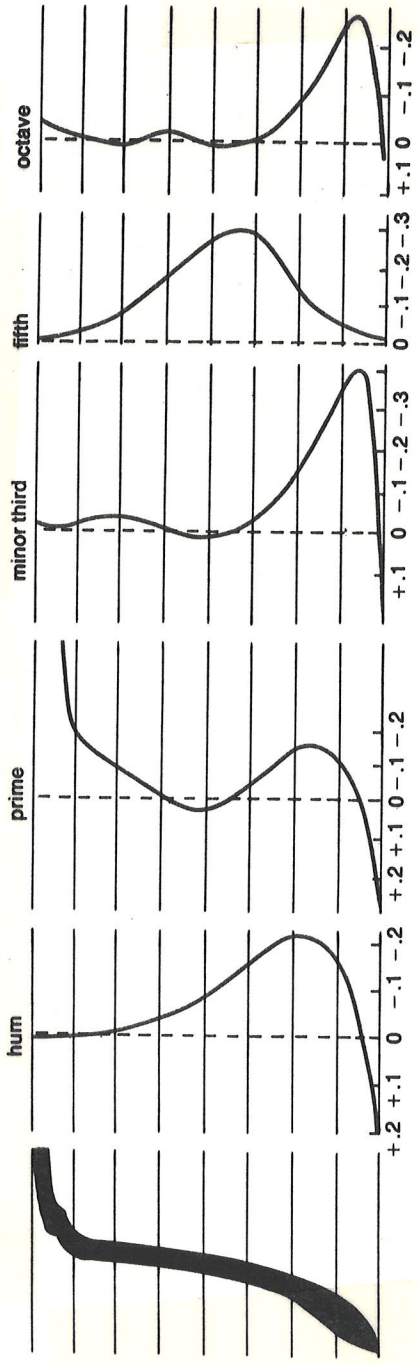

Figure 7. Bell tuning curves show how the first five partials change in frequency when metal is removed from various locations on the inside surface, which appears in cross section at the left. Removing metal from the mouth raises all five partials, whereas a little above the mouth all five are lowered, but by different amounts. Frequency changes are given in tenths of a semitone. (After van Heuven 1949.)

Look first at fundamental mode Rayleigh wave T = 128 sec:

——— $\partial c / \partial \beta(r)$ in km/s

..... $\partial c / \partial \alpha(r)$ in km/s

— — — $\partial c / \partial \rho(r)$ in gm/cm^3

Note sensitivity to $\alpha(r)$ is slight compared to $\beta(r)$, this even more true for shorter period, note "rule of thumb", sees down to about 250 km.

Other figures show partial derivatives for <u>higher mode Rayleigh waves</u>, $n = 1-5$, $T = 28-32$, much shorter period but see much deeper down to 500 km, sensitivity to $\alpha(r)$ now negligible, $\beta(r)$ dominant.

Until recently almost all work has been with fundamental.
<u>A reason</u>: shallow focus quakes are inefficient at <u>exciting</u> higher modes.
Typical shallow focus quake excites fundamental predominantly.

<u>Deep-focus quakes</u> excite very weak surface waves. Source acts essentially at <u>node</u> of motion.

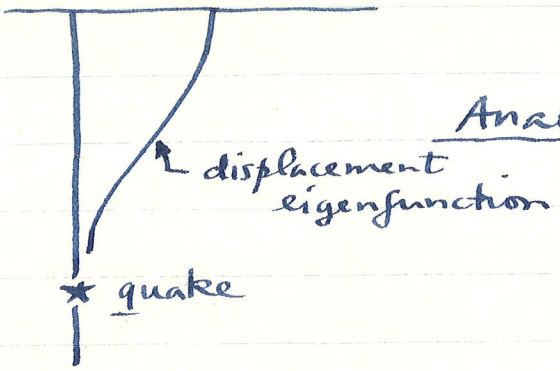

Analogy: violin string

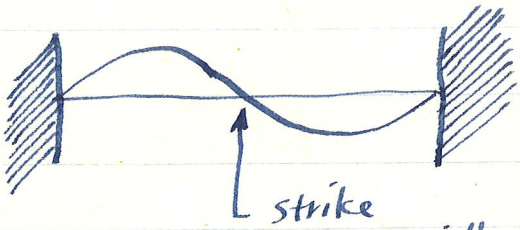

Body waves, core phases, etc. best studied using deep focus quakes, since not obscured by surface waves.

Intermediate-focus quakes most useful for studying higher modes (100-200 km depth) but even then array techniques must be used to separate them and measure their dispersion

Examples of such studies: Cara Fig. 3 employed 100-200 km deep quakes in New Hebrides, WWSSN stations in US.

Fig. 4 shows seismograms arranged in order of increasing Δ, can trace P, sP, PP, etc.

Energy arriving with apparent velocities (actually group velocities) 4.4 km/s – 3.6 km/s is combination of fundamental + higher mode Rayleigh waves, fundamental not dominant as it would be for surface focus.

Fig. 9 shows 1st higher mode filtered out by an array technique.

Fig. 8 shows c(T) measured across US for higher modes $n = 1, 2, 3$ periods $T = 20 - 100$ s.

Fig. 6.4 from Nolet's thesis shows results from similar study using events in Japan recorded by stations in Europe, fundamental Rayleigh c(T) [redacted] plus first six higher modes.

~~Note cutoff of higher modes at longer~~ ~~wavelengths~~ Higher modes are always seen at higher frequencies than

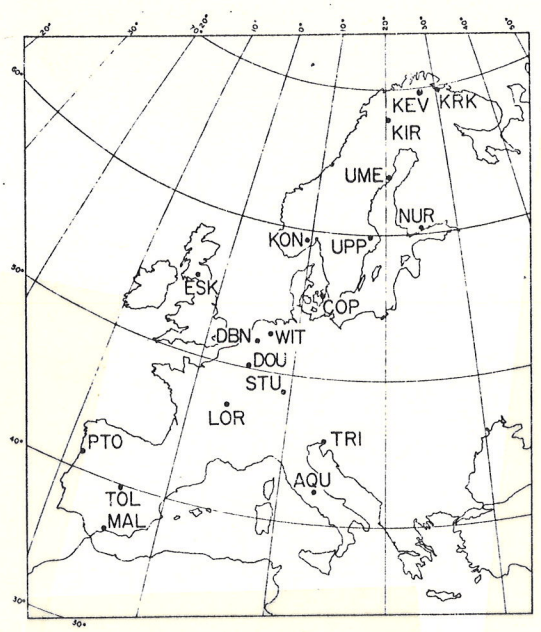

Figure 6.1
The network of long period stations

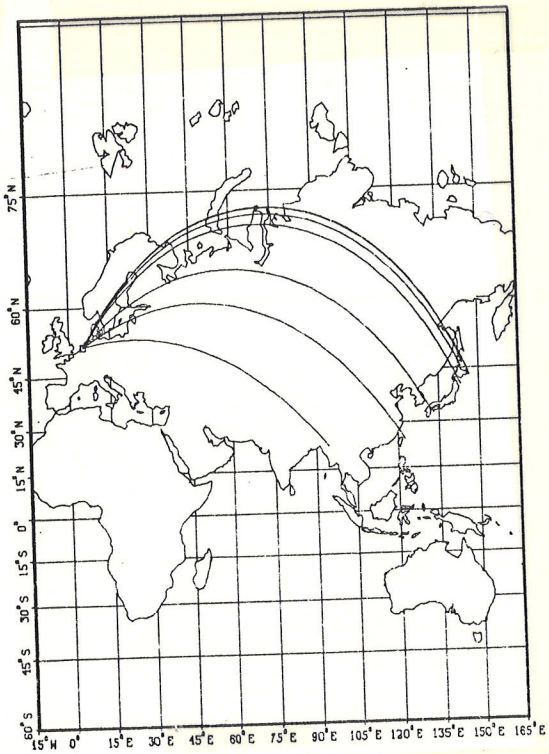

Figure 6.2
Great circle paths from the epicentres to station De Bilt (DBN). The paths for events 3 and 6, both located in Hokkaido, coincide.

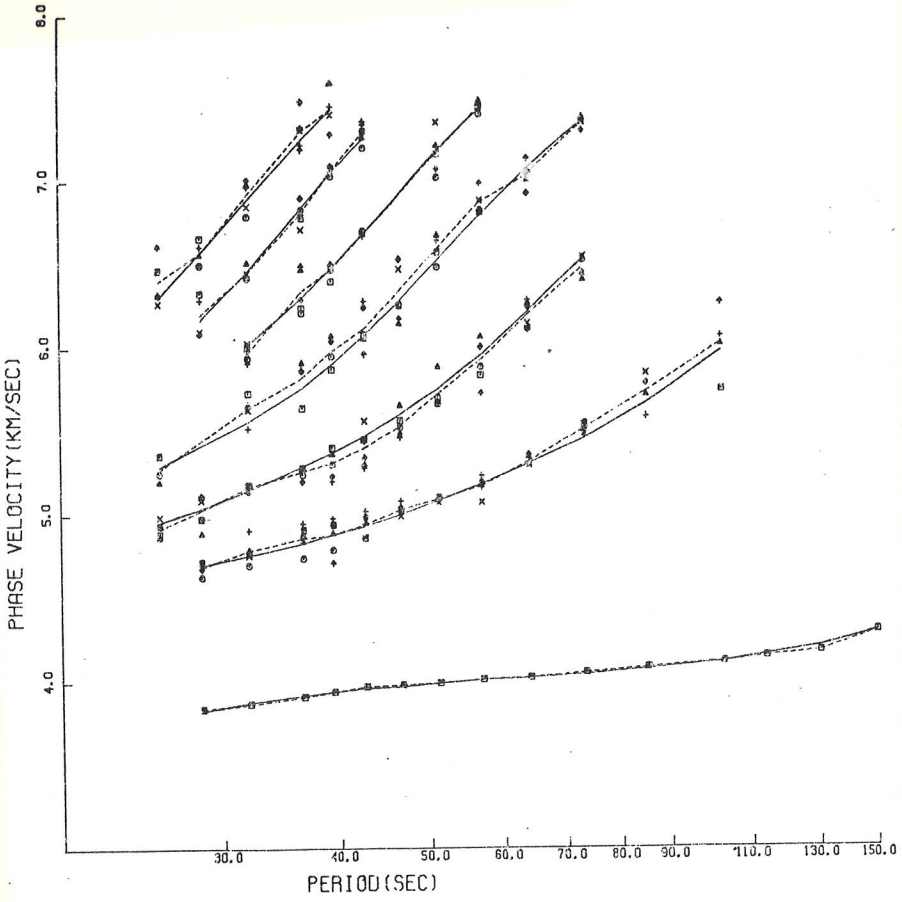

Figure 6.4 Rayleigh wave phase velocity measurements over an array of stations in W. Europe for the 7 events listed in table 6.1. The dotted line connects the average values, the solid curves represent the theoretical values for model 7. The curve for the fundamental mode is at the bottom, the curves for 6 higher modes follow in order of increasing phase velocity.

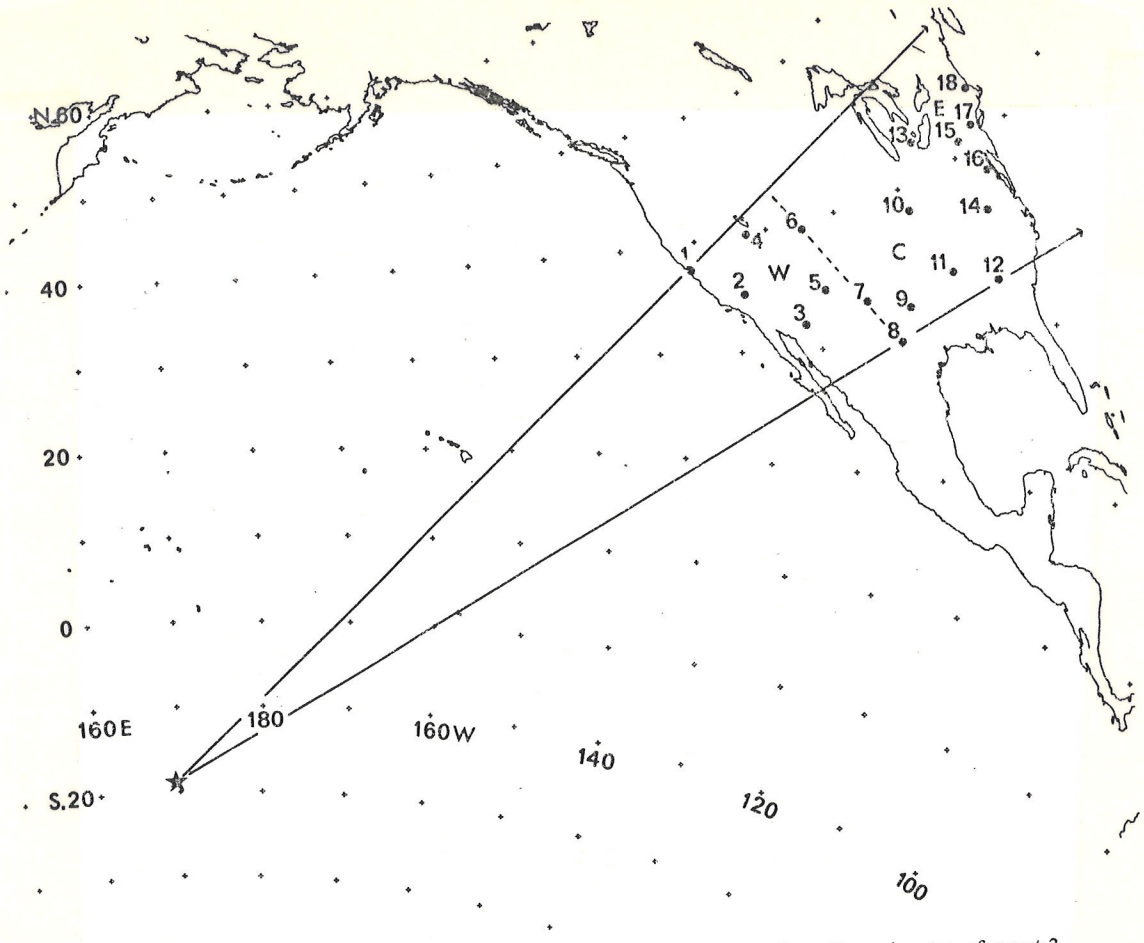

Figure 3. Location of the stations in a polar equidistant projection centred on the epicentre of event 3. The dashed line is the boundary between the western (W) and central (C) block defined in the text. The eastern block is marked by the letter E.

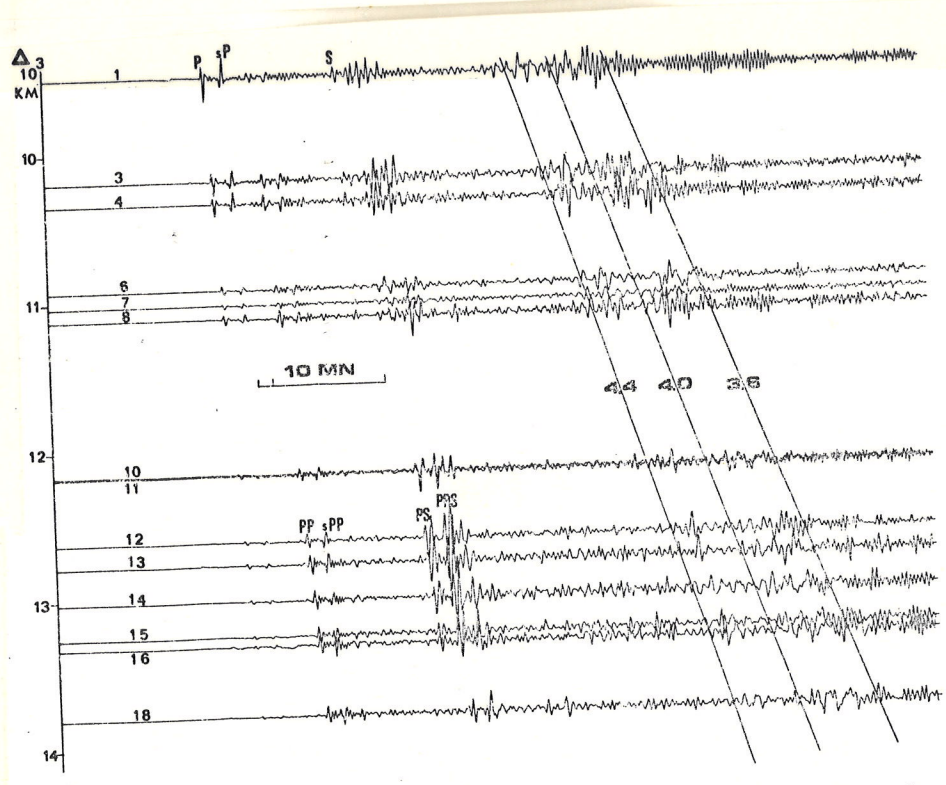

Figure 4. Vertical components for event 3 versus epicentral distance. Each record begins at the origin time of the earthquake. Arrival times corresponding to the group velocities 4.4, 4.0, 3.6 km/s are plotted. Same magnification for each record.

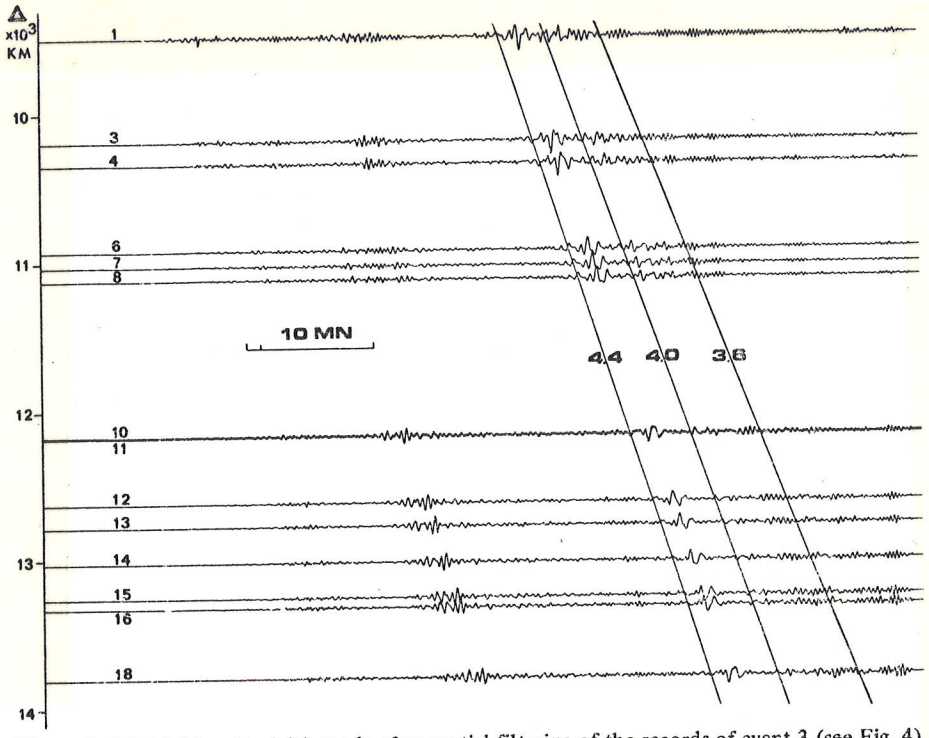

Figure 9. First higher Rayleigh mode after spatial filtering of the records of event 3 (see Fig. 4).

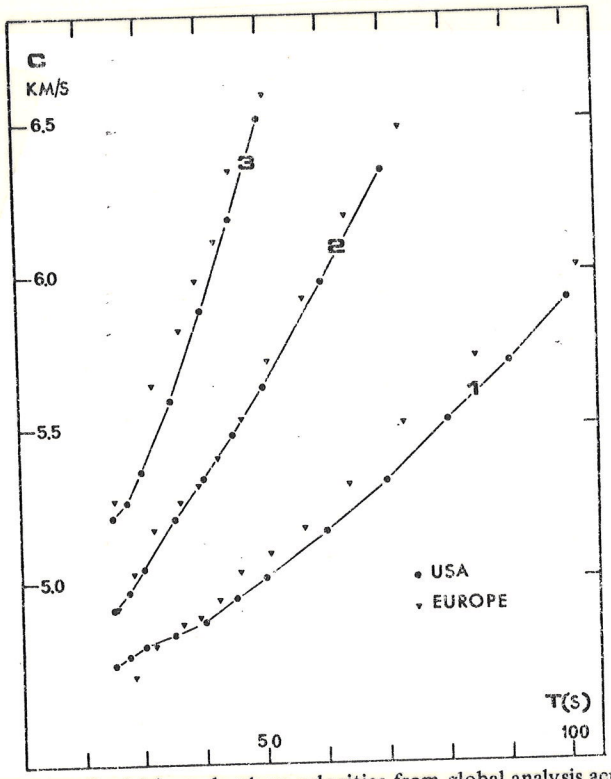

Figure 8. Three first higher Rayleigh mode phase velocities from global analysis across the United States and comparison with Nolet's results in western Europe.

fundamental. Phase velocity c(T) higher at fixed T.

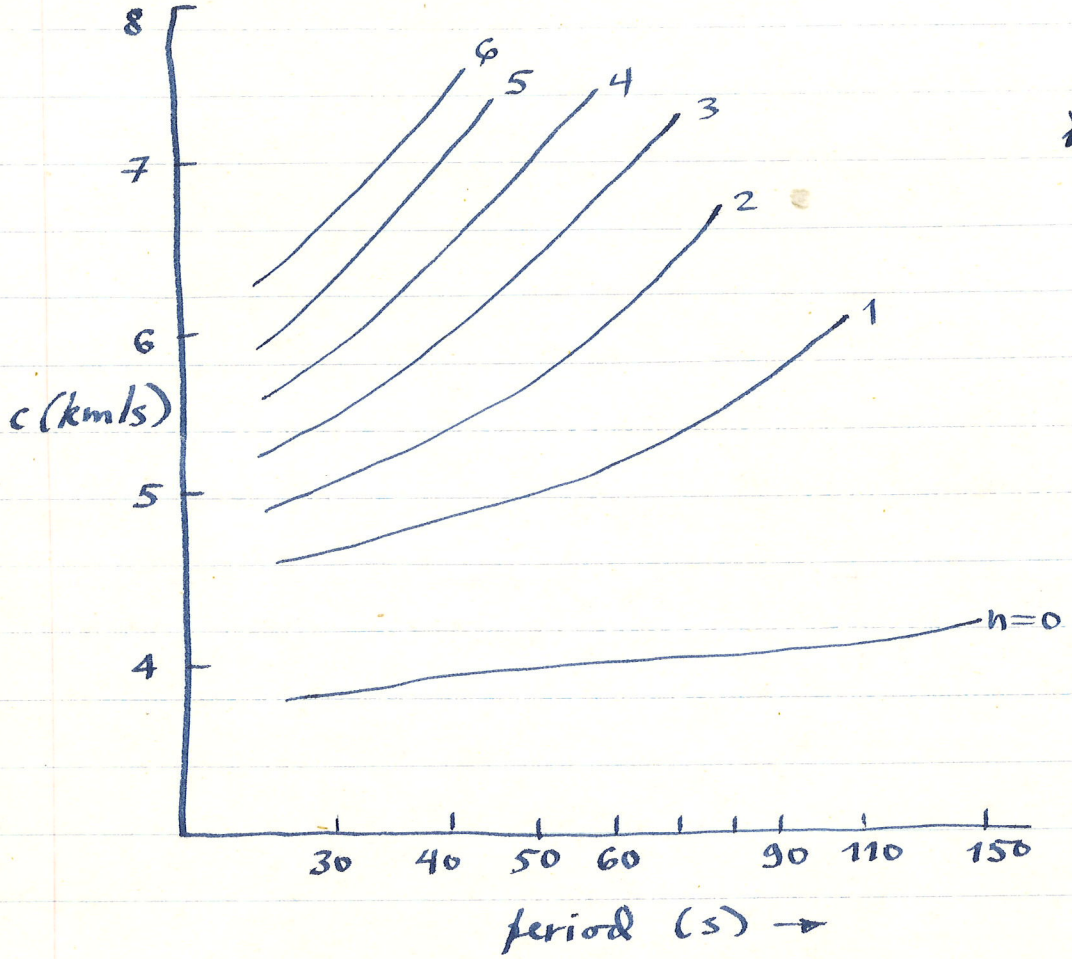

Rayleigh wave dispersion curves, phase velocity vs. period

Surface waves on a sphere: very little difference esp. for short periods, for $T \gtrsim 100$ s sphericity and self-gravitation must be taken into account for quantitative work.

[redacted]

For a flat ⊕ there is always a sharp cutoff phenomenon, corresponds to distinction between body and surface waves. Recall for simple layer over half-space, higher Love wave cutoff occurs at critical angle

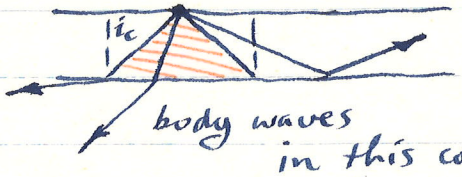

More generally for a layered structure

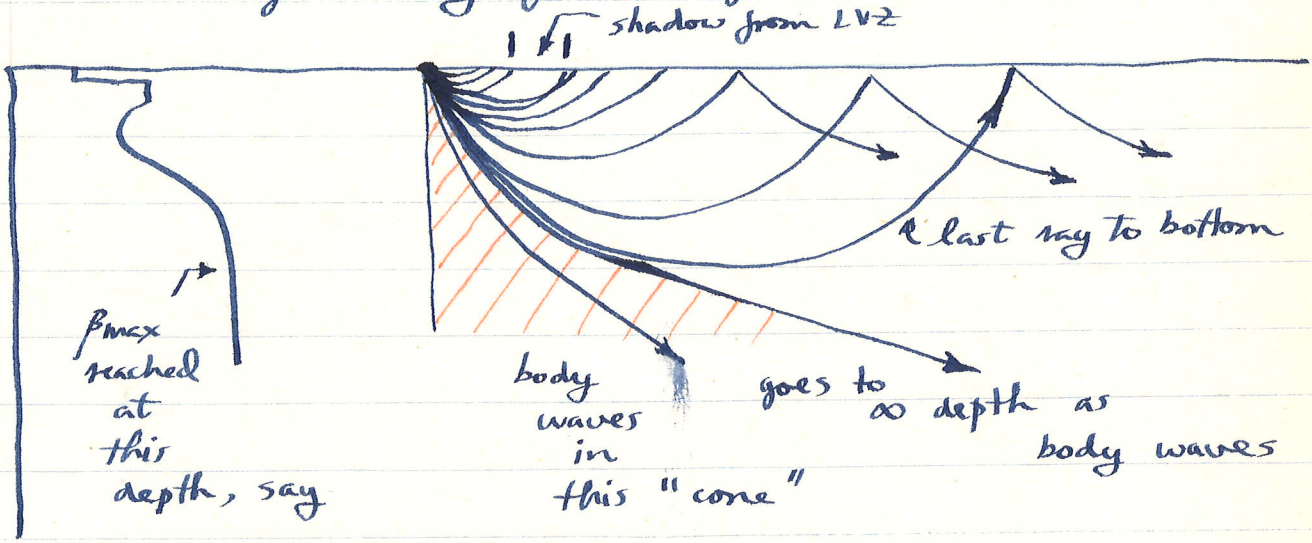

The rays which bottom interfere constructively to make surface waves. On a sphere no rays go to ∞, all emerge at some Δ, cutoff per se does not exist, merely a transition from a regime where it is convenient to study waves to one convenient to study body waves.

Amplitudes:

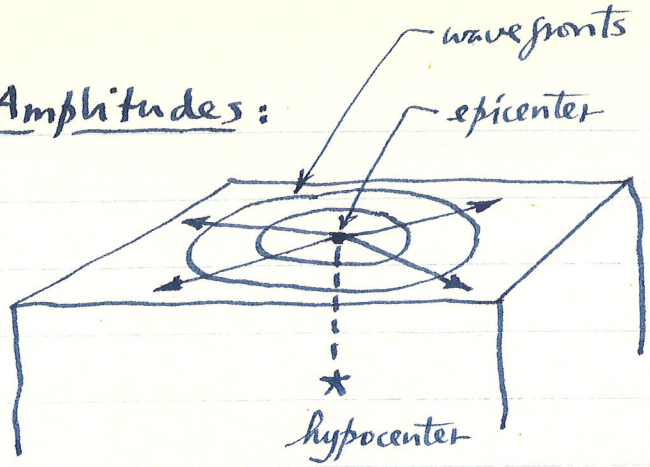

If there is a source in a half-space, surface waves spread out from source.

If D is horizontal distance from epicenter, in absence of attenuation,

$$\text{amplitude} \sim 1/\sqrt{D}$$

Reason: amplitude $\sim \sqrt{\text{energy density}}$ $\sim$ "area" (actually circumference) of circle radius D.

Surface waves $\sim \frac{1}{\sqrt{D}} \cos(kD - \omega t)$

Similarly on a sphere: geometrical attenuation $\sim 1/\sqrt{\sin\Delta}$, Δ = epicentral distance

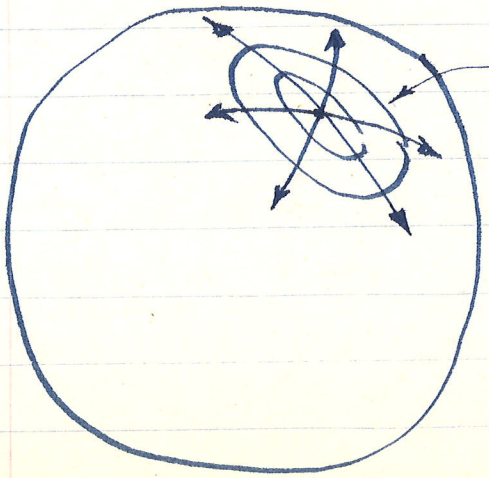

$$\text{motion} \sim \frac{1}{\sqrt{\sin\Delta}} \cos(k\Delta - \omega t)$$

Note: for a surface focus quake surface waves, esp. fundamentally, are predominant signal to arrive, generally much larger amplitude than body waves. For very weak distant events across an ocean basin 20 sec Rayleigh wave can be only visible signal (why 20 s we shall see), useful for nuclear detection problem.

Surface waves only spread out in two dimensions, body waves in three, surface waves are trapped in the third dimension. This accounts for their large amplitudes.

After a large shallow focus quake, several passages of the fundamental surface waves may be observed.

Nomenclature: R for Rayleigh, G (not L) for Love, R1 and G1 short path, etc.

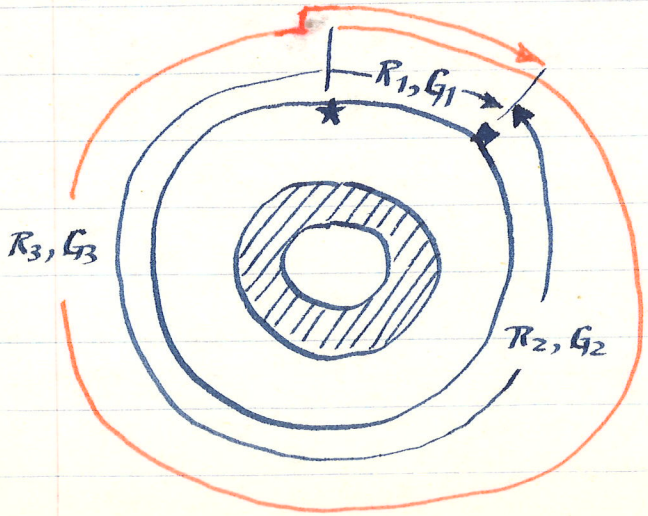

See e.g. Fig. 3a from Dziewonski and Landisman

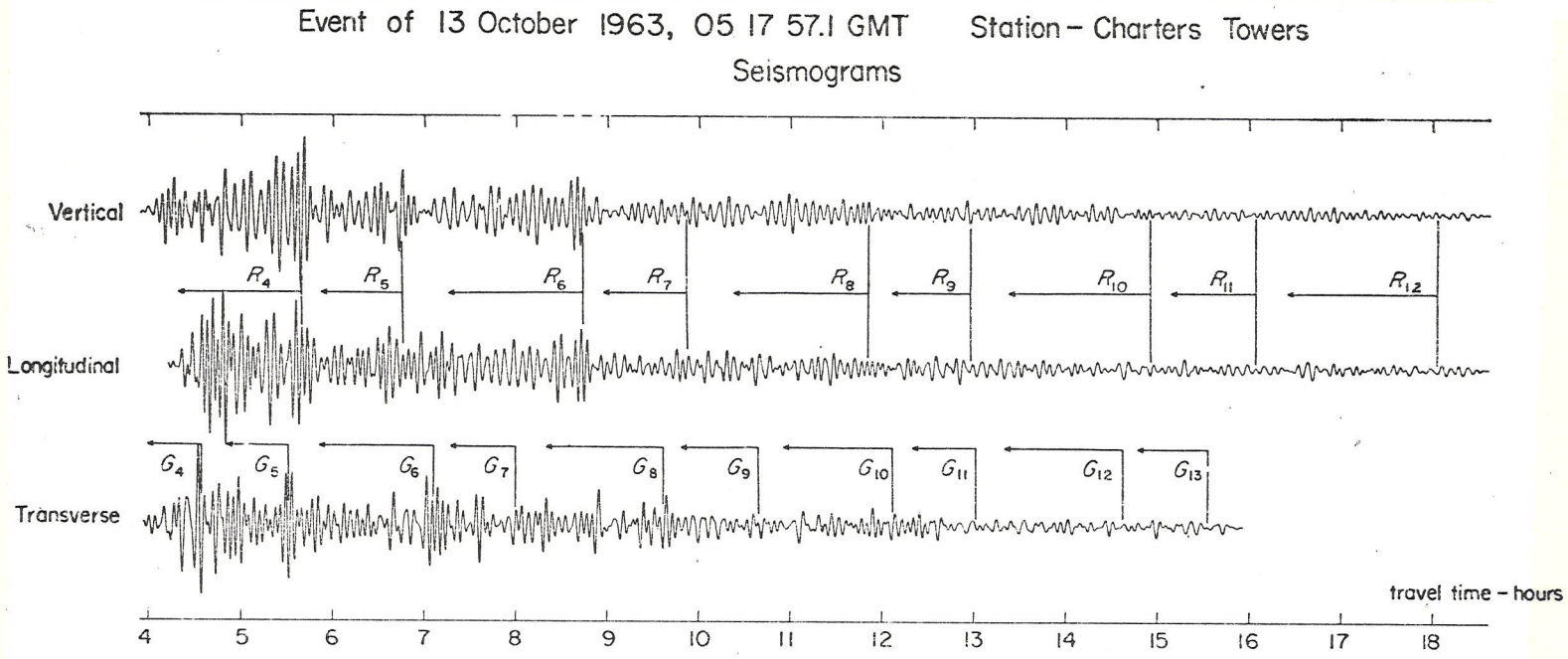

FIG. 3a. Seismograms of the Kurile Islands earthquake of 1963 October 13, 05 h 17 m 57·1 s GMT, recorded at Charters Towers, Australia. A low pass filter with a cut-off period of 150 s was applied to the seismograms before plotting, for clarity of presentation. Vertical stripes indicate the arrival of the slowest portions of wave trains of various types and order numbers.

Event $M \sim 8$ in Kurile Islands, $h \sim 60$ km recorded in CTA Australia, due south of event so EW component records SH or Love waves, vertical and NS record P-SV or Rayleigh waves. Event so large that seismometer off scale for 4 hours after quake. This record shows 4-18 hours after quake, has been low-pass filtered with cut at $T = 150$ secs, see very long-period mantle waves, periods up to $T = 500 - 600$ secs, these "see" down to 1000 - 1200 km.

Decay of successive arrivals due to finite Q_μ, can be used to study $Q_\mu(r)$.

Note: R1 and R2 arrive at same time at antipode $\Delta = 180°$, also amplitude $\sim 1/\sqrt{\sin\Delta} \to \infty$, this a failure of simple amplitude theory, in fact both source and antipode are surface wave caustics (caustic points or focal points, "degenerate" caustic surfaces)!

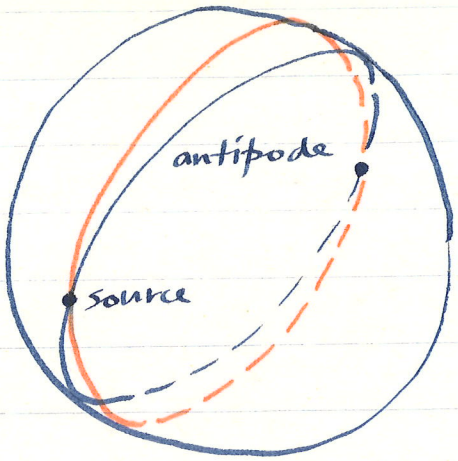

Note adjacent ray paths cross. Surface waves suffer $\pi/2$ phase advance every time they pass through antipode or source (polar phase shift).

Must be taken into account in measuring phase velocity of these long-period surface waves. First pointed out by Brune + others ~ 1960.

Did an experiment to demonstrate this effect:

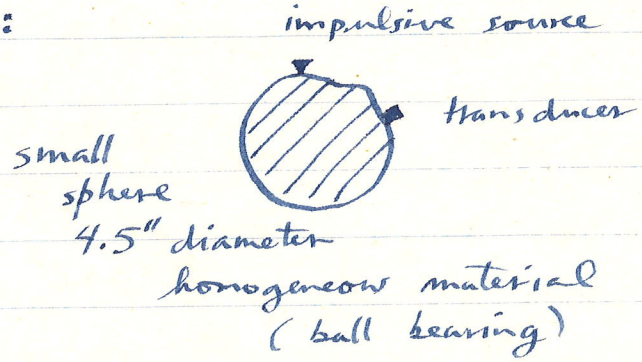

The pulses show little dispersion since homog. sphere like a half-space, but $\pi/2$ phase shifts show up clearly, R1 down, R3 up.

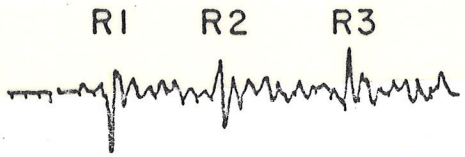

FIG. 3. Observations on a 4.46 inch diameter sphere of R_1 , R_2 , and R_3 . The phase R_3 is shifted 180° with respect to R_1 because of the polar phase shifts.

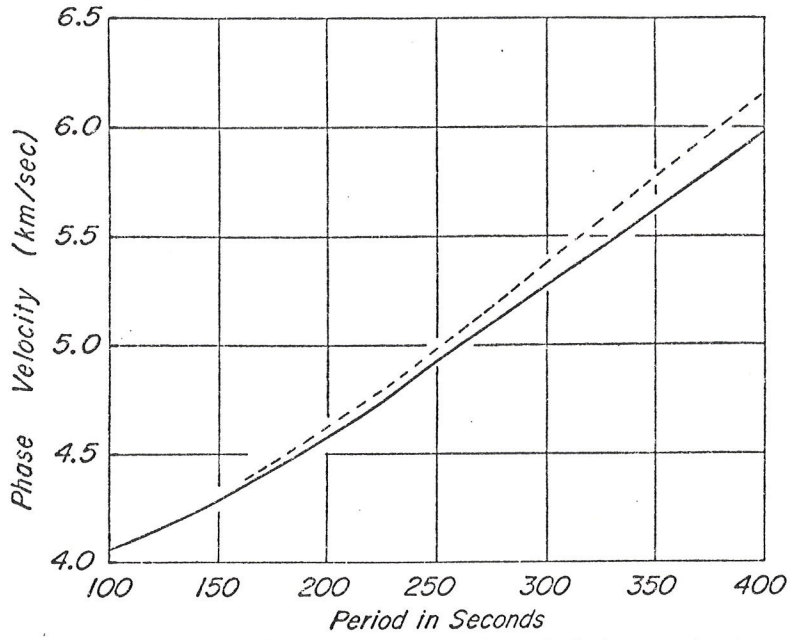

FIG. 4. Observed Rayleigh wave phase velocities. The dashed curve is the previously published result which was uncorrected for polar phase shift. The solid curve includes the polar phase shift correction.

The excitation of surface waves : group velocity.

What will surface waves look like on a seismogram?

Consider the simplest case : excitation of plane Love waves by an SH line source.

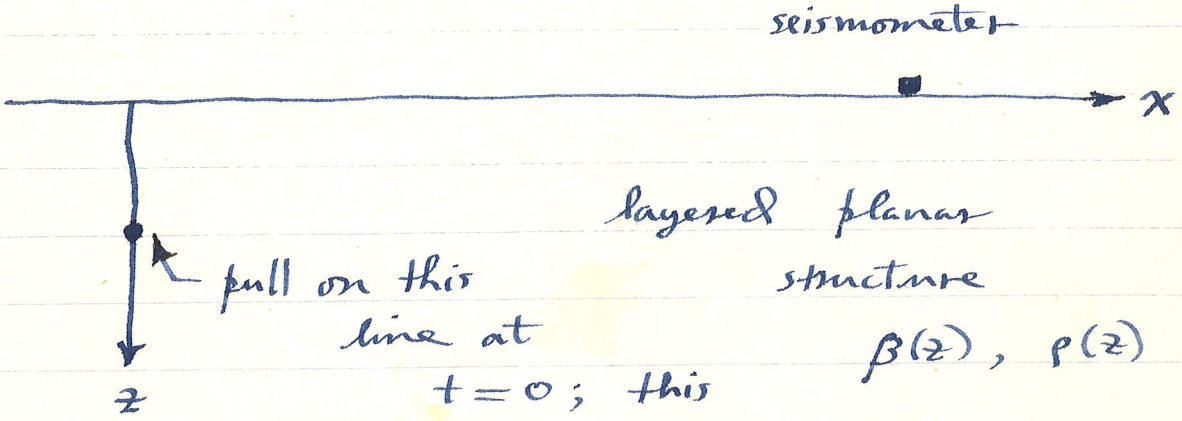

Propagation in ±x directions. All modes will in general be excited.

The surface SH displacement at point x will be of the form : denote it by $u(x,t)$

$\Rightarrow$ SH surface wave motion recorded at seismic station a distance x away.

To be specific we suppose the recorder is to the right of the source. Then

$$u(x,t) = \sum_{n=0}^{\infty} \int_0^{\infty} dk\, A_n(k) \cos[kx - \omega_n(k)t]$$

sum over all modes

excitation amplitude

frequency of nth mode

Simply a sum of propagating waves, all modes and all wavenumbers.
We shall consider each mode separately. For shallow focus quake fundamental mode dominates.
Let us drop n, from now on $n = 0$ will be understood although analysis applies to others as well.

$$u(x,t) = \int_0^{\infty} dk\, A(k) \cos[kx - \omega(k)t]$$

Sum over all wavenumbers, each of different amplitude $A(k)$. Emphasize the sum over wave of all different wavenumbers
Excitation amplitude depends on source

(source depth, time function, etc.)
We have assumed source is such that the amplitudes $A(k)$ are <u>real</u>. In general in seismology they need not be (waves of different wavenumbers leave the source with different phases). More generally then:

$$u(x,t) = \mathrm{Re} \int_0^\infty dk\ A(k)\ e^{i[kx - \omega(k)t]}$$

Say <u>x is large</u> (far from the source and we seek the solution for <u>large t</u> (with x/t fixed)

Rewrite the above as:

$$u(x,t) = \mathrm{Re} \int_0^\infty dk\ A(k)\ e^{it\phi(k)}$$

(t: large)

$$\phi(k) = k\frac{x}{t} - \omega(k)$$

($\frac{x}{t}$: fixed)

$\exists$ a general method for the asymptotic

evaluation of such integrals, Kelvin's method of stationary phase.

Provides great insight into propagation of dispersive waves, leads to concept of group velocity.

Another point of view: consider $t=0$

$$u(x,0) = \mathrm{Re} \int_0^\infty dk\, A(k)\, e^{ikx}$$

↑ this is the initial state

By Fourier transform inversion can be shown that

$$\frac{1}{4\pi} A(k) = \int_{-\infty}^{\infty} u(x,0)\, e^{-ikx}\, dx$$

Thus amplitude $A(k)$ is a constant times F.T. of initial displacement. We seek the evolution of this initial state as disturbance propagates away from source. If $u(x,0)$ is localized near $x=0$ then by the uncertainty principle $A(k)$ will be broad and smooth.

Our argument heuristic but can be made rigorous.

Consider the integrand as a function of k:

$$A(k)\, e^{it\phi(k)}$$

↖ product of two terms

Both $A(k)$ and $\phi(k) = k\frac{x}{t} - \omega(k)$ will be broad and smooth, e.g.

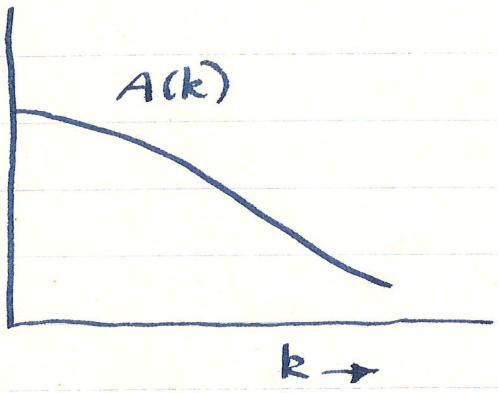

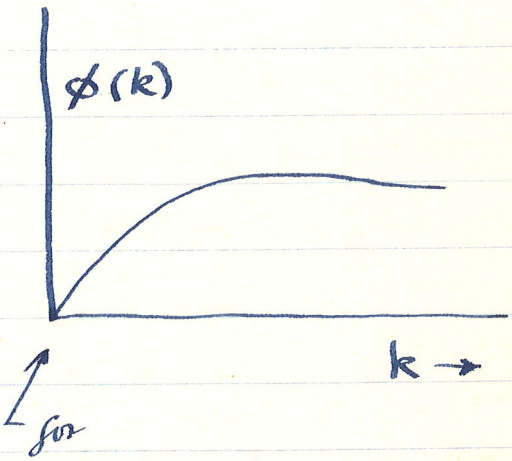

↖ for fundamental

$\omega(0) = 0$ so $\phi(0) = 0$

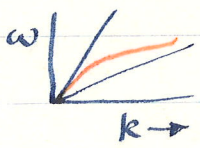

Actually, our $\phi(k)$ looks more like

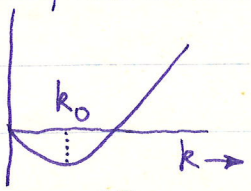

But $e^{it\phi(k)} = \cos t\phi(k) + i\sin t\phi(k)$

for t large will be very wiggly, e.g.

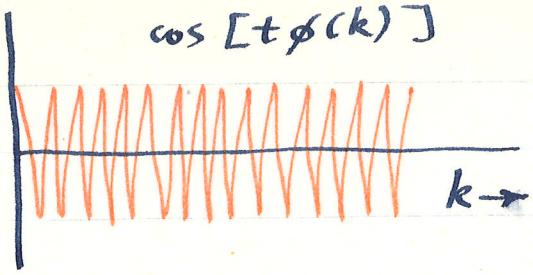

The integrand is the product $A(k) \cos[t\phi(k)]$

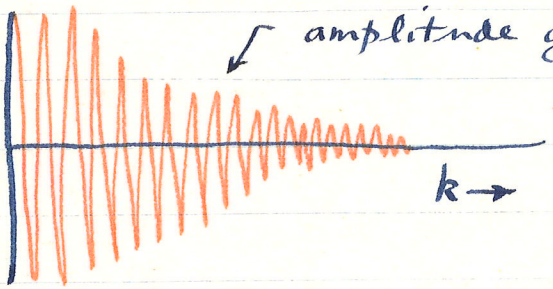

The contributions to the integral oscillate from + to − very rapidly. There is little net contribution.

The maximum contribution comes from so-called points of stationary phase where

$$\boxed{d\phi(k)/dk = 0}$$

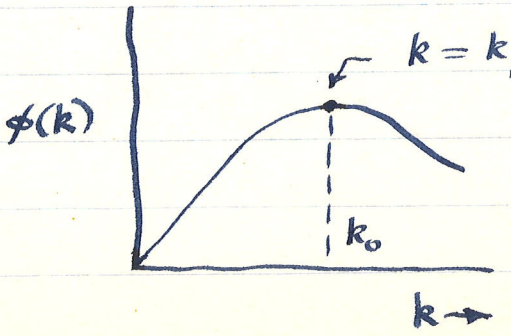

In the nbhd of k_0, $\phi(k)$ changes slowly as k changes.

Thus $\cos[t\phi(k)]$ looks like this:

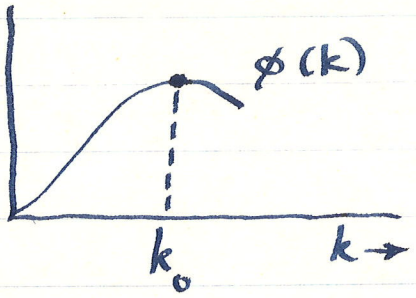

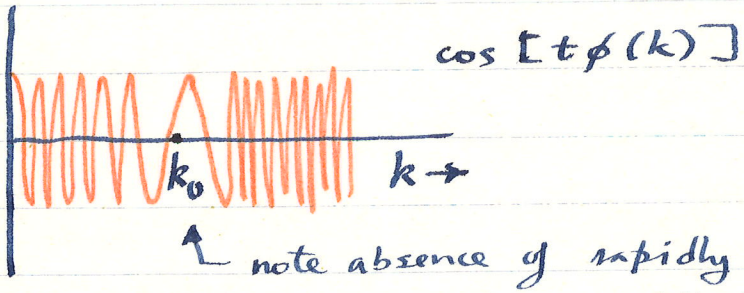

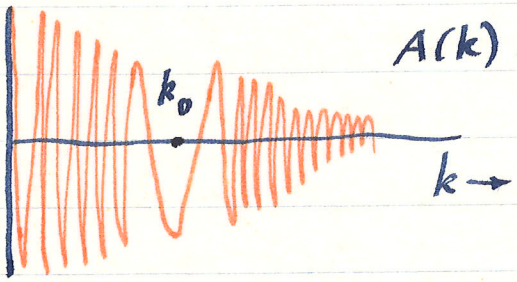

In limit of large t integral gets its dominant contribution from vicinity of k_0.

What are the points of stationary phase in our case?

$$d\phi(k)/dk = 0 = \frac{x}{t} - \frac{d\omega(k)}{dk}$$

We first plot the phase $xh(\omega)$ versus ω in Fig. 1.24(a) in the vicinity of a maximum or stationary point of $h(\omega)$. Fig. 1.24(b) shows that for ω in the vicinity of the maximum, $\cos xh(\omega)$ oscillates slowly whereas for ω away from the stationary point, there are many oscillation for small changes in ω. Fig. 1.24(c) shows the resulting behaviour of $\cos xh(\omega)$. The necessity for having x large should be apparent from Fig. 1.24(a). Large x accentuates the

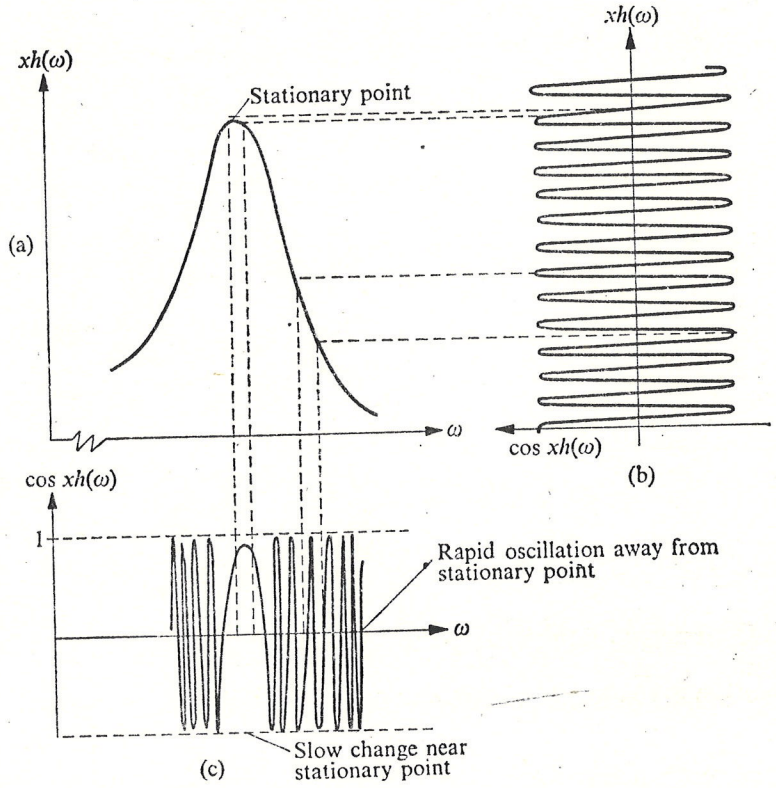

FIG. 1.24. The behaviour of $\cos xh(\omega)$ near a stationary point of $h(\omega)$.

maximum of $h(\omega)$ which increases the oscillatory nature of $\cos xh(\omega)$ away from the critical point.

To evaluate (1.6.22), making use of the ideas just described, we first expand $h(\omega)$ about ω_0. This gives

$$h(\omega) = h(\omega_0)+h'(\omega_0)(\omega-\omega_0)+(\tfrac{1}{2})h''(\omega_0)(\omega-\omega_0)^2+\ldots. \qquad (1.6.25)$$

If ω_0 is a stationary point, then $h'(\omega_0) = 0$ and the phase is given by

$$xh(\omega) \cong x\{h(\omega_0)+(\tfrac{1}{2})h''(\omega_0)(\omega-\omega_0)^2\}, \qquad (1.6.26)$$

Stationary phase points are defined by:

$$x = \frac{d\omega(k)}{dk}\, t$$

Recall $\omega(k)$ looks like:

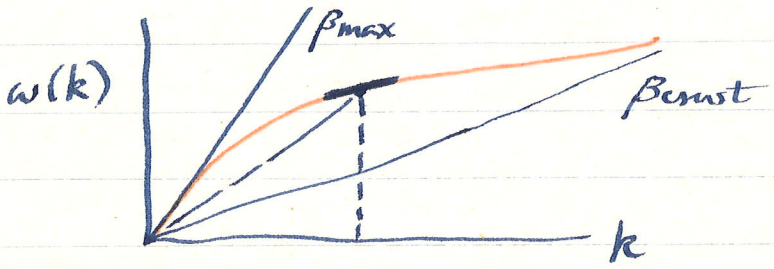

At a given k, $\frac{d\omega}{dk}$ is slope of dispersion curve, called the group velocity. Recall $c(k) = \omega(k)/k$ the phase velocity is slope of straight line from origin to point.

Group velocity vs. k tends to look like

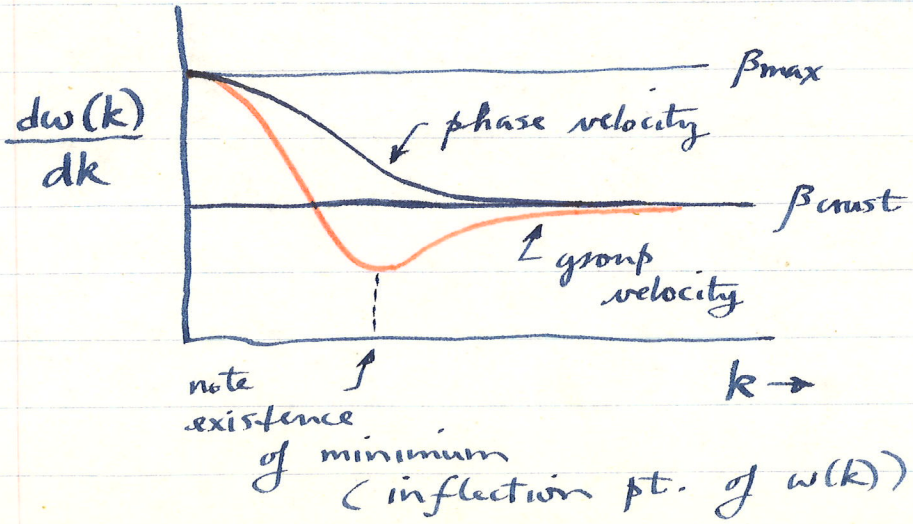

For a given value of x/t $\exists$ <u>one or two or no</u> stationary phase points

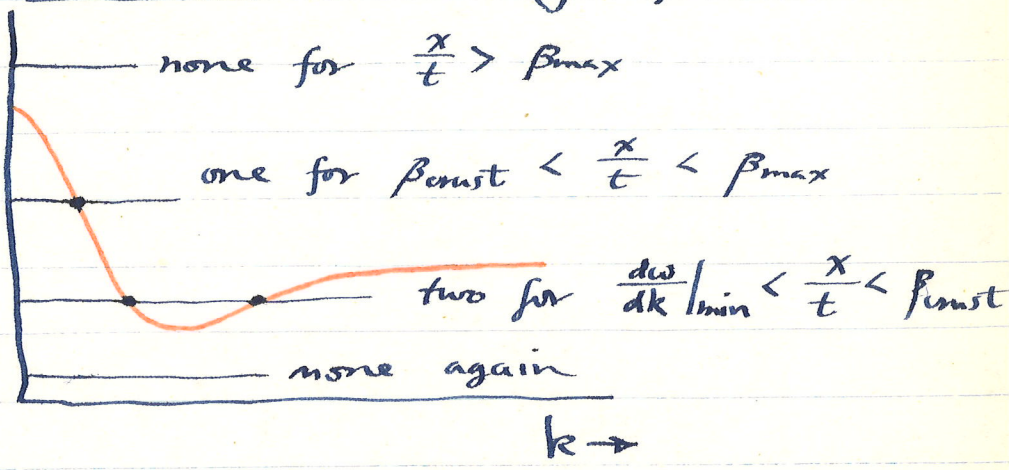

This has implications as we shall see.

In the vicinity of every stationary phase pt. k_0 we expand $A(k)$ and $\phi(k)$ in <u>Taylor series</u>:

$$\phi(k) = \phi(k_0) + \cancel{\phi'(k_0)}\,(k-k_0) + \frac{1}{2}\phi''(k_0)(k-k_0)^2 + \cdots$$

(zero at k_0 by defn)

$$A(k) = A(k_0) + \cdots$$

To find <u>dominant</u> contribution we ignore ....

Note: at minimum $\phi''(k_0) = \frac{d}{dk}\left(\frac{x}{t} - \omega'\right)\Big|_{k_0}$

$= -\omega''(k_0)$. The term we "keep" before .... is zero, must instead keep next term. This point and its vicinity thus deserve special attention.

Substituting in:

$$u(x,t) \approx \mathrm{Re} \sum_{k_0} \int_0^\infty dk\, A(k_0)\, e^{it[\phi(k_0)+\frac{1}{2}\phi''(k_0)(k-k_0)^2 - \ldots]}$$

sum over all possible stationary phase pts

this is $e^{i[k_0 x - \omega(k_0)t]}$

$$= \mathrm{Re} \sum_{k_0} A(k_0)\, e^{it\phi(k_0)} \cdot \int_0^\infty dk\, e^{\frac{1}{2}it\phi''(k_0)(k-k_0)^2}$$

this integral depends on k only here, it is readily evaluated

The <u>error integral</u> is given by

$$\int_{-\infty}^{\infty} e^{-\alpha x^2}\, dx = \sqrt{\frac{\pi}{\alpha}}$$

Our integral gets its dominant contribution

from $k \sim k_0$ so the lower limit can be replaced by $-\infty$ with little error. Thus must evaluate

$$\int_{-\infty}^{\infty} dk\ e^{-\frac{1}{2} i t \omega''(k_0)(k-k_0)^2}$$

↑ we've replaced $\phi''(k_0)$ by $-\omega''(k_0)$.

In our case

$$\alpha = \tfrac{1}{2} t\, |\omega''(k_0)|\, e^{-i\pi/2 \operatorname{sgn} \omega''(k_0)}$$

"sign fcn": $\operatorname{sgn} = \begin{cases} +1 & \text{if positive} \\ -1 & \text{if negative} \end{cases}$

We get the final result

$$u(x,t) \approx \operatorname{Re} \sum_{k_0} A(k_0) \left[2\pi / t\, |\omega''(k_0)| \right]^{1/2}$$

$$\exp i \left[k_0 x - \omega(k_0) t - \frac{\pi}{4} \operatorname{sgn} \omega''(k_0) \right]$$

↑ this is just a phase shift of $\pm \pi/4$

sum over all <u>stationary</u> phase pts. k_0

Maybe just write as $\pm \pi/4$

The signal at x, t, which is actually a superposition of many waves of different wavenumbers looks like (at any instant) a single wave (or maybe two) with wavenumber k_0.

Recall that dw/dk looks roughly like

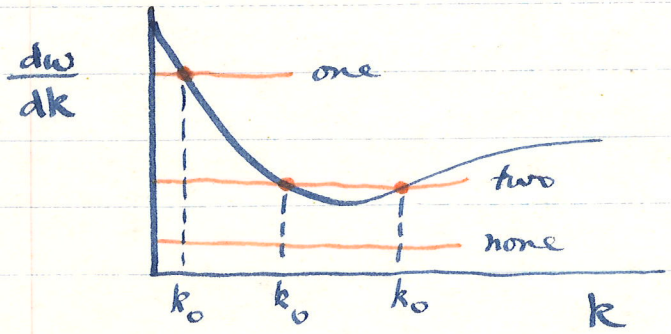

Recall k_0 is defined by:

$$\boxed{x = \omega'(k_0)\,t = \left[\frac{dw}{dk}\Big|_{k_0}\right] t}$$

At time t waves of wavenumber k_0 and frequency $\omega(k_0)$ are found at position $x = \omega'(k_0)\,t$.

Thus $\omega'(k_0)$ is the velocity of that position which always contains waves of wavenumber k_0. A group of waves with that wavenumber will be

observed to travel with velocity $w'(k_0)$, called the group velocity.

Any individual wave crest or trough within the group still travels with the phase velocity $c(k_0) = w(k_0)/k_0$. But the position that always contains waves of wavenumber k_0 moves with the group velocity. If $c(k_0)$ and $w(k_0)$ are different (they are only the same in the absence of dispersion) then a given wave crest must change its wavelength as it moves.

To measure phase velocity requires an array of stations. One must be able to observe a single phase move across the array. One thus measures the phase velocity under the array.

Now what will a surface wave seismogram look like? It is

$$u(x_{fixed}, t).$$

It will look like the passage of a

wavetrain with a variable frequency. The frequency of waves arriving at time t will be $\omega(k_0)$ where $\omega'(k_0) = \frac{x}{t}$.

For a simple 1-layer Love waveguide:

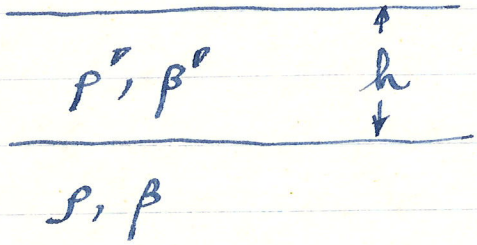

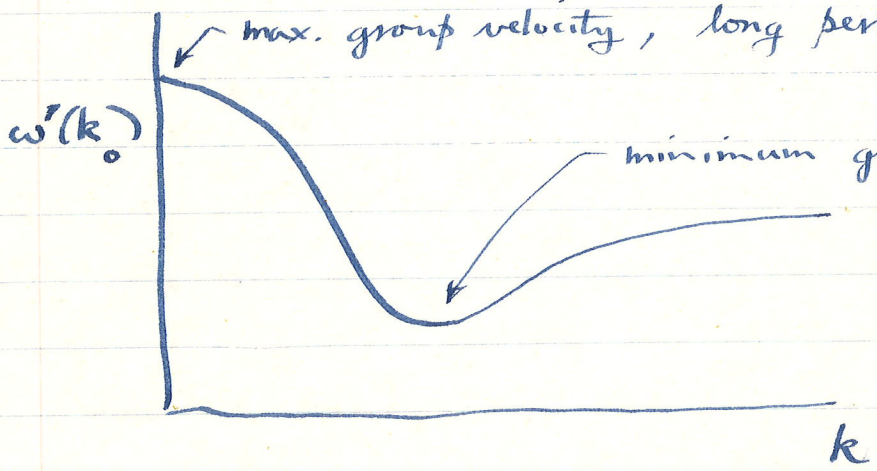

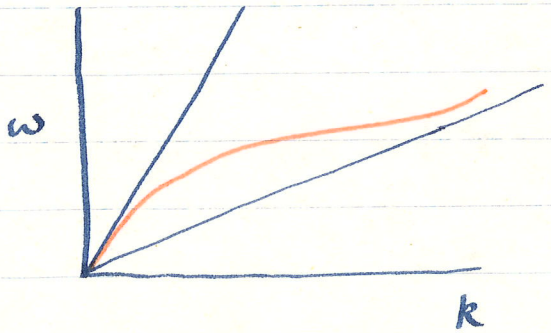

Long wavelength long period waves arrive first. They "see" deeper into the

higher velocity structure and as a result travel faster.

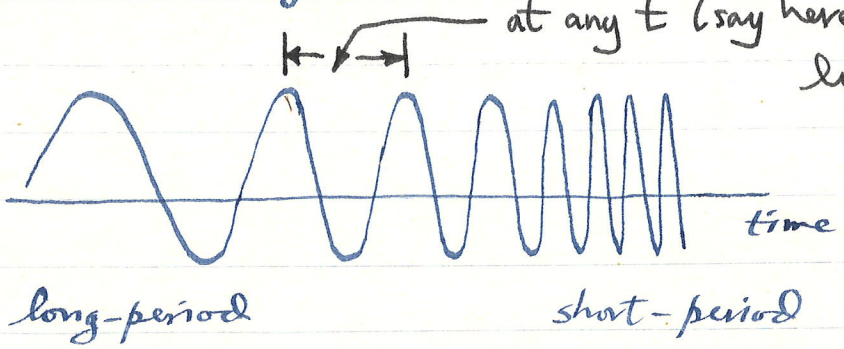

This is typical of seismic surface wave dispersion in the 10–40 sec range, these are the dominant signals from the majority of earthquakes, $M = 5-7$, intermediate in size.

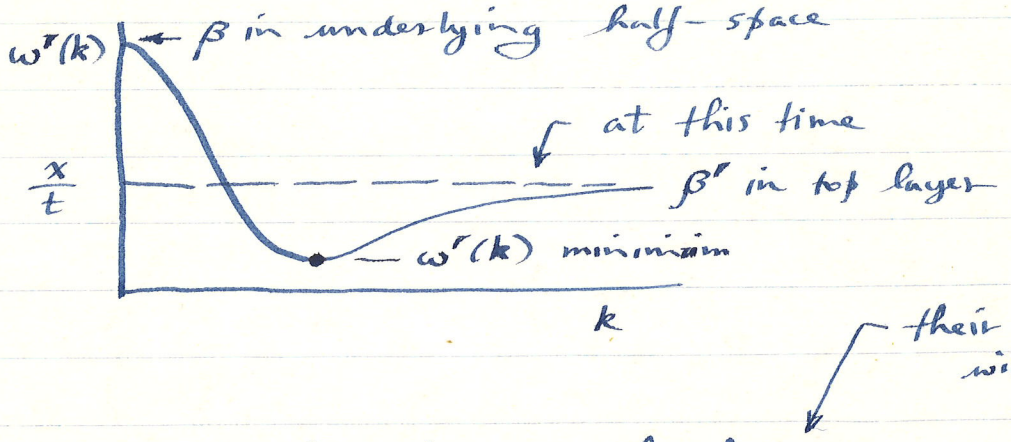

At the time shown high frequency waves should start to arrive superimposed on the lower frequency waves. In practice these are seldom seen partly because they are heavily damped and scattered, partly because of the limited passbands of seismometers (long-

period WWSSN peaks ~ 20 sec period, one of the reasons for the predominance of 20 s surface waves). Another reason discussed below.

The last surface waves to arrive: both high and low frequencies merge into a so-called Airy phase at group velocity minimum.

Our theory predicts amplitude ~ $|\omega''(k_0)|^{-1/2}$, infinite at group velocity minimum, theory breaks down, must consider next term in Taylor series, first done by Airy, leads to so-called Airy function

$$Ai(x) = \frac{1}{\pi}\int_0^\infty \cos\left(xt + \frac{1}{3}t^3\right) dt$$

t^3 from next term in Taylor series

Principal result: amplitudes are enhanced at the Airy phase, as the divergence of our theory suggests.

An application where all the above phenomena can be seen easily:

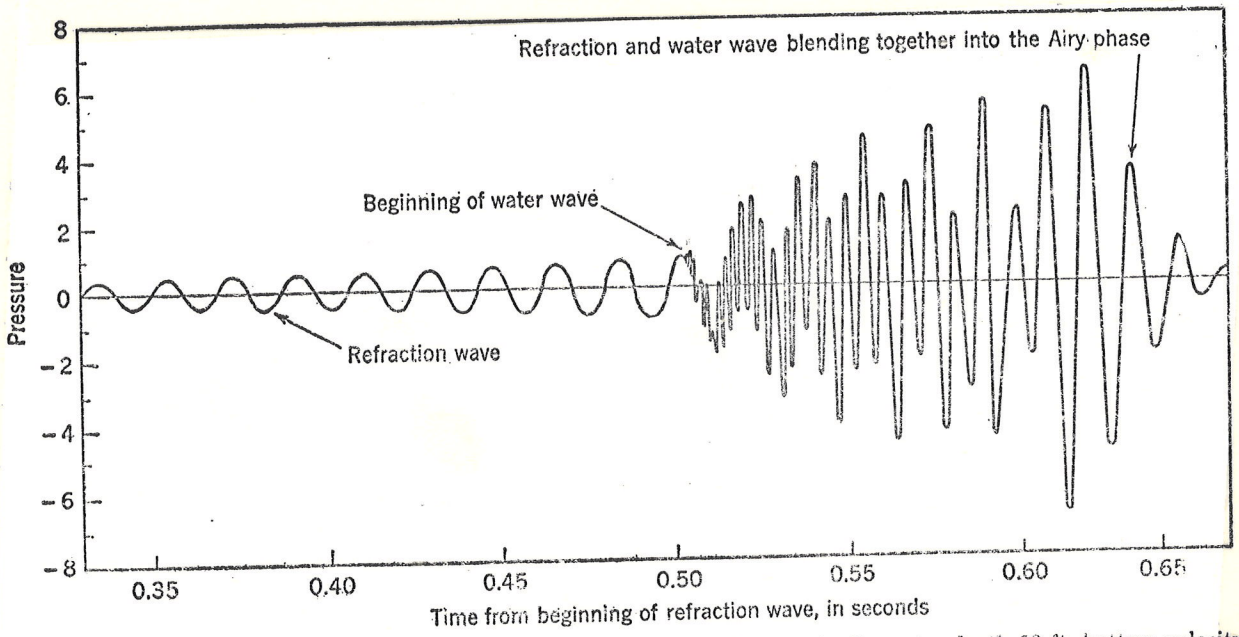

FIG. 4–13. Theoretical wave motion in first mode for range 460 times water depth, water depth 60 ft, bottom velocity 1.1 times velocity in water, density 2.0, charge weight 5 lb. (*After Pekeris.*)

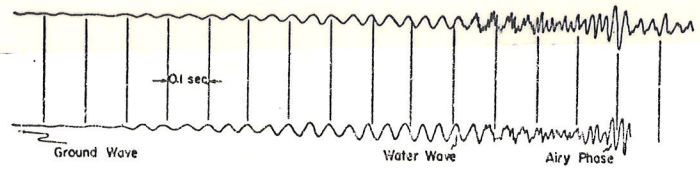

FIG. 4–12. Waves (through two different filters) from an explosive charge of 55 lb observed at a range of 1,030 times water depth, water depth = 90 ft. Bottom sediment thickness = 220 ft, bottom sound velocity = 1.13 times velocity in water. Source and receiver in water. (*Courtesy of C. L. Drake.*)

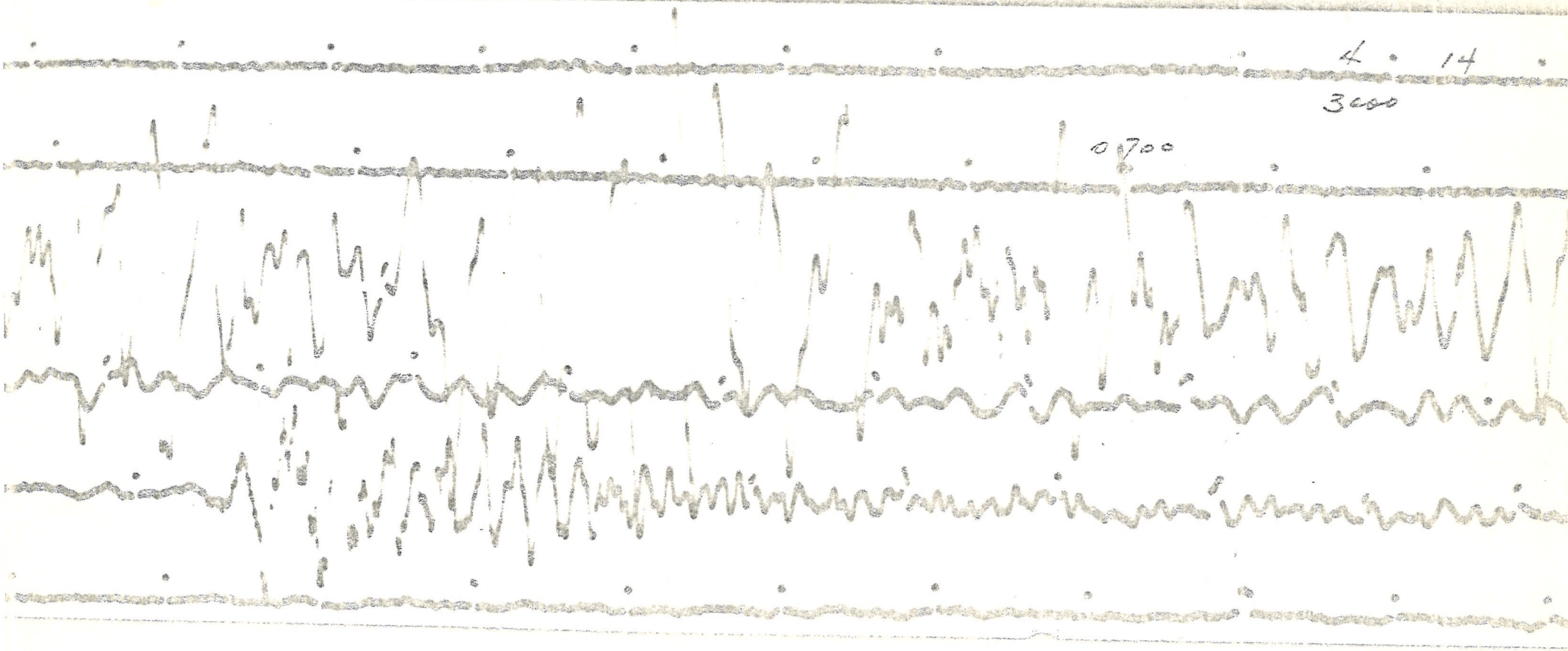
4 . 14
3000
0700

explosions in shallow water, the surface waves are Rayleigh, not Love waves.

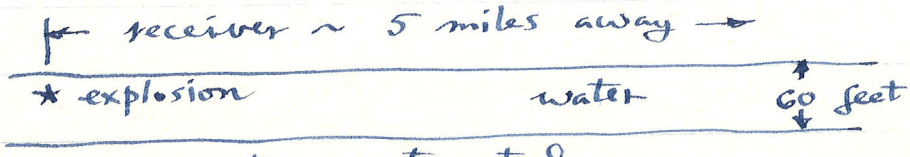

water-saturated sediments, can be modelled as a fluid.

Fig. 4-13 from EJP shows a synthetic seismogram (after Pekeris) for the above geometry.

Some data from an experiment with similar geometry shown in Fig. 4-12, the onset of the high frequency waves with group velocity = speed of sound in H_2O is clear as is the enhanced amplitude of the Airy phase.

One of the seismograms from the lab exercise shows a similar phenomenon, station BAG, a local submarine quake near Luzon, the geometry is presumably something like:

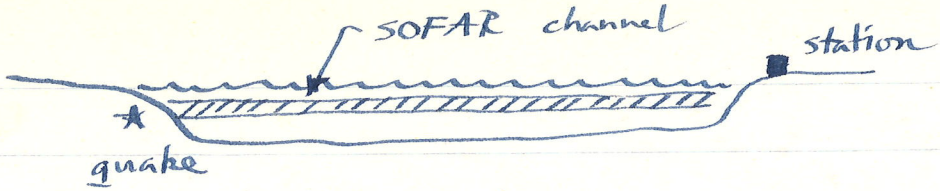

The high-frequency water wave superimposed on the P wave is clearly visible, called a T phase, most easily seen when quake occurs at same depth as SOFAR channel, this traps high-frequency energy and it propagates to long distances with little attenuation.

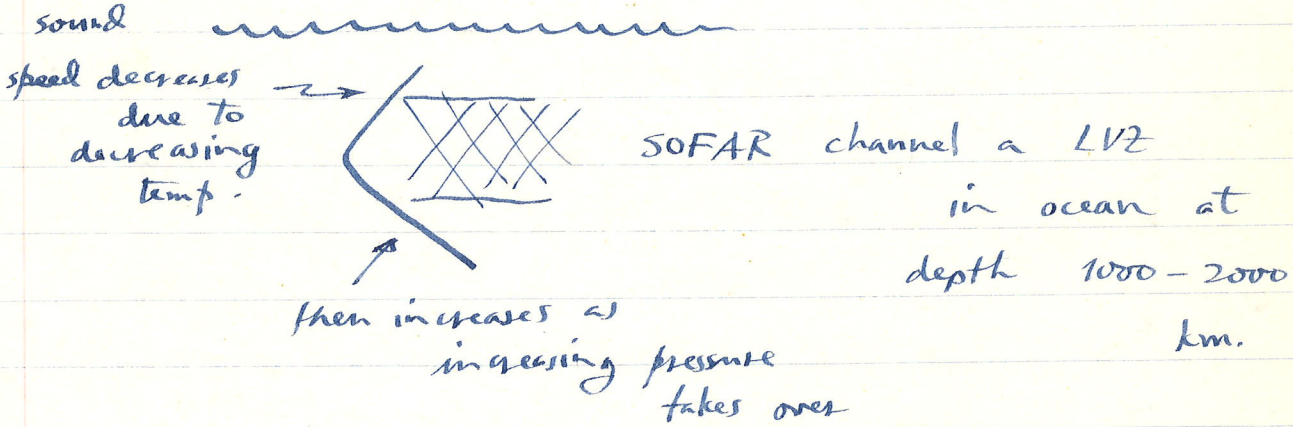

SOFAR channel used for communication purposes in ocean.

Summary of observed surface wave dispersion:

Group velocity can be easily measured at a single station if Δ and t are known. This will be the subject of a lab exercise. A possible procedure is to plot t_{peak} vs. peak number (Press and Ewings 1950's). See their Fig. 2.

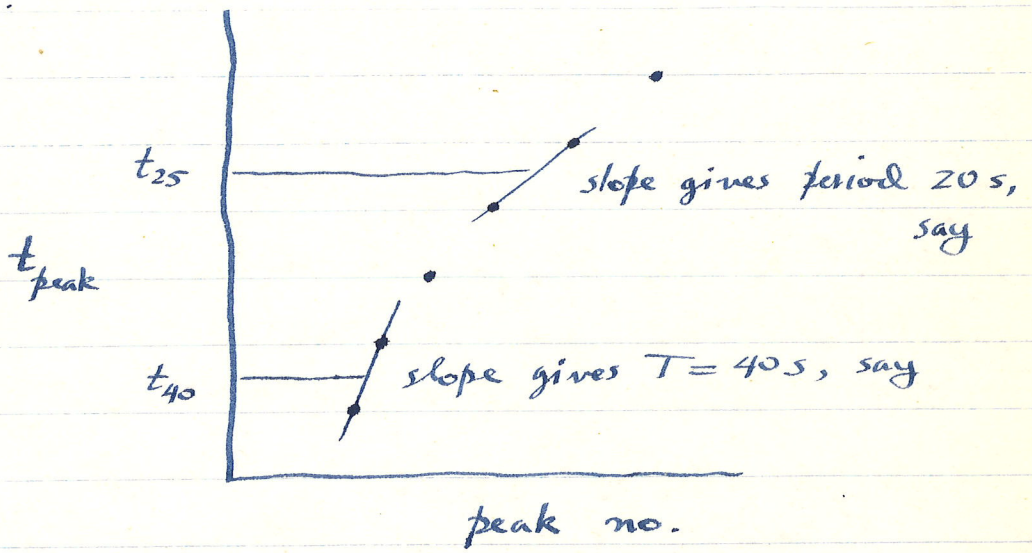

For an intermediate magnitude quake WWSSN long-period response can be used to measure dispersion in range 40 – 10 s, generally speaking.

"Typical" dispersion in this range looks like:

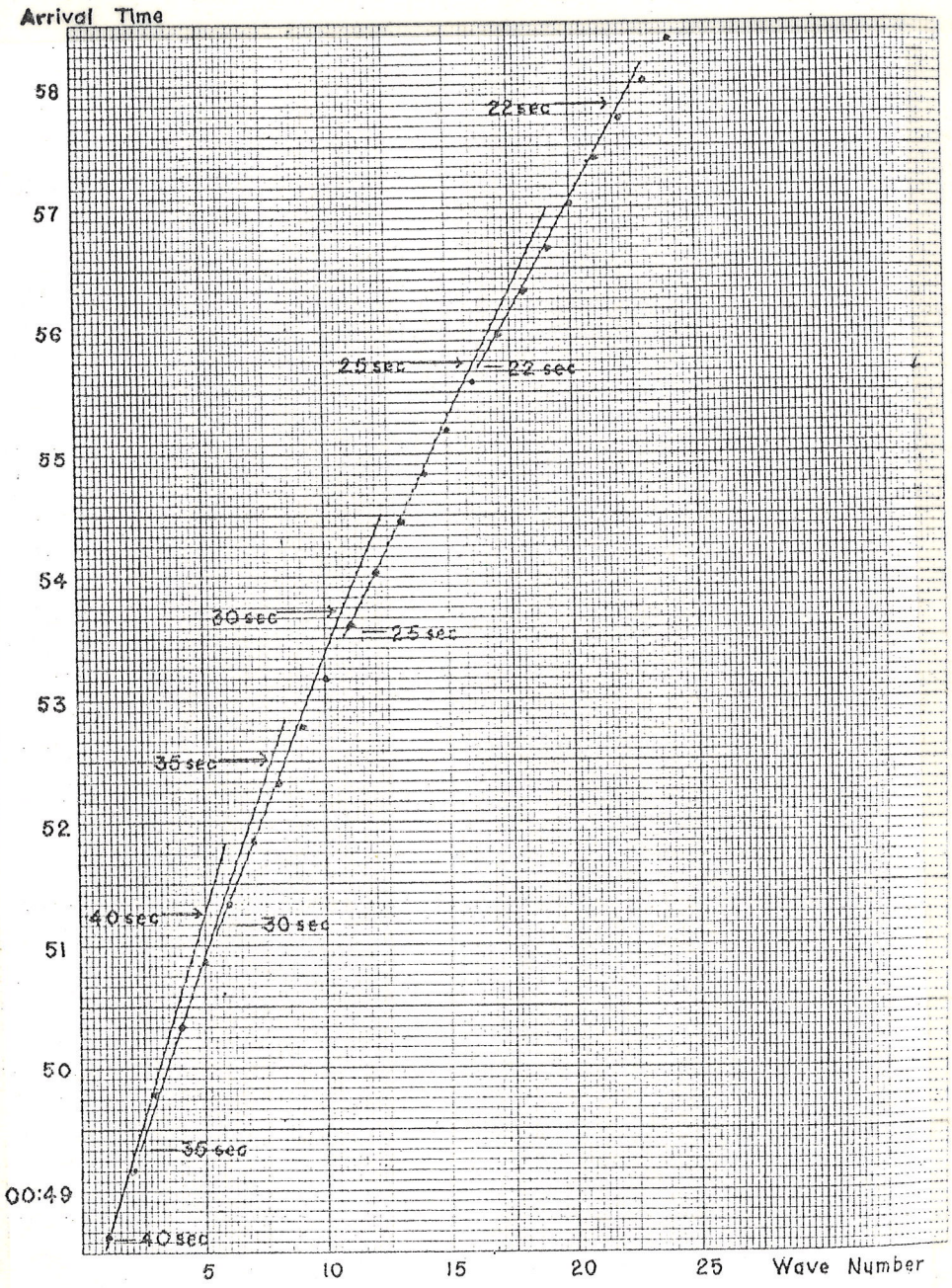

Fig. 2. Example of method of obtaining arrival time of waves of different periods in early part of seismogram.

location of steep part ⌈ depends on H_2O depth: see Fig. 3.13 of Gubbins

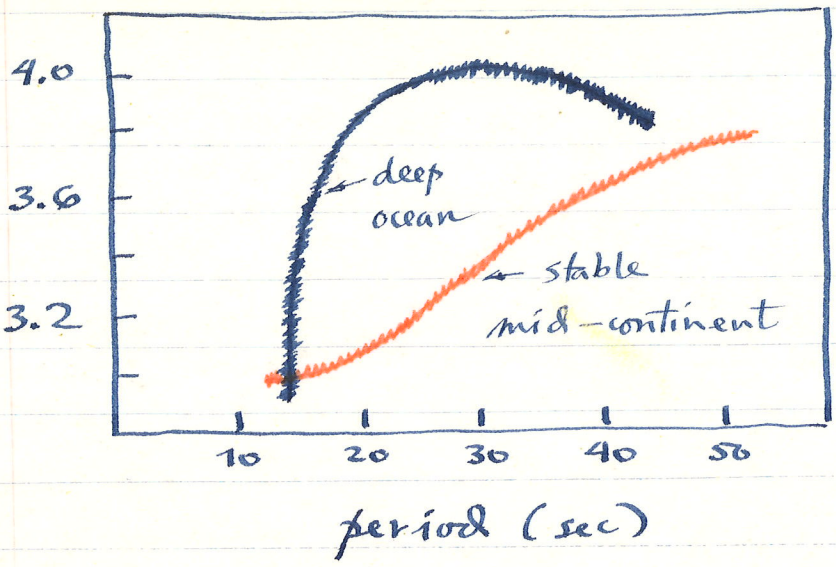

"typical" fundamental mode Rayleigh wave group velocity (km/sec)

The above corresponds to this part only

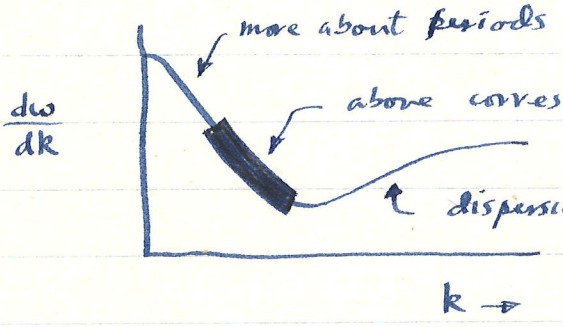

Note: in oceanic case (more "typical" since ⊕ surface 2/3 oceans) 15 second waves travel with group velocities between 2 and 4 km/s. Hence they get very dispersed, one sees very long 15 sec wavetrains. Continental

dispersion is more gradual.

emphasize this: it's the reason for the name dispersion

In general the greater Δ the more dispersed the waves get, for obvious reasons. Dispersion is not easy to measure on short paths $\Delta = 10° - 20°$, say.

The oceanic and continental curves both go to their minima at about 15 secs

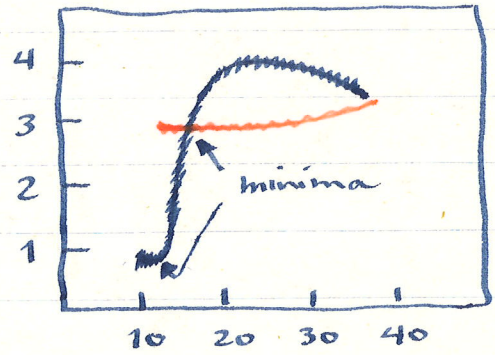

This then corresponds to the Airy phase, for this season typically largest signal on a vertical seismogram, used for detection of weak events, see dispersed 15 sec (or so) surface waves, esp. on oceanic paths.

Continental paths also are more heterogeneous (accreted terranes, etc.); oceanic more uniform, leading to "nicer" looking surface waves.

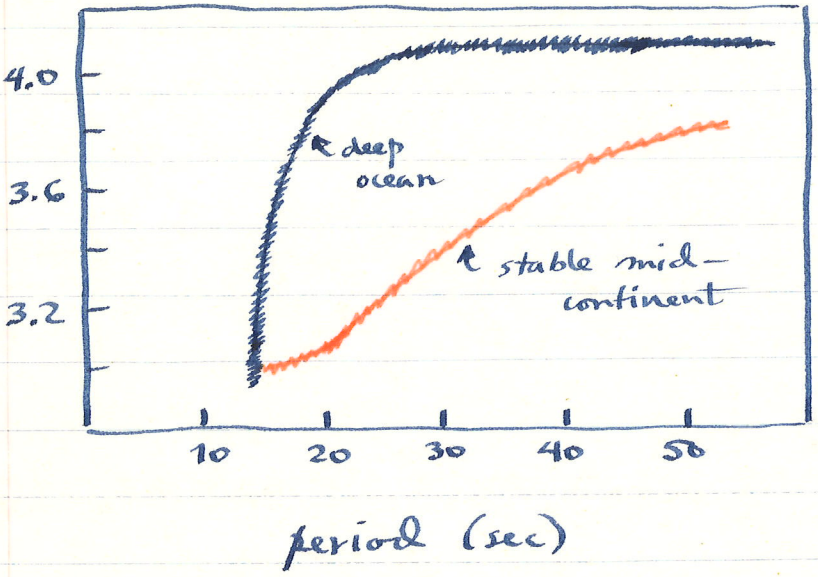

"typical" fundamental Love wave dispersion

An important feature in this case is the very flat Love wave dispersion curve for periods greater than 20-30 sec all the way up to > 100 s. This gives rise to the so-called G wave an impulsive-looking surface wave arrival with a velocity of about 4.5 km/sec, essentially the velocity of the lid over the LVZ.

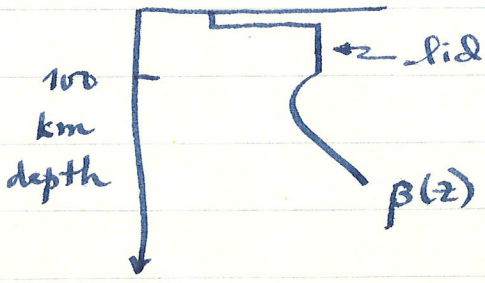

The G wave can be thought of as trapped in the lid.

Rayleigh waves "see" deeper, and don't get trapped in the lid over such a broad frequency range ($\lambda/2$ vs. $\lambda/4$).

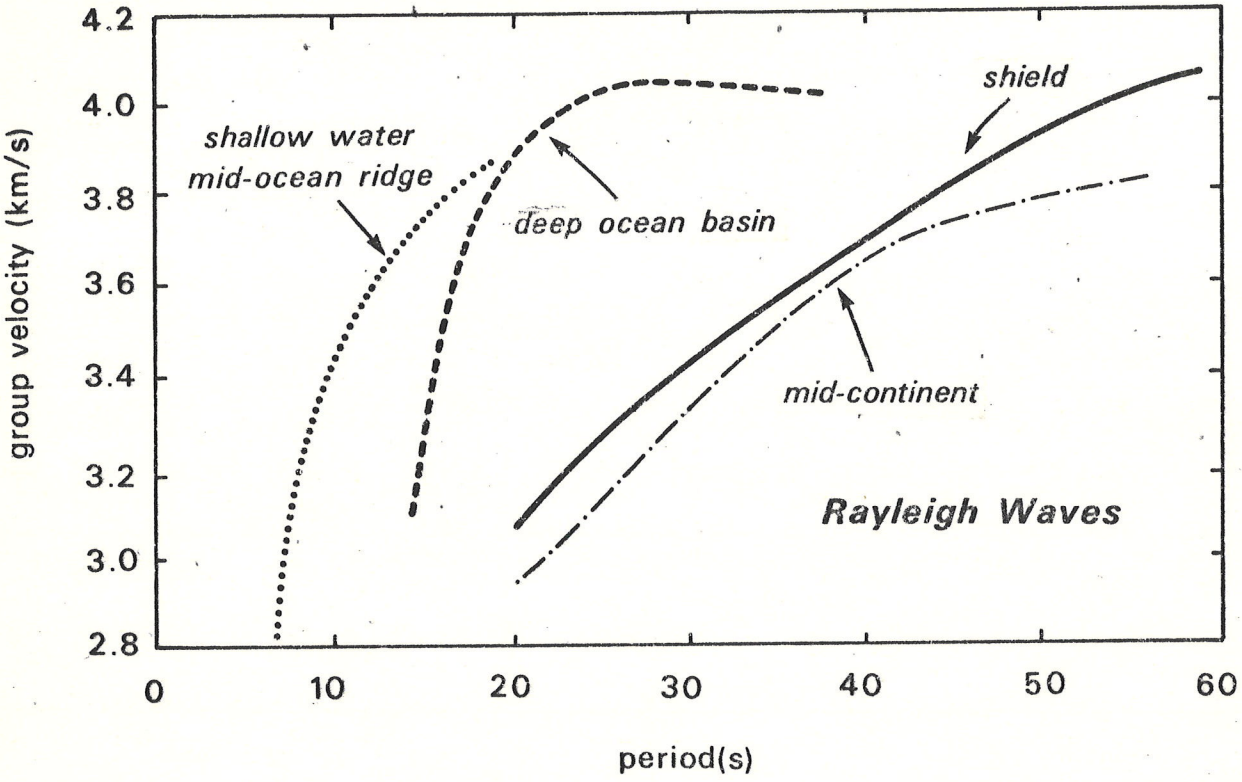
group velocity (km/s)
4.2
4.0
3.8
3.6
3.4
3.2
3.0
2.8
0
10
20
30
40
50
60
period(s)
shallow water
mid-ocean ridge
deep ocean basin
shield
mid-continent
Rayleigh Waves

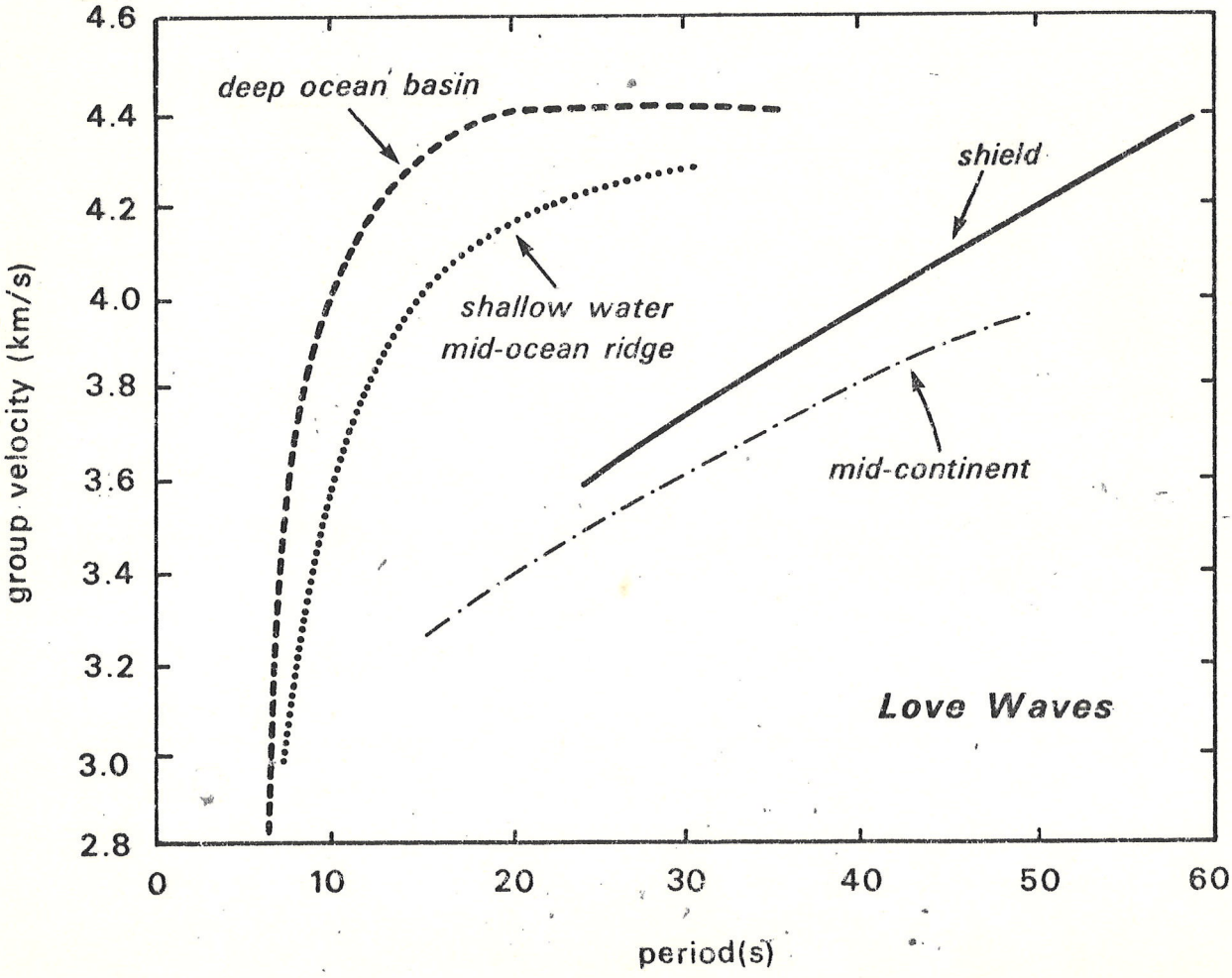
group velocity (km/s)
4.6
4.4
4.2
4.0
3.8
3.6
3.4
3.2
3.0
2.8
0
10
20
30
40
50
60
period(s)
deep ocean basin
shallow water
mid-ocean ridge
shield
mid-continent
Love Waves

The main reason for this difference between oceans and continents is the thinner oceanic crust, the waves can "see" the higher velocity mantle at a higher frequency.

in oceans

Because of the thin crust Rayleigh wave group velocities reach high values (4.1 km/s) at periods of only 35 secs.

The Love waves are not influenced by the water and rise steeply at ~ 10 secs to flatten out at about 4.5 km/s (the lid velocity)

(esp. for Rayleigh waves)

The position of the steep rise can vary from ~ 5 secs to ~ 15 secs depending on the sediment thickness (~ 5 secs when ∃ little or no sediment, 15 secs when ∃ 1.5 – 2 km of sediment)

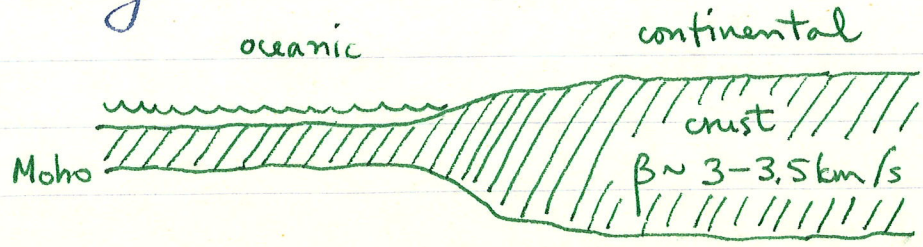

β ~ 4.6 km/s in mantle

Consider the typical curves compiled by Brune for shields, stable platforms with sediment cover, deep oceans and ocean ridges.

The latter have little or no sediment cover and the steep region is ~ 5 seconds.

Shields and platforms are similar for periods $\gtrsim$ 25–30 seconds. Below that it is variable depending on the amount of sediment cover.

Note the <u>higher modes</u>. They are high frequency (< 10 seconds) and high group velocity. For intermediate focus events (50–100 km) they show up ahead of the fundamental Rayleigh on the vertical, e.g.

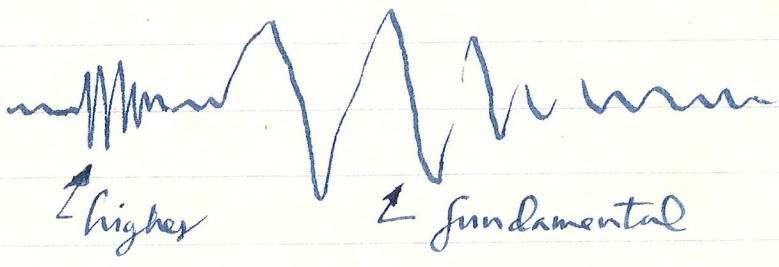

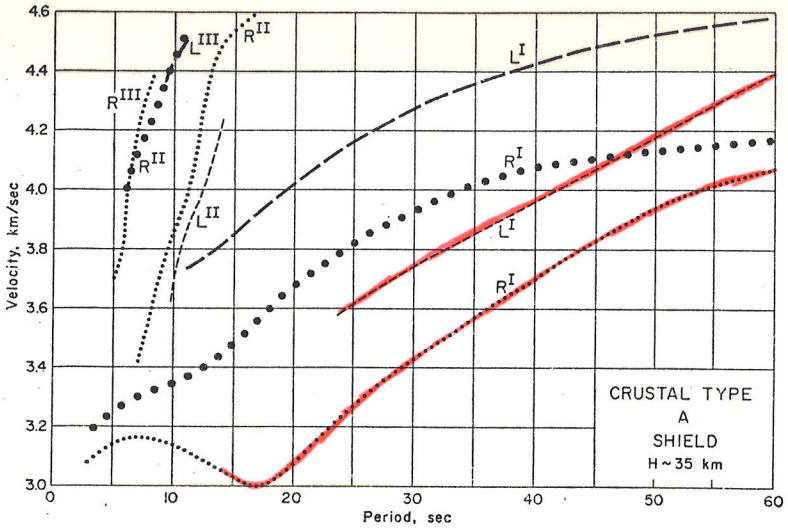

Fig. 1. Dispersion curves for crustal type *A*, shield. Small dots and dashes represent Rayleigh-wave and Love-wave group velocities. Large dots and dashes represent Rayleigh-wave and Love-wave phase velocities. R^{I} signifies the first Rayleigh mode, L^{II} signifies the second Love mode, etc.

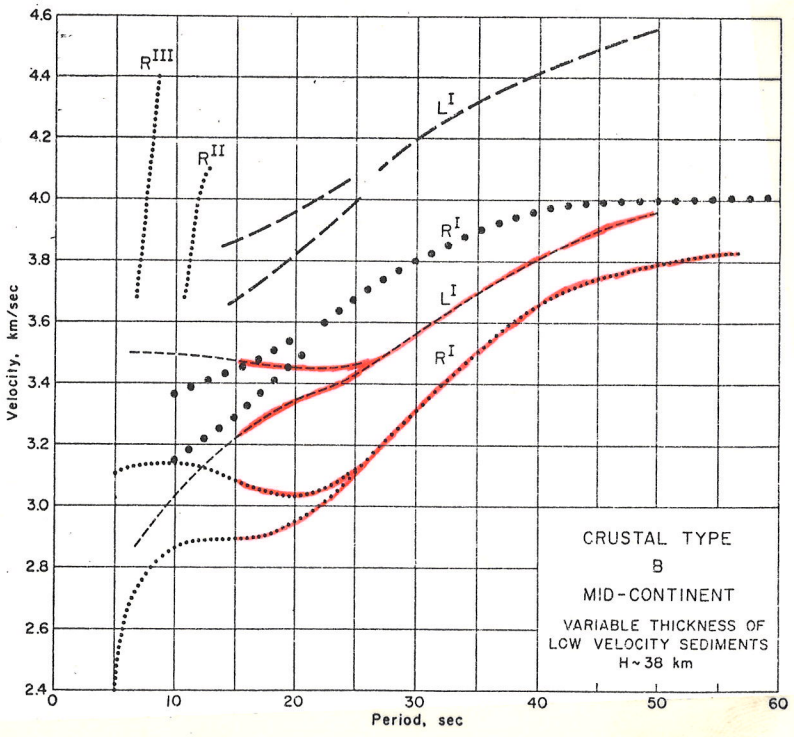

Fig. 2. Dispersion curves for crustal type *B*, mid-continent. See Figure 1 for legend.

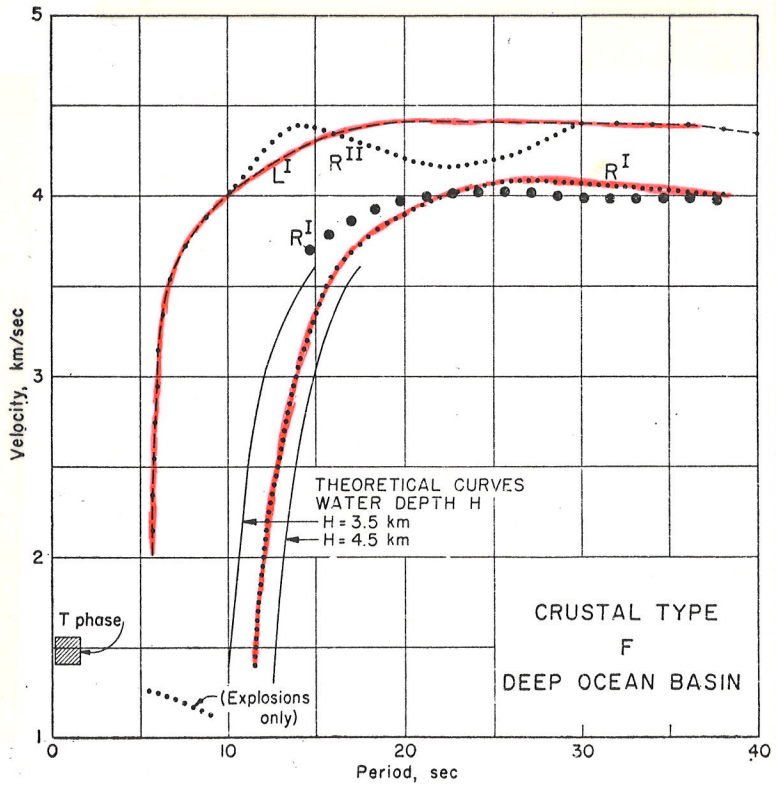

Fig. 6. Dispersion curves for crustal type *F*, deep ocean basin.

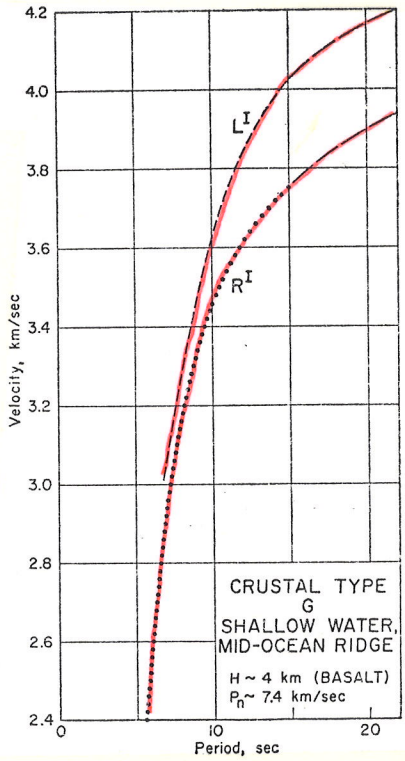

Fig. 7. Dispersion curves for crustal type *G*, shallow water mid-ocean ridge.

Very large events excite lower frequency waves and allow the dispersion curves to be measured all the way up to several hundred seconds.

This requires careful numerical analysis, time-variable filtration, residual measurement methods, etc.

A summary of the observed long period dispersion is seen in Figs. 1 and 2 from article by Dorman.

Note oceanic and continental merge at ~ 100 secs period, structural differences below 100 – 200 km are slight.

Love is flat to very long periods but Rayleigh exhibits another minimum in vicinity of 250 secs, i.e. 250 sec waves are slower (3.5 km/s) than 20–30 sec waves (4.0 km/s). This phenomenon is a consequence of general velocity increase in mantle, LVZ merely perturbs this minimum and Love plateau

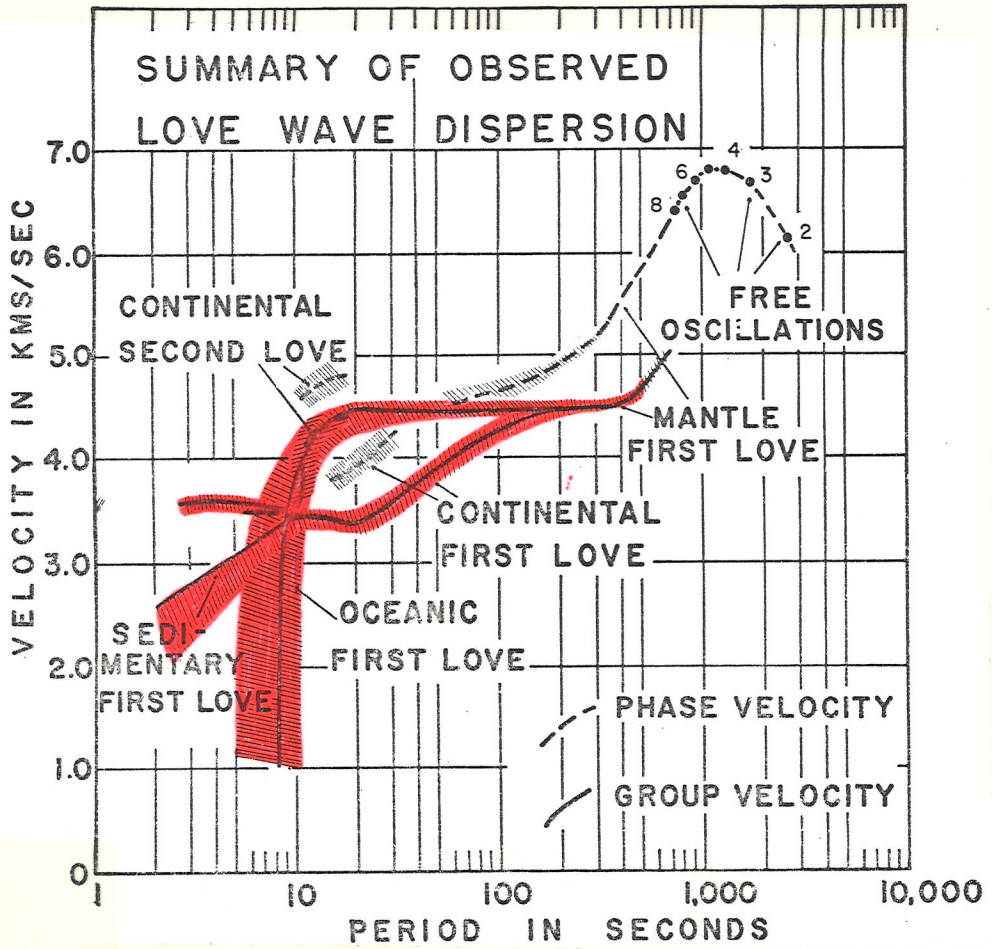

FIG. 1. Summary of observed Love wave dispersion.

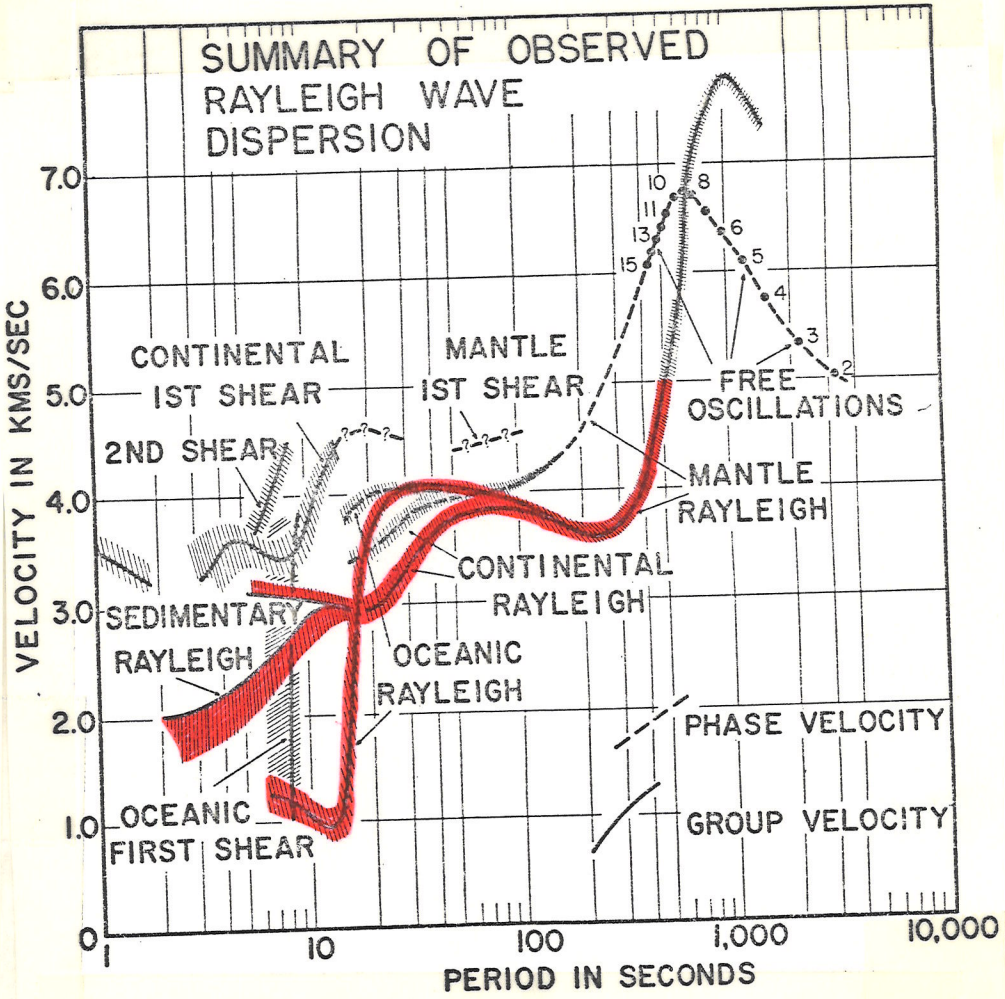

FIG. 2. Summary of observed Rayleigh wave dispersion.

To see it need not only large events but long-period seismometers. WWSSN response peaks ~ 20 secs (designed to detect weak "events", in Soviet Union primarily), very poor response above 100 secs.

Compare Fig. 3 from Wier's thesis showing a "typical" largely oceanic R1 and no visible R3 on WWSSN with R3 seen on an HGLP at same site (OGD). Note slow group velocity of longer period waves. Also note Airy phase at beginning corresponding to U_{max} at 50–100 sec. Above 250 secs both Love and Rayleigh group velocities rise once again to ~ 5 km/sec at 500–600 seconds period. These are true mantle waves, "see" to depths of 500 – 1000 km (Rayleigh see deeper) where $\beta(r)$ is larger so they go faster. They are really the first-arriving surface waves but can only be seen after very large quakes and after application of low-pass filters to seismograms. These waves are low amplitude but fast.

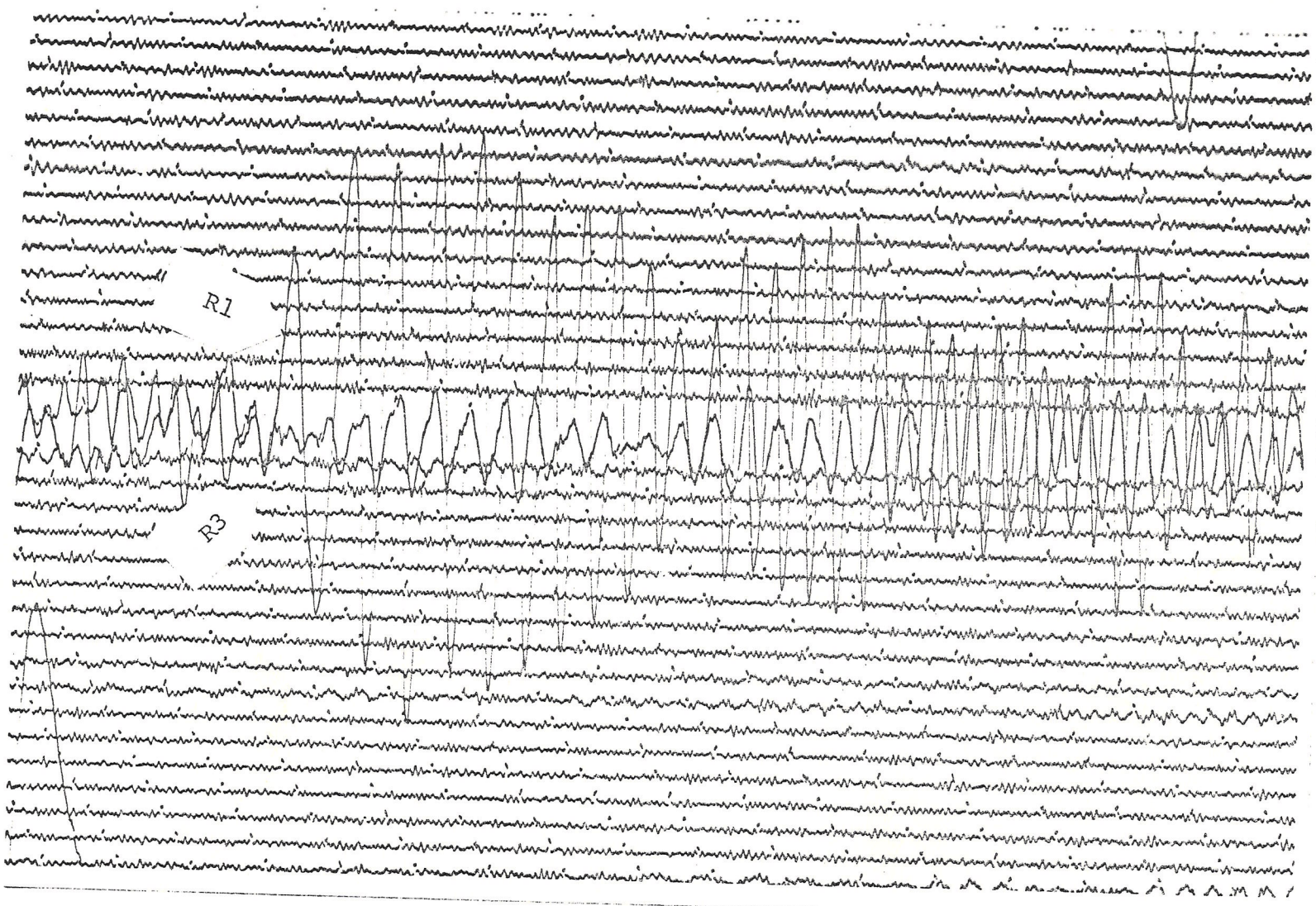

Fig. 3-13. Part of the recording of the event of 12/30/73 (MS 6.6) made by WWSSN seismographs at station OGD. The first passage of the Rayleigh wave (R1) is prominent but little or no signal is observable when the third passage is expected (R3). Vertical component, magnification 3000 times. Compare to the Frontispiece.

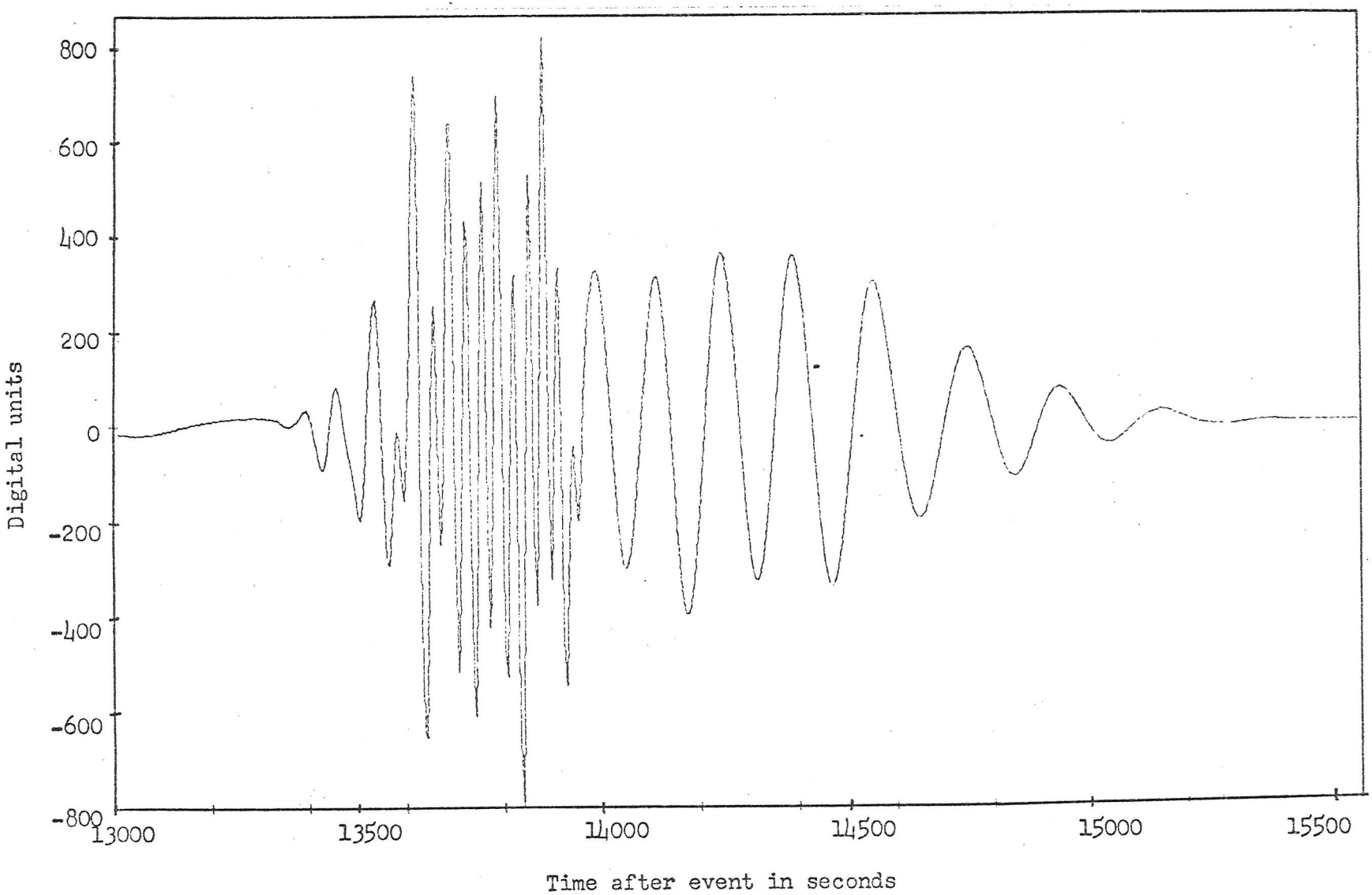

Frontispiece: The advantages of digitally recorded seismic data: seismogram of vertical R3 recorded at OGD from the event of 12/30/73. Compare to Figure 3-12.

See Figs. 2, 11 and 14 from study by Dziewonski + Landisman showing long-period Rayleigh and Love dispersion for a single path around the world, note alignment of path so Love and Rayleigh are separated as in our lab exercise. Note fast arriving low amplitude long-period waves at about 2 hr 20 min travel time, [redacted] the time to circumnavigate the ⊕ once at ~ 5 km/sec.

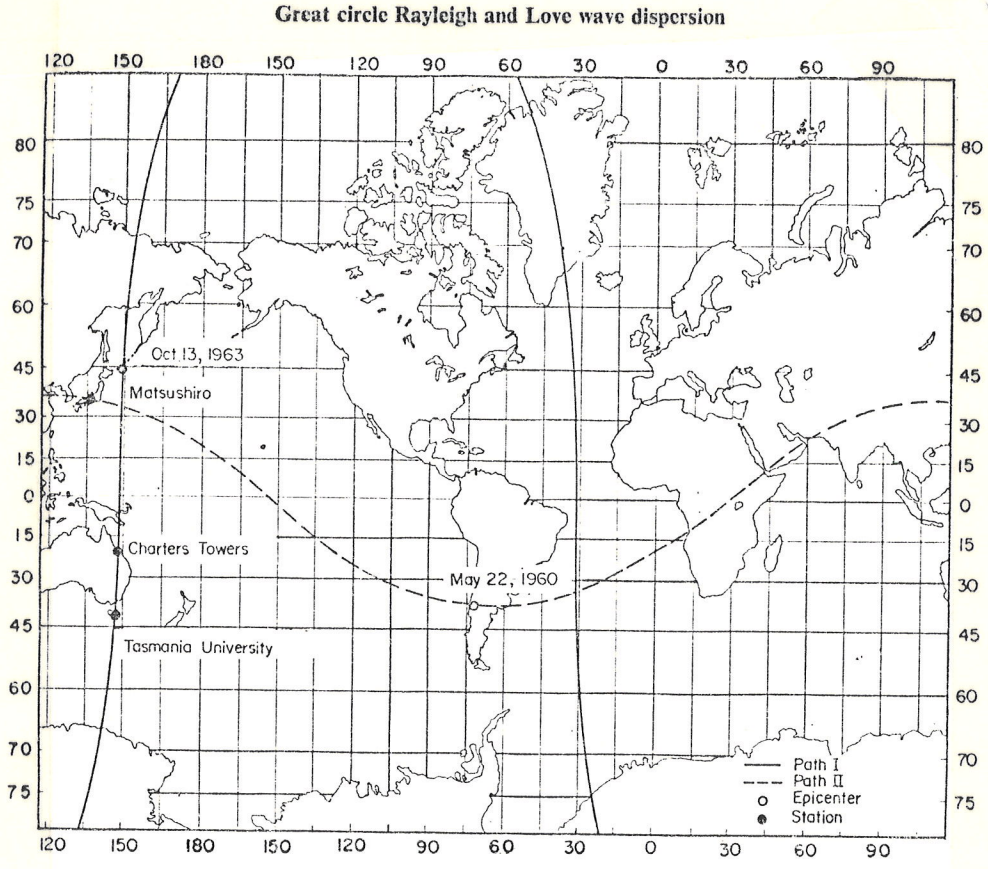

FIG. 2. World map showing the sources, stations and world circling paths considered in the present study.

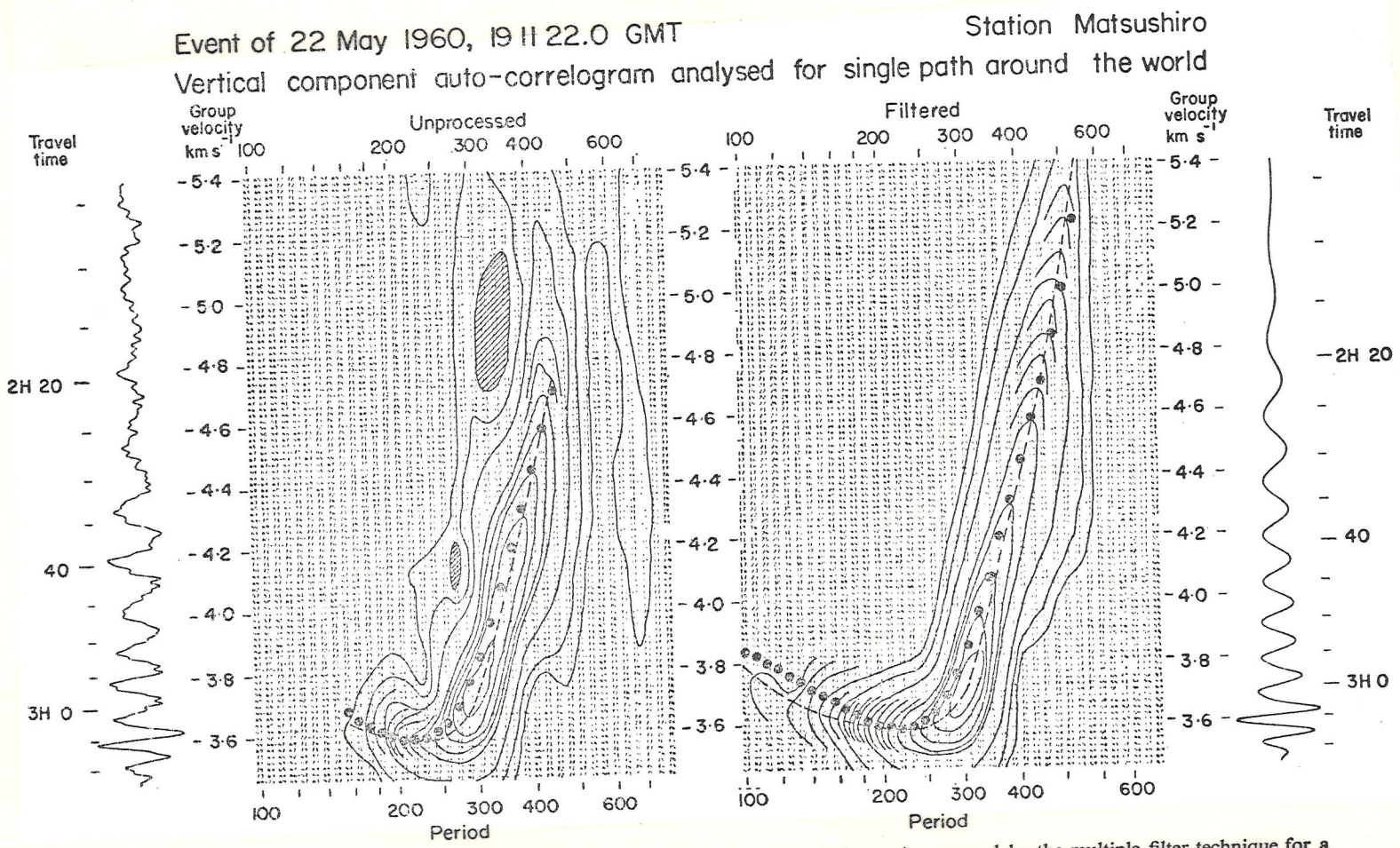

FIG. 11. Vertical component auto-correlogram of the Matsushiro recording (Fig. 5, bottom) processed by the multiple filter technique for a single passage of Rayleigh waves around the world. For details see caption to Fig. 10.

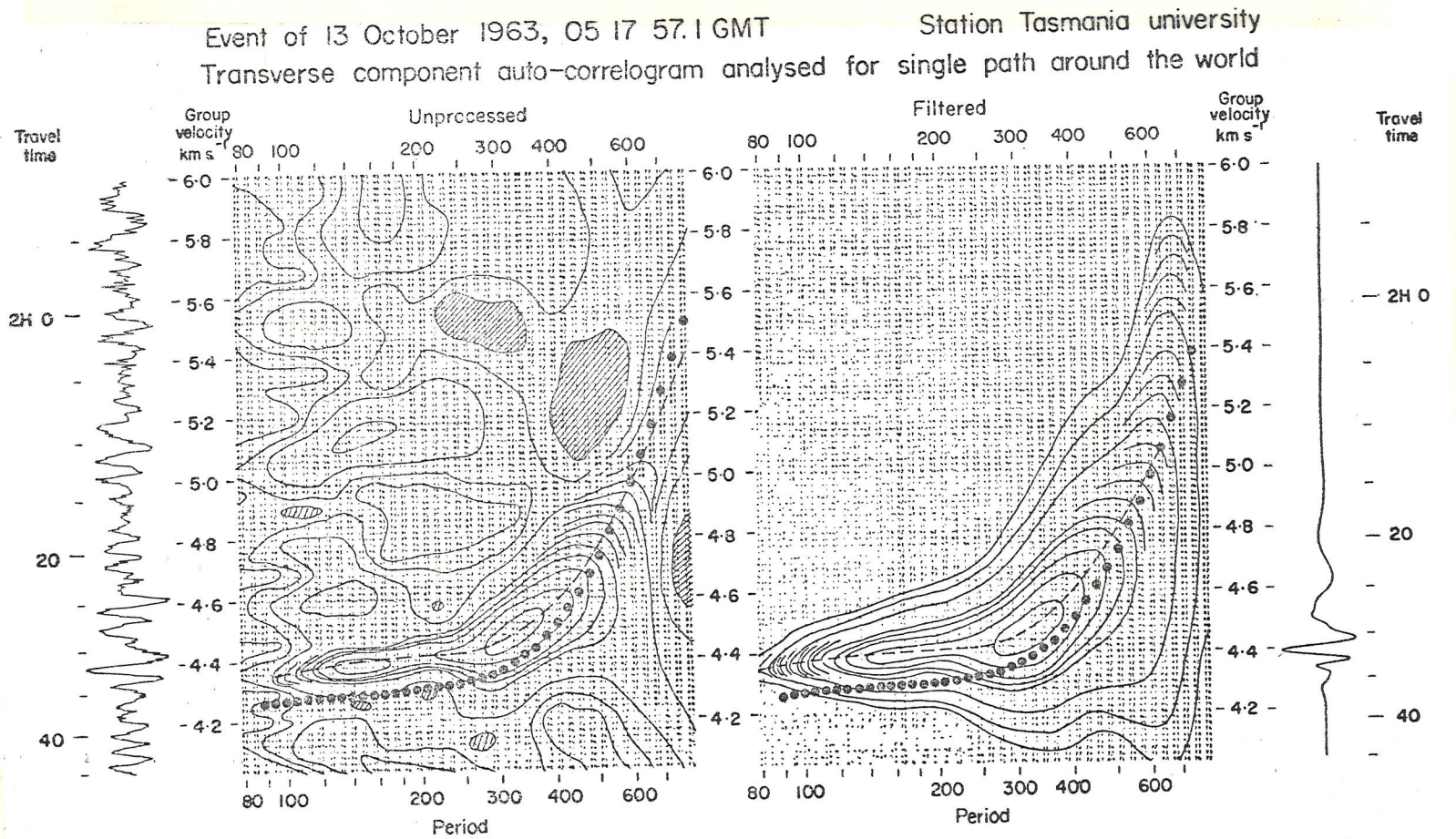

FIG. 14. Transverse component auto-correlogram of the Tasmania University recording (Fig. 4b, bottom) processed by the multiple filter technique for a single passage of Love waves around the world. For details see caption to Fig. 10.

Phase velocities cannot be measured over a "pure" path using a single station. Two common methods:

1. two-station technique: to see how method works suppose first 3 two stations on same great circle path very close together, on the order of a wavelength

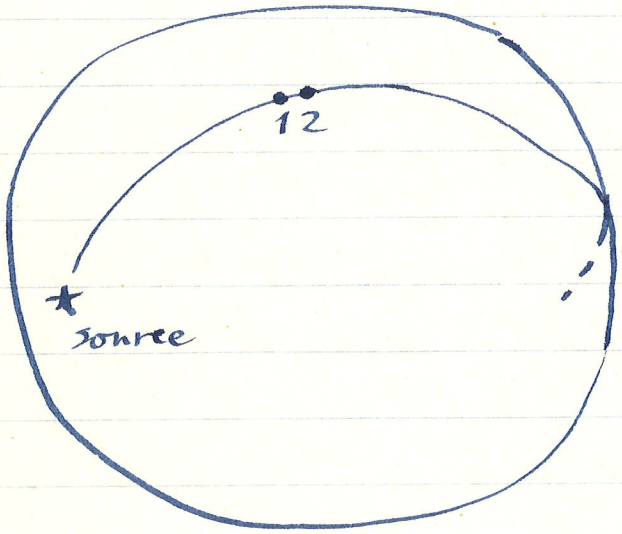

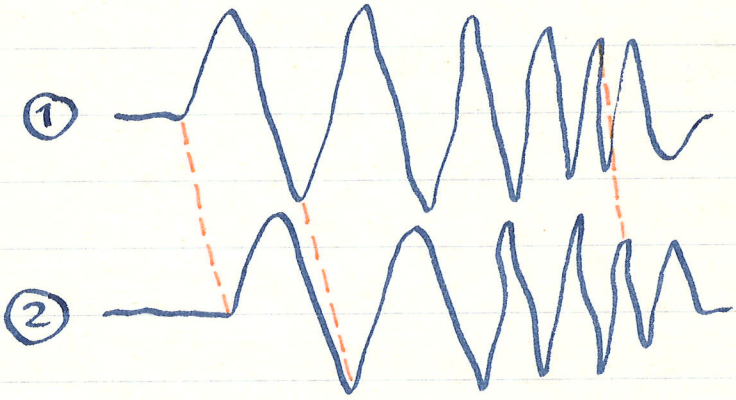

can then correlate peaks and troughs.

Can then keep track of individual waves, measure their velocity, this yields phase velocity for path between the two stations.

Using Fourier analysis, can use same method but with more distant stations. One measures the phase $\phi(\omega)$ at 1 and 2, then

$$c(T) = \frac{a\Delta/T}{\left[\frac{1}{2\pi}(\phi_2 - \phi_1)\right]}.$$

Note rather stringent geometry requirements.

2. great circle method: use a single station, compare (say) R3 and R1. This used for long-period mantle waves.

This measures c_{ave} averaged over a great circle path. A common method of interpretation is to divide the path up into (say) old oceans, young oceans, shields, etc. Then

$$\frac{1}{c_{ave}} = \frac{l_1}{c_1} + \frac{l_2}{c_2} + \cdots \frac{l_n}{c_n}$$

where l_n are the path fractions satisfying $l_1 + \cdots l_n = 1$.
Whether this geometrical optics approx. is valid is a matter of debate.

Water waves : one of the simplest applications of the concepts of dispersion, group velocity, etc.

Easily generated : throw a stone into a pond, e.g. Lake Carnegie.

The restoring force for elastic waves is the elasticity of rock — rigidity and incompressibility. Restoring force for surface water waves is gravity

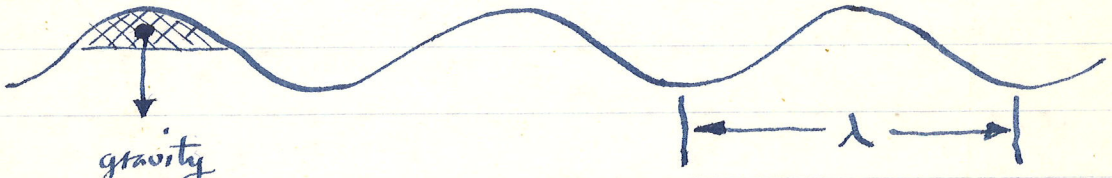

gravity pulls this down, wave propagates

wavenumber $k = \frac{2\pi}{\lambda}$

ang. freq. ω

phase velocity $c = \frac{\omega}{k}$

Phase velocity is speed of an individual wave crest of wavenumber k.

By solving an appropriate b.v. problem it can be shown that <u>dispersion relation</u> for surface gravity waves is

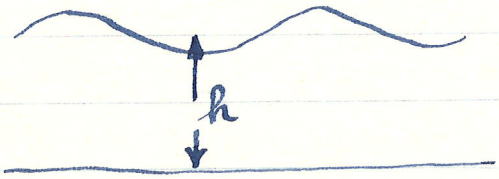

depth = h

$$\omega = (gk \tanh kh)^{1/2}$$

tanh 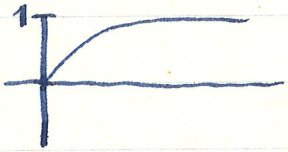

$\tanh x \sim x$ for $x \ll 1$

$\tanh x \sim 1$ for $x \gg 1$

Shallow H_2O waves $c = \sqrt{gH}$, speed depends on $\sqrt{\text{water depth}}$

Let us consider only <u>deep water waves</u> for simplicity, $kh \gg 1$ or

$h \gg \lambda$, depth much greater than wavelength, this condition easily checked

Then $kh \to 1$ and

$$\boxed{\omega = \sqrt{gk}}$$

Particle motions in the deep water case are <u>circular</u>, waves do not "feel" the bottom

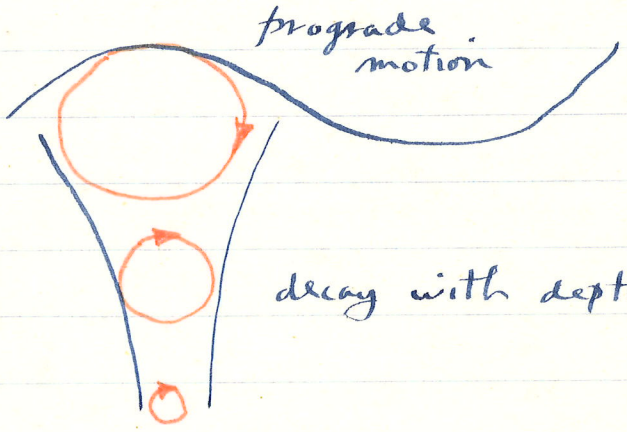

decay with depth like e^{-kz}

What is the <u>phase velocity</u>?

$$c = \omega/k \quad , \quad c = \sqrt{g/k}$$

$$\boxed{c(\lambda) = (g\lambda/2\pi)^{1/2}}$$

Use λ as independent variable, most easily observed in rock in pond "experiment".

Group velocity $u = d\omega/dk = \sqrt{g} \cdot \frac{1}{2} k^{-1/2}$

$$u = \frac{1}{2}\sqrt{g/k}$$

$$\boxed{u(\lambda) = \tfrac{1}{2}\, c(\lambda)}$$

The group velocity is 1/2 the phase velocity for all wavelengths.

The above results are not valid for <u>short wavelength</u> waves. There another phenomenon becomes important: <u>surface tension</u>.

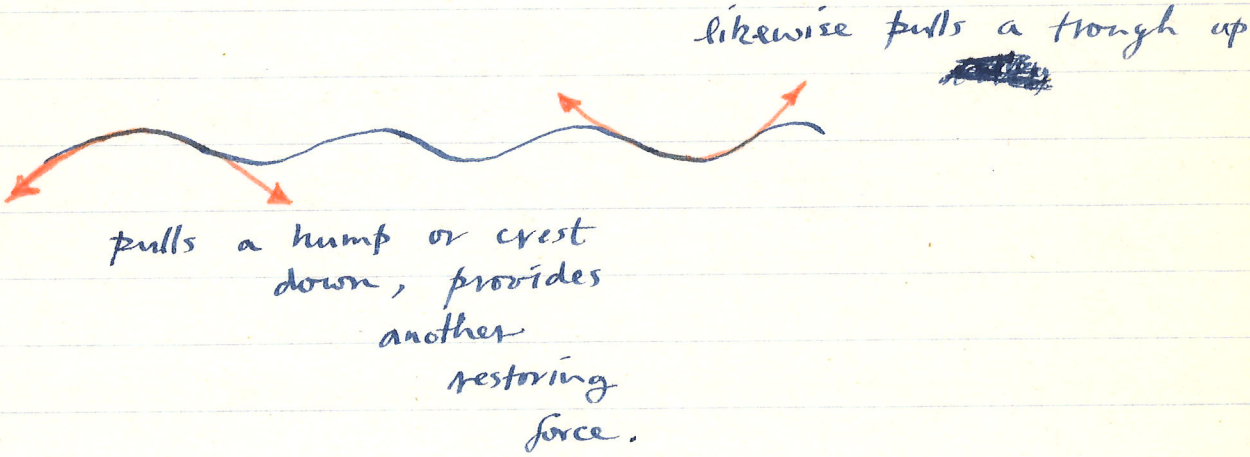

The restoring force provided by surface tension depends on the <u>curvature</u> of the wave crests, hence greater for shorter wavelength waves.

It can be shown that its effect is exactly to replace:

$$g \longrightarrow g + \frac{Tk^2}{\rho}$$

ρ = density of water

$\leftarrow$ dependence on k^2 arises from dependence on curvature

T = surface tension coefficient, "strength" of surface tension, for air–water interface, can be measured, find for distilled H_2O:

$$T = 74 \text{ dyne/cm}$$

Now what is the phase velocity?

$$\omega = \sqrt{(g + Tk^2/\rho)k}$$

$$c = \omega/k$$

$$c = \left[\frac{g + Tk^2/\rho}{k} \right]^{1/2}$$

This has a minimum where $dc/dk = 0$

We note that c^2 has its minimum where c does, so

$$-gk^{-2} + T/\rho = 0$$

$$k_{min} = (\rho g/T)^{1/2}$$

The corresponding wavelength is

$$\boxed{\lambda_m = \frac{2\pi}{k_m} = 2\pi (T/\rho g)^{1/2}}$$

with $T = 74$ dyne/cm and $\rho = 1.0$ gm/cm^3 find

$$\boxed{\lambda_m = 1.7 \text{ cm}}$$

less than an inch

The corresponding minimum phase velocity is

$$\boxed{c_m = \left(\frac{2g}{k_m}\right)^{1/2} = 23 \text{ cm/sec}}$$

A plot of $c(\lambda)$ thus looks like:

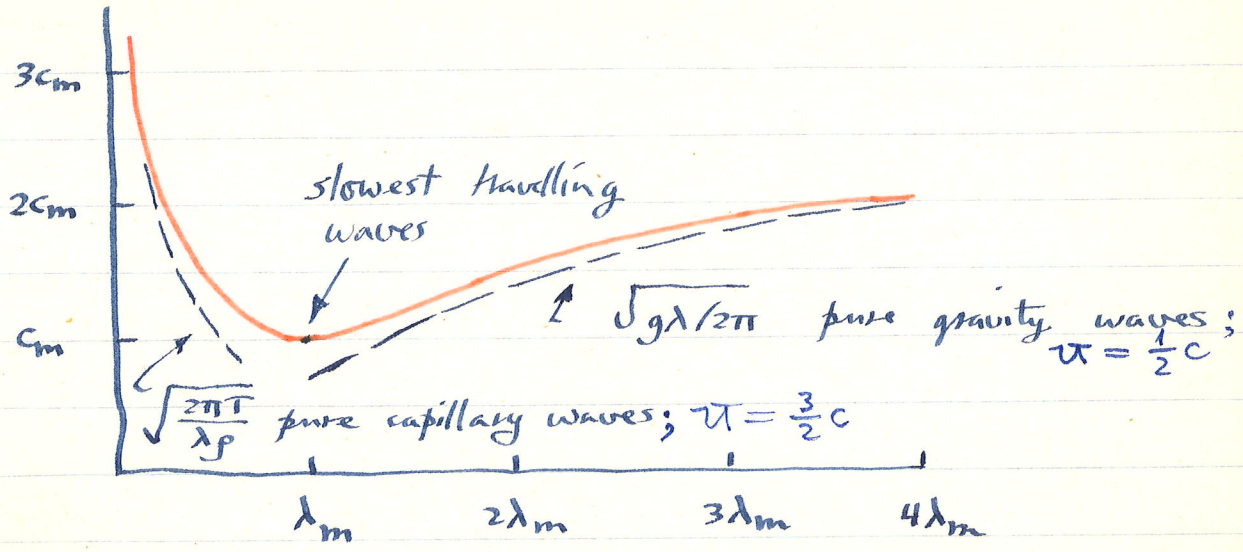

For $\lambda \gg \lambda_m$, i.e. > a few inches, the effect of surface tension is negligible, behave as pure gravity waves.

For $\lambda \ll \lambda_m$ surface tension takes over, raises the phase speed (more restoring force), called capillary waves, their dispersion relation obtained by neglecting gravity

$$\boxed{\omega = \sqrt{Tk^3/\rho}\ , \quad c(\lambda) = \sqrt{2\pi T/\lambda\rho}}$$

Their group velocity is thus

$$v = \frac{d\omega}{dk} = \frac{3}{2}\frac{\omega}{k} \qquad \boxed{v = \frac{3}{2}c}$$

The group velocity of capillary waves is 3/2 the phase velocity.

Now note that

$$U = \frac{d\omega}{dk} = \frac{d(kc)}{dk}$$

$$= c + k\frac{dc}{dk} \quad \text{or since } \frac{dk}{k} = -\frac{d\lambda}{\lambda}$$

$$\boxed{U = c - \lambda\frac{dc}{d\lambda}}$$

Graphical construction to find $U(\lambda)$:

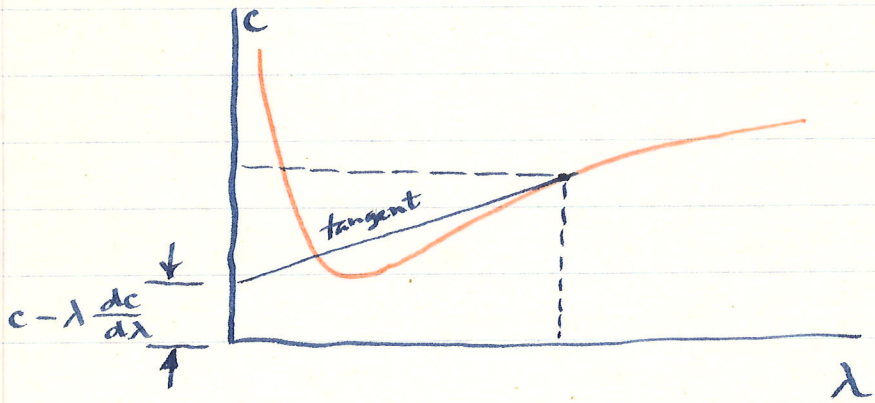

$U(\lambda)$ is intercept of tangent to $c(\lambda)$ curve

Clear then that $U(\lambda)$ will have a minimum at inflection pt. of $c(\lambda)$, i.e.

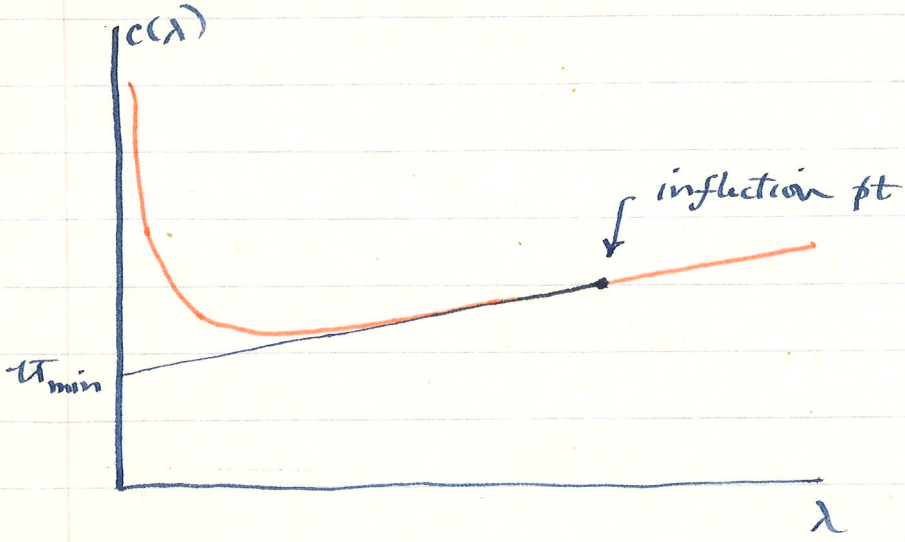

A little analysis shows that u_{min} occurs at $\lambda = 2.54\,\lambda_{min} = 4.3$ cm

The corresponding phase speed is $c = \sqrt{1.21}\,c_m$ $= 28$ cm/sec and the group velocity at the minimum [redacted] is $u = 0.767\,c_m$:

$u_{min} =$ [redacted]^{18} cm/sec, 4.3 cm waves

$u = 0.64\,c$ ($c = 28$ cm/sec) at the minimum

Now, knowing this, we can predict the pattern a stone in a pond will make.

A plot of u vs. λ looks like :

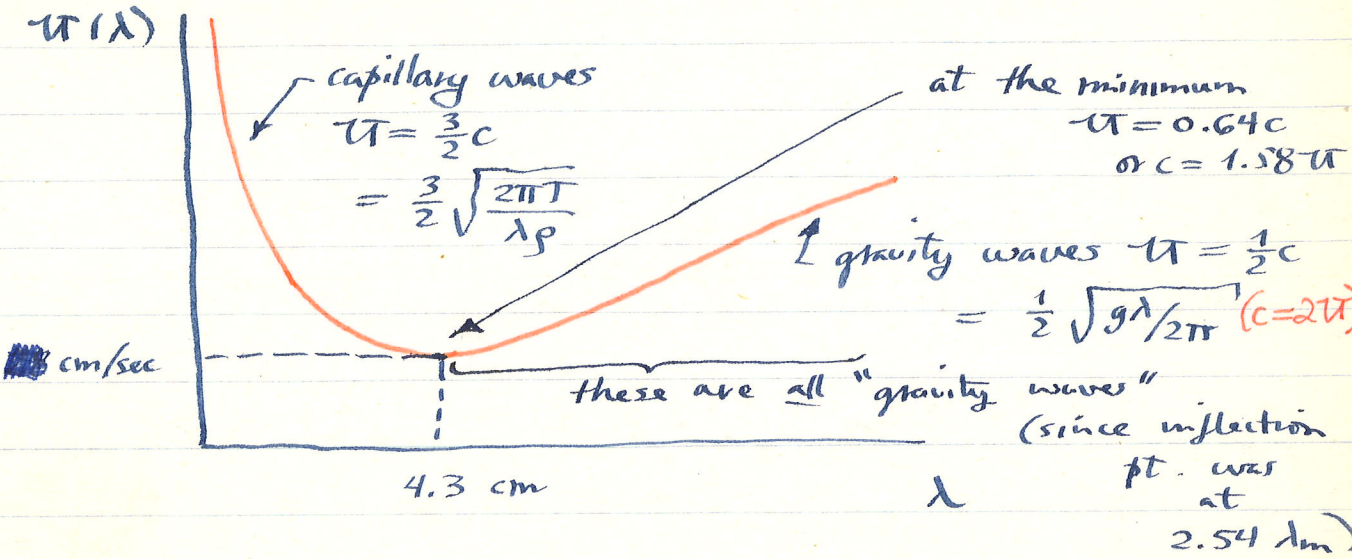

In practice only the gravity waves are visible to the unaided eye, the capillary waves are subject to rapid damping and are quickly attenuated.

All the energy moves away from the splash faster than 18 cm/sec. Throw a stone into a pond, wait a few seconds (recall Kelvin's analysis for $t \to \infty$) to let things sort out.

A calm region soon appears in the middle surrounded by waves of length 1–5 cm. Their crests will seem to be emerging "from nowhere" i.e. from the calmed central region since their phase velocities exceed their group velocity.

The longest waves generated will typically be about 10 times the size of the stone (this a property of the "source"). For, say, a 2" or 5 cm stone the longest waves will have $\lambda \sim 1/2$ m and since $v \sim \sqrt{\lambda}$ will be travelling about 3-4 times as fast as the slowest waves. The pattern will thus look roughly like.

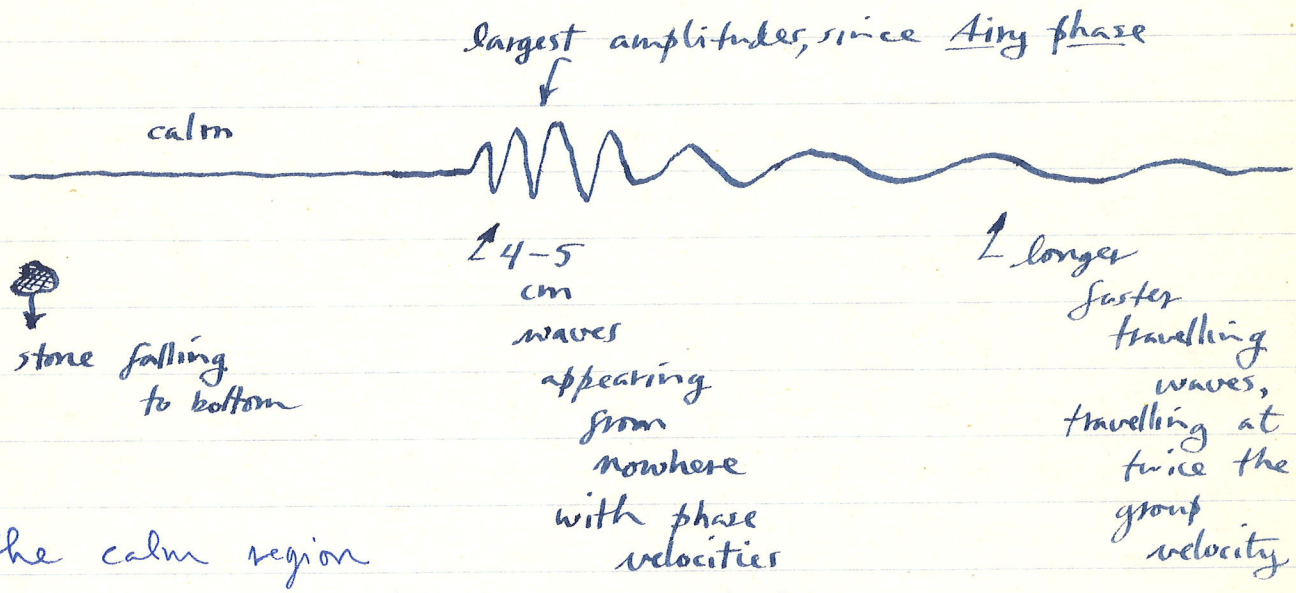

In the calm region all the individual waves are cancelling each other out. At the caustic or Airy phase 4-5 cm waves appear travelling at a speed 1.58 times the speed of the Airy "group" itself

These must be capillary waves : sets scale of print.

47. Rimpeling - Rippled surface - Gekräuselte Wasserfläche - Cercles dans l'eau - Ringar på vattnet

48. Drie werelden - Three worlds - Drei Welten - Trois mondes - Tre världar

Consider these long (gravity) waves on the outer edge of the pattern. If you try to follow a single wave crest with your eye you'll lose it. Let's see what the motion of a single wave crest is.

Waves move at $c = 2\pi$. Thus they must increase their period and speed as they move.

$$\text{defn:} \quad kx - \omega t = \text{constant}$$

A single constituent wave is

$$\cos[kx - \omega(k)t].$$

We also know that waves of wavenumber k are found at $x/t = \omega(k)$.

We must solve simultaneously

$$kx - \omega t = \text{const}$$
$$x = \omega(k)\, t$$

Now for gravity waves $\omega = \sqrt{gk}$, $\omega = \frac{1}{2}\sqrt{g/k}$

$$\left[k\,\tfrac{1}{2}\sqrt{g/k} - \sqrt{gk}\right]t = \text{const}$$

or

$$\sqrt{gk}\, t = \text{const} \quad \text{or}$$

$$\omega t = \text{const}$$

$$t/T = \text{constant}, \quad T = \text{period}$$

If one could follow a single crest its period would increase linearly with time.

Furthermore $$x = \frac{1}{2}\sqrt{\frac{g}{k}}\, t$$

$$kx = \frac{1}{2}\sqrt{gk}\, t = \frac{1}{2}\omega t = \text{const.}$$

$$\frac{x}{\lambda} = \text{const}$$

this constant is twice as big as the first →

When a wave has travelled twice as far it's twice as long.

Now suppose you pick out a single wave at some fixed time t_0. What is its subsequent motion?

$$kx = k_0 x_0, \quad \omega t = \omega_0 t_0$$

where k_0 and ω_0 are its initial wavenumber and frequency.

$$x = \frac{k_0 x_0}{k} = \frac{k_0 x_0}{\omega^2/g} = g\frac{k_0 x_0}{\omega^2}$$

$$= g\frac{k_0 x_0}{\omega_0^2 t_0^2/t^2} = \left(\frac{k_0 x_0}{\omega_0^2 t_0^2}\right) g t^2$$

$$t_0 = \frac{x_0}{1\pi} = 2x_0\sqrt{\frac{k_0}{g}} \qquad \text{and} \quad \omega_0^2 = g k_0$$
$$\omega_0^2 t_0^2 = 4 k_0^2 x_0^2$$

$$x = \left(\frac{g}{4 k_0 x_0}\right) t^2 \qquad \text{or finally in terms of wavelength}$$

$$\boxed{x = \left(\frac{g}{8\pi}\,\frac{\lambda_0}{x_0}\right) t^2}$$

A given wavecrest moves with a constant acceleration!

In the pond experiment $\lambda_0 \sim \frac{1}{2}$ m out on the edge and $x_0 \sim 10$ m so $\lambda_0/x_0 \sim 1/20$ and the acceleration is about $\frac{1}{500}\,g$, not very much.

The Bond experiment on a big scale: the 1966 Pacific ocean swell experiment of Munk et al.

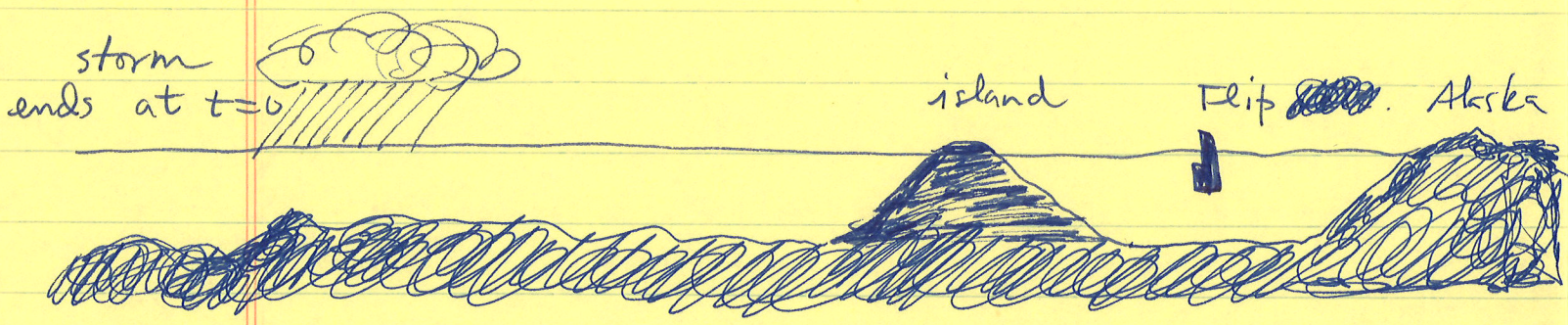

When will deep water waves of frequency ω be found a distance x away?

Answer: at $t = \frac{x}{v_g}$; $v_g = \frac{1}{2}\frac{g}{\omega}$, so

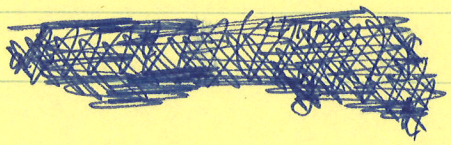

> Waves of frequency ω arrive at station at x at $t = \frac{2x}{g}\omega$

High frequency waves take longer. Frequency of peak in power spectrum observed to vary linearly with arrival time as expected.

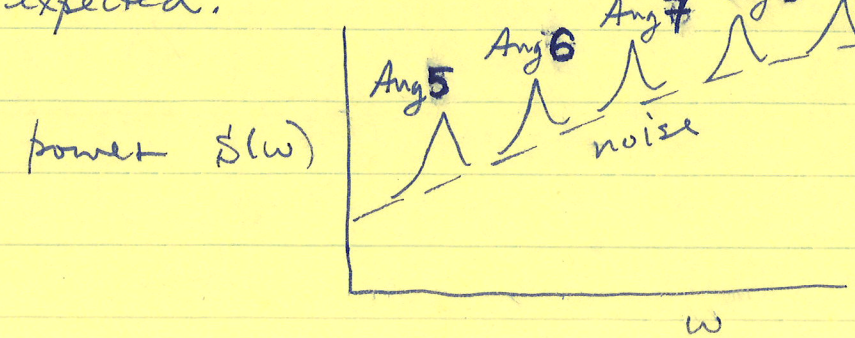

Or presented differently, in three dimensions, on a frequency–time plot

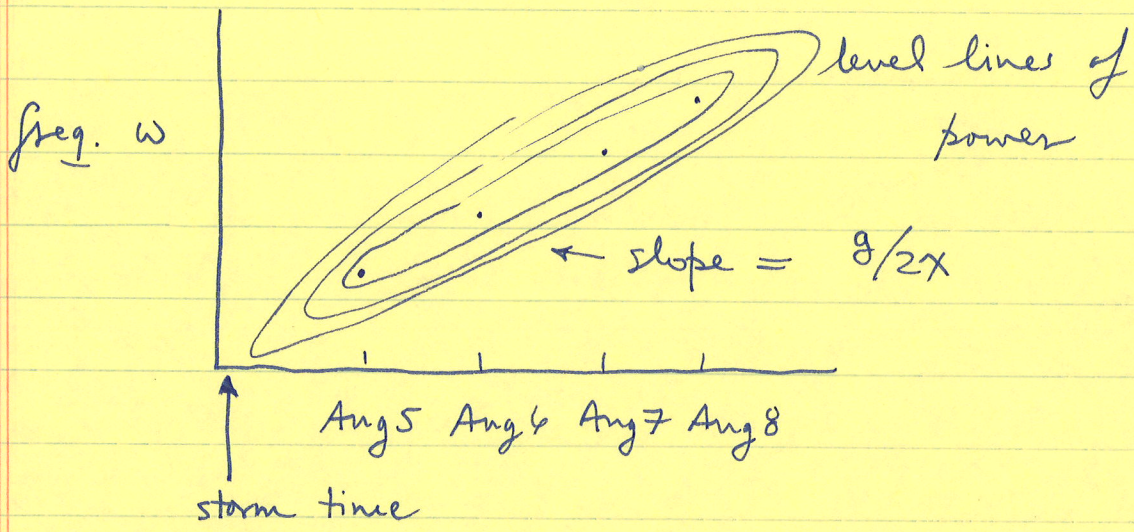

Intercept on date or time axis at $\omega = 0$ is time of arrival of wave of zero frequency ($T = \infty$). This gives time of storm. ~~[illegible]~~. The slope of the "ridge lines" gives the storm distance, since $\omega = gt/2x$

or $\omega = (g/2x)t$

↑ slope

Good agreement with meteorological location and time of storms was found. Farther storms have lower slopes. Wave from storms as far as 180° were detected.

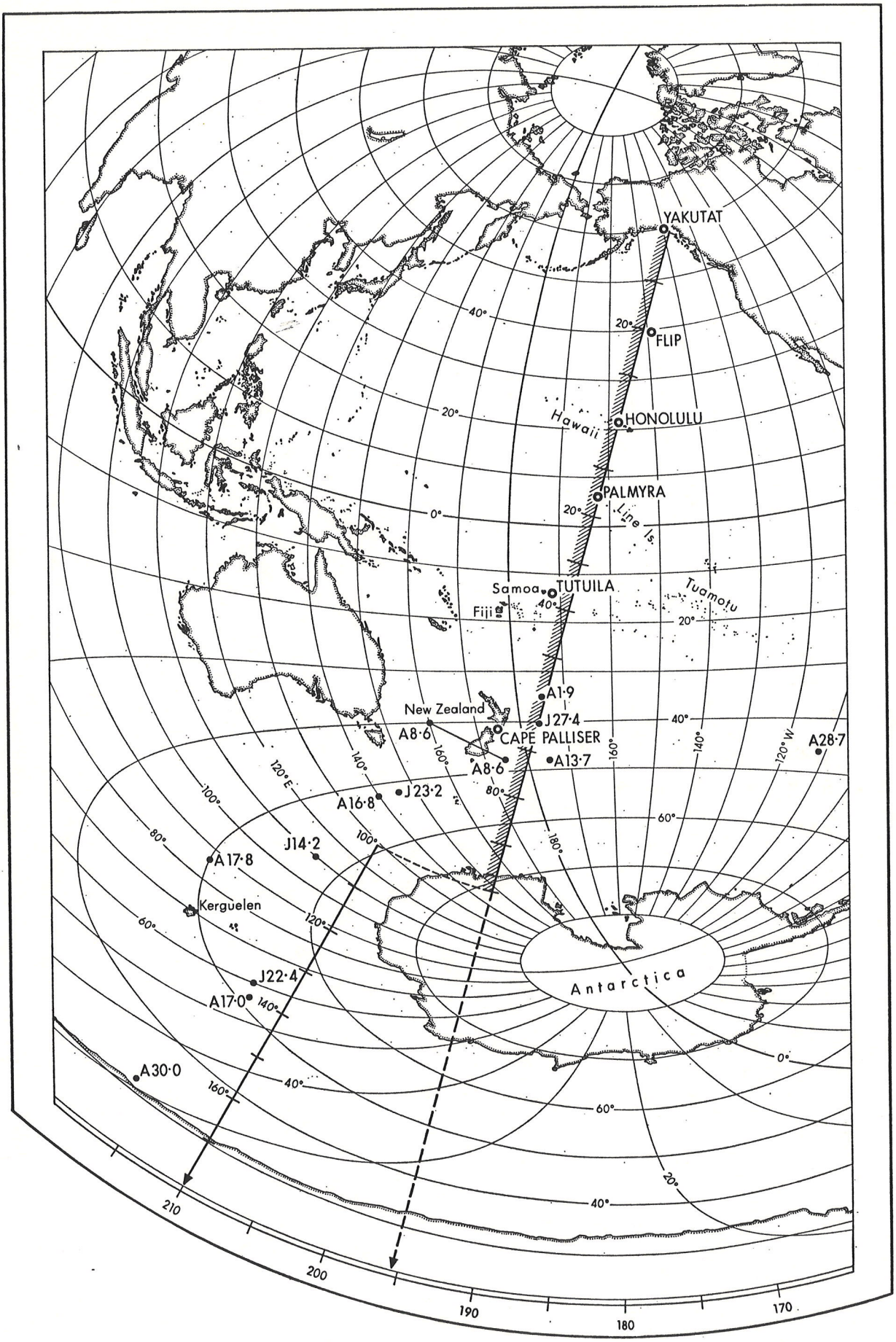

FIGURE 1. Great-circle chart based on Honolulu showing the location of the six wave instruments and of the principal storm sources. The 'reference great-circle' is in the direction 195·5° T from Honolulu; the Tasman window into the Indian Ocean bears 210° T. Distances from Honolulu are in degrees (1° = 60 nautical miles). Each storm is marked by a dot and its fractional date (J27·4 means 27 July, 9·6 h G.M.T.).

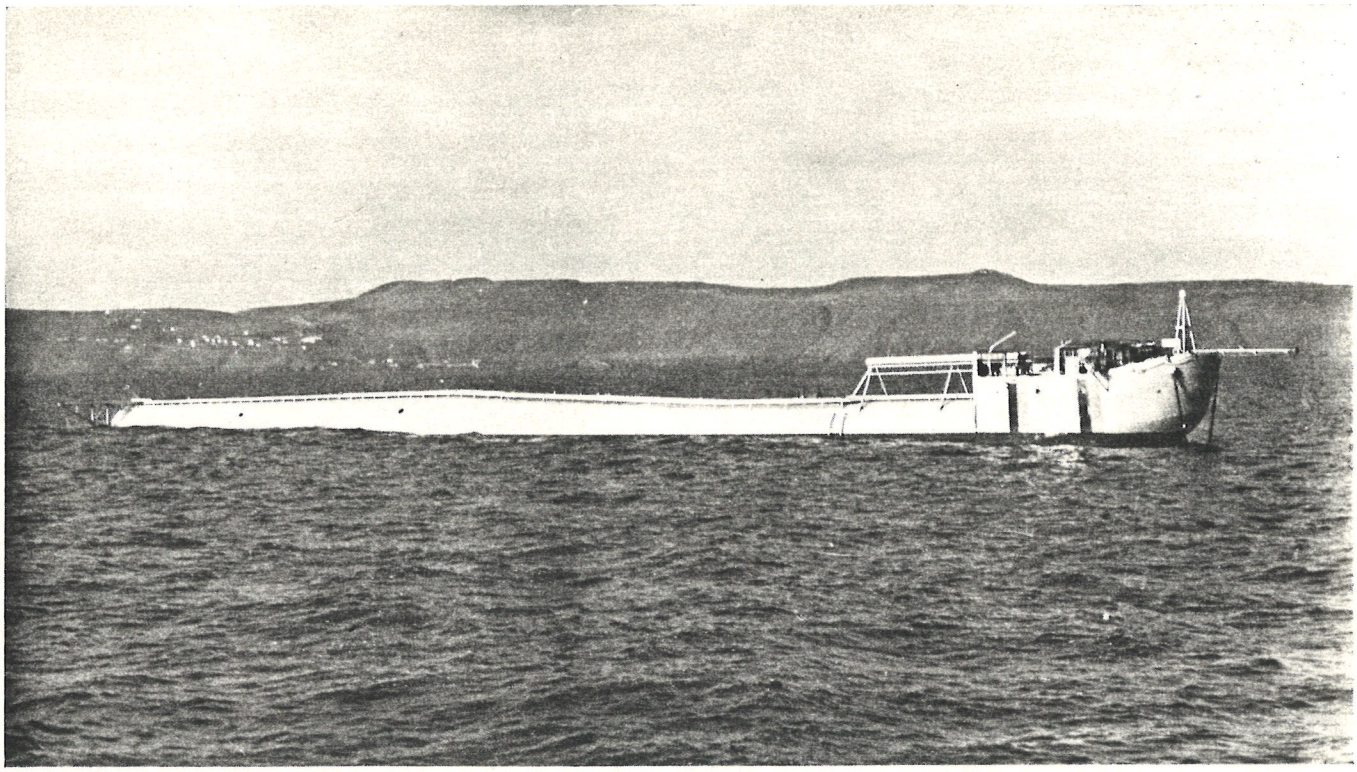

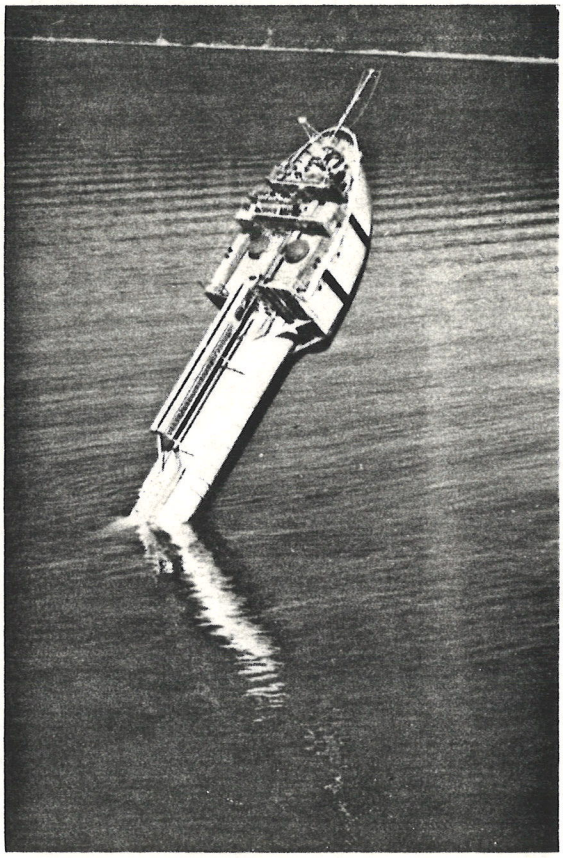

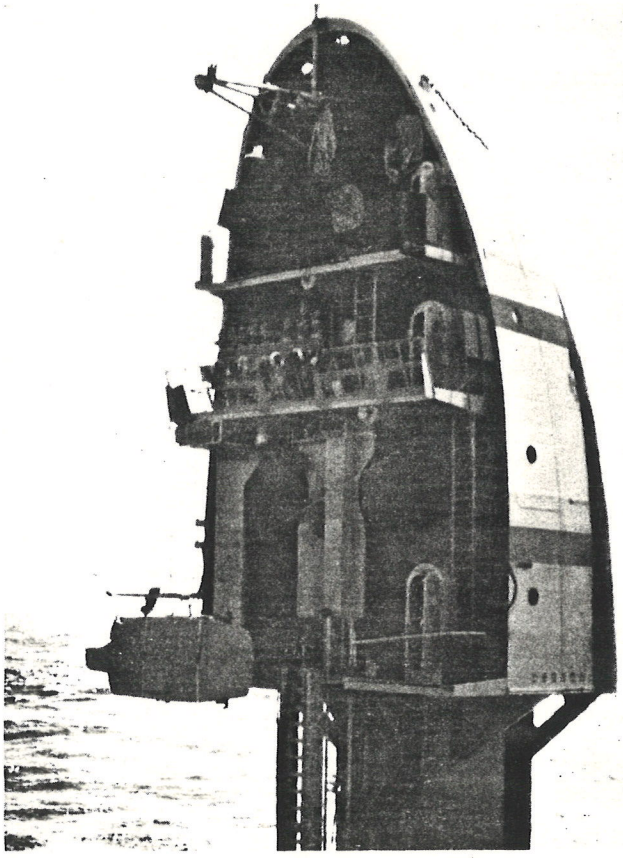

FIGURE 6. The vessel *Flip* in horizontal position, during flipping operation, and in vertical position (from Fisher & Spiess 1963).

(*Facing p.* 439)

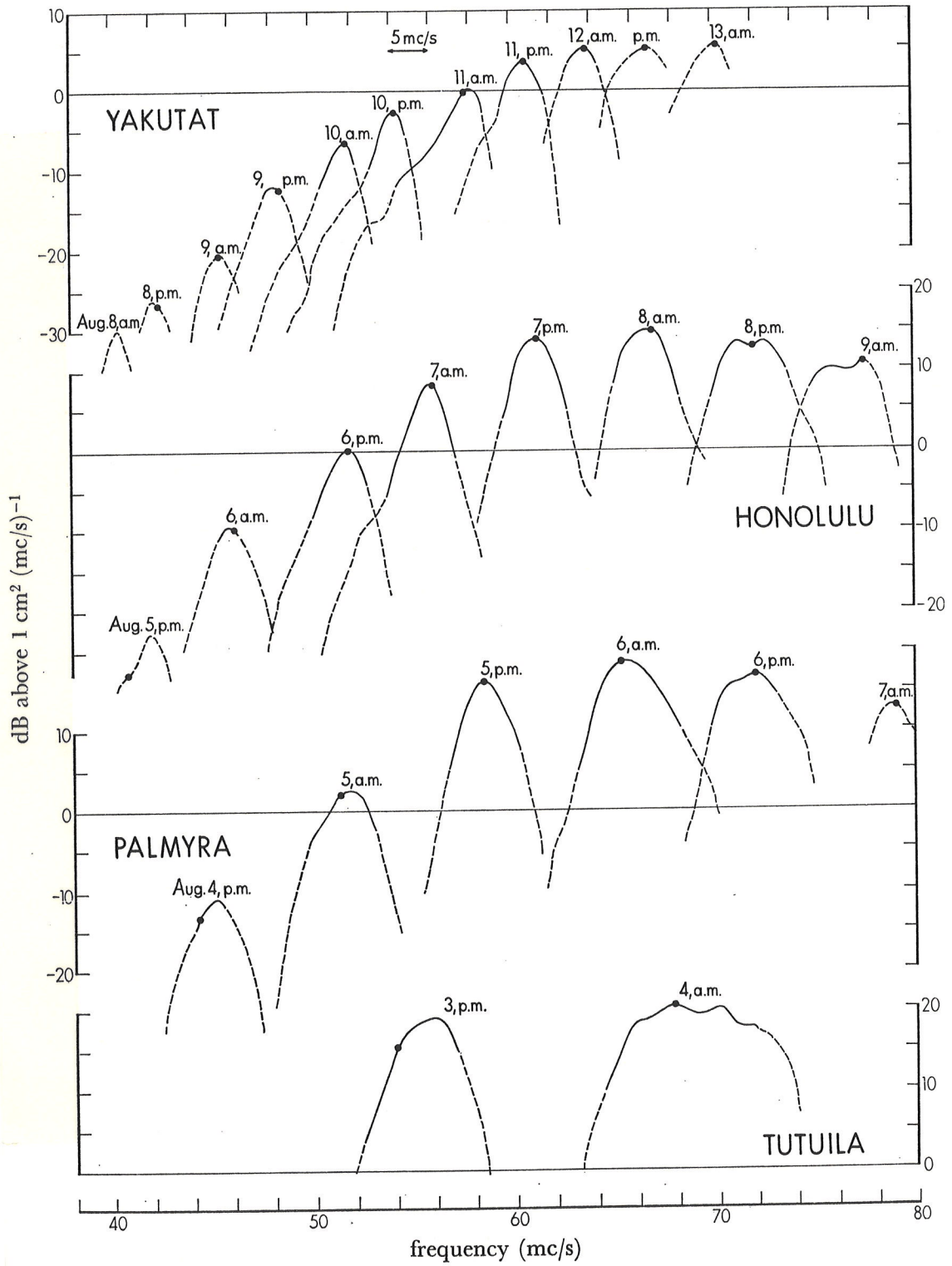

IGURE 20. Successive spectra at the four stations for the event of 1·9 August. The dots correspond to the chosen ridge line for this particular event (see figure 16), and they are positioned relative to the bottom frequency scale. The spectra to either side are drawn on a compressed frequency scale to avoid overlap; the width of a 5 mc/s band is shown by the arrow.

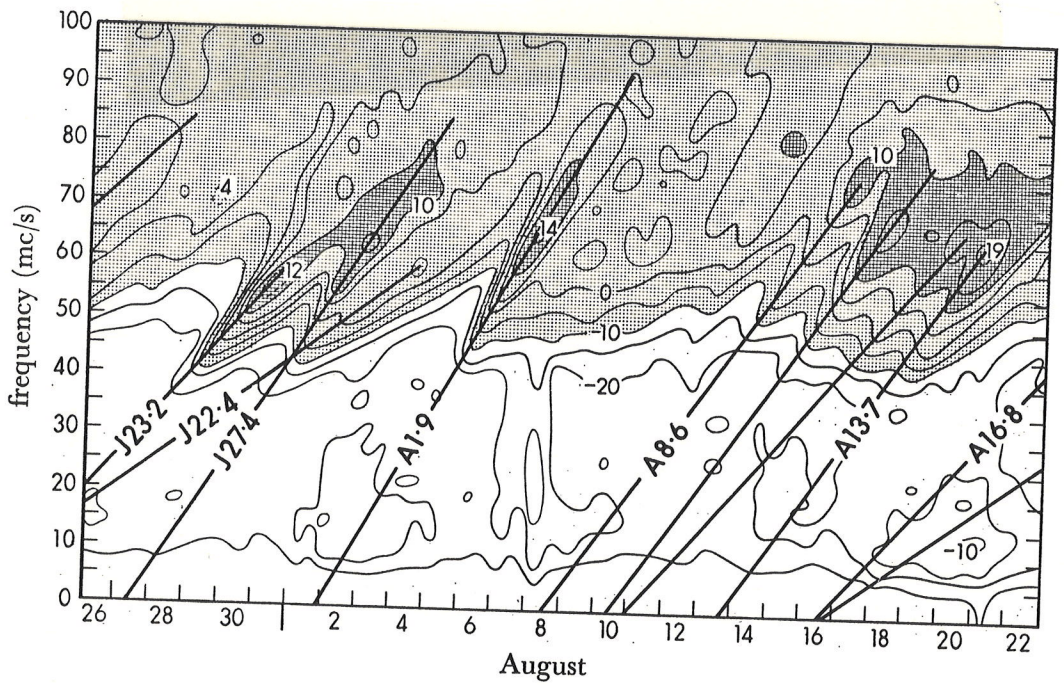

FIGURE 15. Contours of equal power density, $E(f, t)$, on a frequency–time plot for one month of Honolulu observations. Contours are drawn for -30, -25 dB, ..., $+25$, 30 dB relative to 1 cm^2 (mc/s)$^{-1}$ (i.e. 10^{-3}, $0{\cdot}316 \times 10^{-3}$, ..., to $0{\cdot}316 \times 10^{3}$, 10^{3} cm^2 (mc/s)$^{-1}$). Additional contours are dashed and labelled. On the time axis the ticks designate midnight G.M.T. The ridges represent dispersive arrivals from the principal events, and are labelled according to the source time (J 27·4 means 27 July, 9·6 h G.M.T.).

J22.4 storm is farthest away.

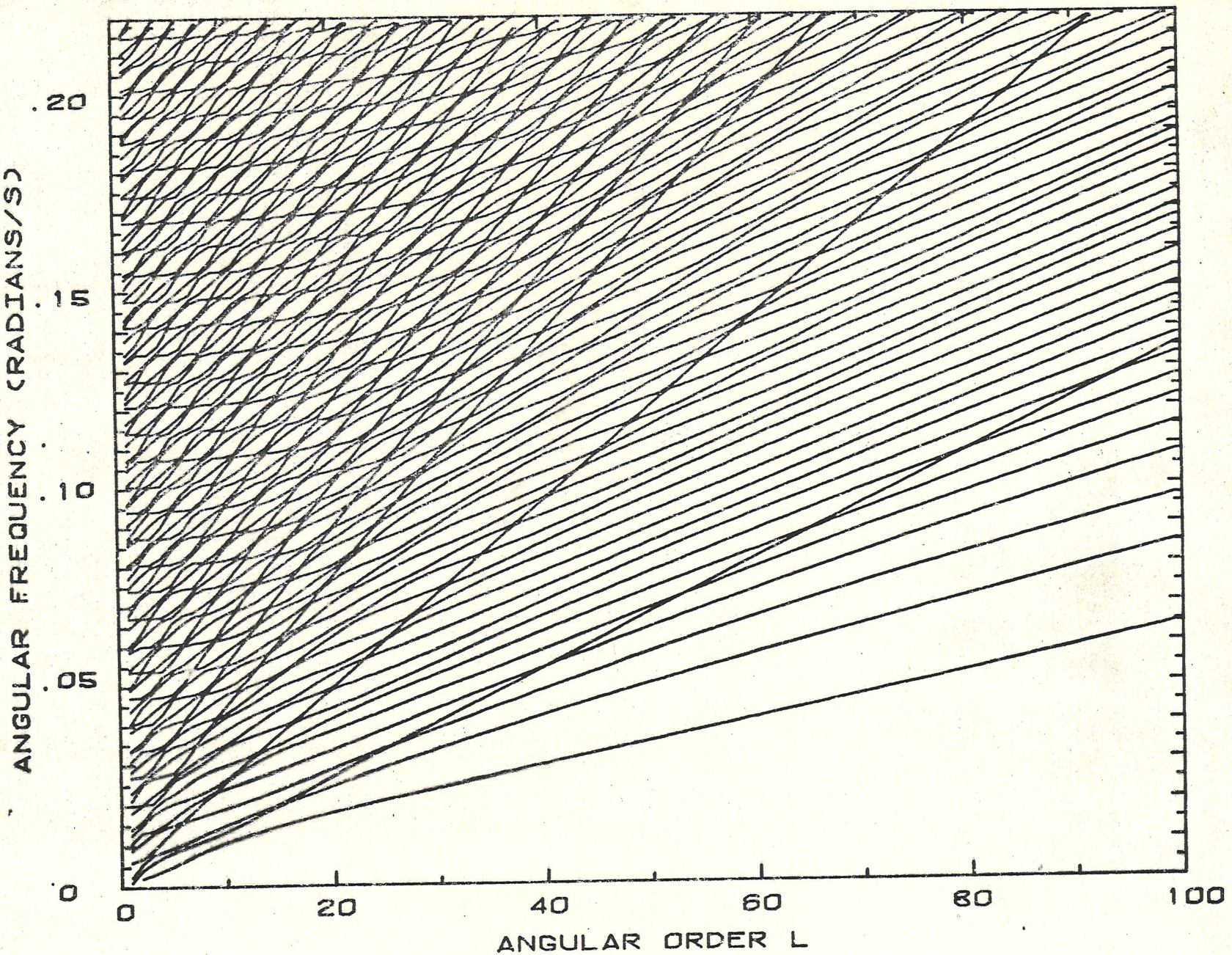

Figure 2. Spheroidal mode eigenfrequencies for PREM; the pertubation in gravitational potential has been neglected.